AD-A060 907 COASTAL ENGINEERING RESEARCH CENTER FORT BELVOIR VA F/G 8/3
SAND RIPPLE GROWTH IN AN OSCILLATORY-FLOW WATER TUNNEL.(U)
AUG 78 K E LOFQUIST
UNCLASSIFIED CERC-TP-78-5 NL

1 OF 2
AD
A060907

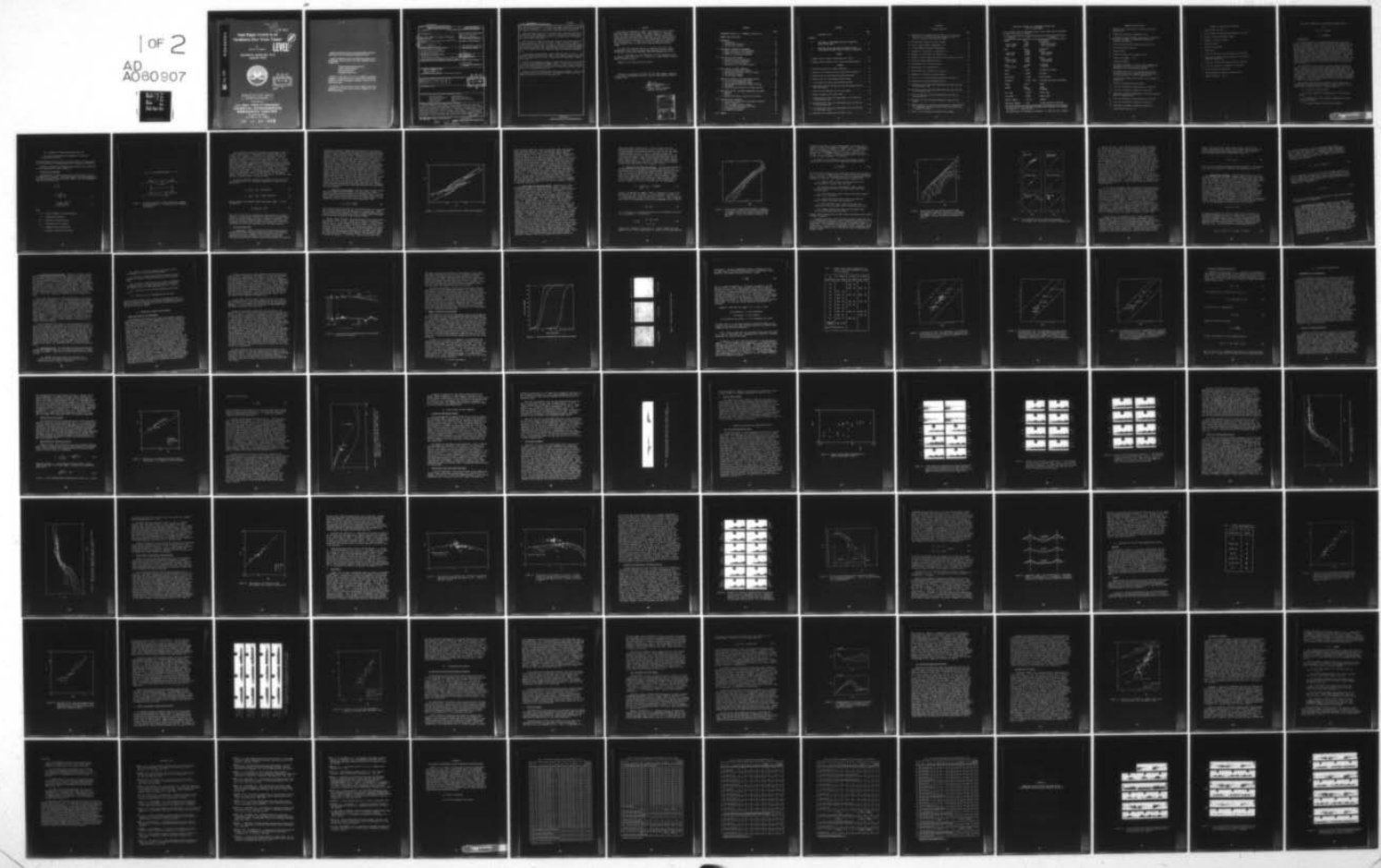

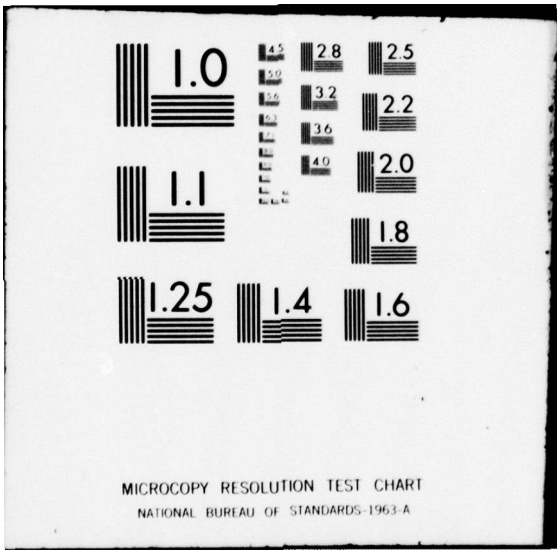
1.0
1.1
1.25
1.4
1.6
1.8
2.0
2.2
2.5
2.8
3.2
3.6
4.0
MICROCOPY RESOLUTION TEST CHART
NATIONAL BUREAU OF STANDARDS-1963-A

TP 78-5

Sand Ripple Growth in an Oscillatory-Flow Water Tunnel

by

Karl E. B. Lofquist

LEVEL II

TECHNICAL PAPER NO. 78-5
AUGUST 1978

Prepared for

U.S. ARMY, CORPS OF ENGINEERS
COASTAL ENGINEERING
RESEARCH CENTER
Kingman Building
Fort Belvoir, Va. 22060

UNCLASSIFIED

SECURITY CLASSIFICATION OF THIS PAGE *(When Data Entered)*

REPORT DOCUMENTATION PAGE

READ INSTRUCTIONS BEFORE COMPLETING FORM

1. REPORT NUMBER: TP 78-5
2. GOVT ACCESSION NO.
3. RECIPIENT'S CATALOG NUMBER

4. TITLE *(and Subtitle)*: SAND RIPPLE GROWTH IN AN OSCILLATORY-FLOW WATER TUNNEL

5. TYPE OF REPORT & PERIOD COVERED: Technical Paper

6. PERFORMING ORG. REPORT NUMBER

7. AUTHOR(s): Karl E. B. Lofquist

8. CONTRACT OR GRANT NUMBER(s): CERC Agreement No. 76-30

9. PERFORMING ORGANIZATION NAME AND ADDRESS
National Bureau of Standards
National Engineering Laboratory
Washington, DC 20234

10. PROGRAM ELEMENT, PROJECT, TASK AREA & WORK UNIT NUMBERS: D31193

11. CONTROLLING OFFICE NAME AND ADDRESS
Department of the Army
Coastal Engineering Research Center (CERRE-CP)
Kingman Building, Fort Belvoir, Virginia 22060

12. REPORT DATE: August 1978

13. NUMBER OF PAGES: 100

14. MONITORING AGENCY NAME & ADDRESS *(If different from Controlling Office)*

15. SECURITY CLASS. *(of this report)*: UNCLASSIFIED

15a. DECLASSIFICATION/DOWNGRADING SCHEDULE

16. DISTRIBUTION STATEMENT *(of this Report)*
103 p.
Approved for public release, distribution unlimited.

17. DISTRIBUTION STATEMENT *(of the abstract entered in Block 20, if different from Report)*
CERC-TP-78-5

DDC RECEIVED NOV 7 1978 B

18. SUPPLEMENTARY NOTES

19. KEY WORDS *(Continue on reverse side if necessary and identify by block number)*

Coastal processes
Equilibrium bed forms
Oscillatory flow
Ripple growth
Ripple profiles
Sand motion initiation
Three-dimensional bed forms
Waves

20. ABSTRACT *(Continue on reverse side if necessary and identify by block number)*

The development of sand ripples in an oscillatory-flow water tunnel was observed in 104 laboratory experiments approximating conditions at the seabed under steady progressive surface waves. The period, T, and amplitude, a, of the water motion were varied over wide ranges. Three quartz sands were used, with mean grain diameters, D = 0.55, 0.21, and 0.18 millimeter. In 24 experiments, with the bed initially leveled, T was reduced until ripples appeared, and their development to final equilibrium form was observed without further change in T.

(Continued)

DD FORM 1 JAN 73 1473 EDITION OF 1 NOV 65 IS OBSOLETE

UNCLASSIFIED

SECURITY CLASSIFICATION OF THIS PAGE *(When Data Entered)*

78 10 25 037 050 735

The remaining 80 experiments investigated the response of previously established bed forms to changes in T or a or both. The ripple length, λ, and height, η, were measured from photos, except when bed forms were three dimensional.

Sand grains began to move on the flat bed at flow velocities generally compatible with earlier observations. A Shields criterion for motion initiation was found in need of modification for use in oscillatory flow. Prior compression of the bed had small effect.

With the grains in motion, ripples were initiated by and would spread from slight irregularities on the bed or around its edge, or could be generated everywhere by a slight increase in velocity. Flow separation and vortex formation occurred at an early stage. Rolling-grain ripples as described by Bagnold (1946) did not always form and seemed unnecessary to vortex ripple development. The initial length of the vortex ripples was small and remarkably independent of a.

During growth, the dimensionless ripple length and height, λ/a and η/a, were expressible as functions of $(D/a)n$, where n is the number of periods since ripples first appeared on the flat bed. Ripple growth was approximately complete when $(D/a)n = 1$.

Profiles of two-dimensional ripples in equilibrium with the flow were generally as described by Mogridge and Kamphuis (1972). In particular, λ/a and η/a were fairly constant over a wide range of intensity of flow. However, with end crests fixed, and a varying, a profile could be "strained" into various stable forms over a considerable range of λ/a.

Both two- and three-dimensional final bed forms were observed. Criteria for these forms were not clearly established, but appeared to depend on both the amplitude and intensity of flow, and the grain size.

PREFACE

This report is published to improve understanding of the occurrence and form of ripples under water waves, since ripples can reduce wave height and affect sand transport. The report summarizes a laboratory study, including prototype offshore conditions, of sand ripple growth in sinusoidal flow. The results will enable the engineer to better predict and interpret equilibrium ripples in the offshore under both laboratory and field conditions. The work was carried out under the coastal processes program of the U.S. Army Coastal Engineering Research Center (CERC).

The report was prepared by Karl E. B. Lofquist, Physicist, Fluid Engineering Division, National Engineering Laboratory, National Bureau of Standards, Gaithersburg, Maryland, under CERC Agreement No. 76-30.

Dr. R. J. Hallermeier was the CERC monitor for this agreement, under the general supervision of Dr. C. J. Galvin, Jr., Chief, Coastal Processes Branch, Research Division.

Comments on this publication are invited.

Published in accordance with Public Law 166, 79th Congress, approved 31 July 1945, as supplemented by Public Law 172, 88th Congress, approved 7 November 1963.

JOHN H. COUSINS
Colonel, Corps of Engineers
Commander and Director

CONTENTS

CONTENTS

TABLES

FIGURES

CONTENTS

FIGURES--Continued

CONVERSION FACTORS, U.S. CUSTOMARY TO METRIC (SI)
UNITS OF MEASUREMENT

U.S. customary units of measurement used in this report can be converted to metric (SI) units as follows:

Multiply	by	To obtain
inches	25.4	millimeters
	2.54	centimeters
square inches	6.452	square centimeters
cubic inches	16.39	cubic centimeters
feet	30.48	centimeters
	0.3048	meters
square feet	0.0929	square meters
cubic feet	0.0283	cubic meters
yards	0.9144	meters
square yards	0.836	square meters
cubic yards	0.7646	cubic meters
miles	1.6093	kilometers
square miles	259.0	hectares
knots	1.852	kilometers per hour
acres	0.4047	hectares
foot-pounds	1.3558	newton meters
millibars	1.0197×10^{-3}	kilograms per square centimeter
ounces	28.35	grams
pounds	453.6	grams
	0.4536	kilograms
ton, long	1.0160	metric tons
ton, short	0.9072	metric tons
degrees (angle)	0.01745	radians
Fahrenheit degrees	5/9	Celsius degrees or Kelvins[1]

[1]To obtain Celsius (C) temperature readings from Fahrenheit (F) readings, use formula: $C = (5/9)(F - 32)$.

To obtain Kelvin (K) readings, use formula: $K = (5/9)(F - 32) + 273.15$.

SYMBOLS AND DEFINITIONS

a	amplitude of the water motion, one half the orbital diameter ($2a$)
D	average grain diameter, equivalent to D_{50}
D_m	a descriptive grain diameter, meaning that m percent of the sand, by weight, is composed of grains with diameters less than D_m
f	bottom friction factor, defined by equation (23)
g	acceleration due to gravity
h	depth of water
H	height of surface wave (trough to crest)
k	surface wave number, $= 2\pi/L$
L	surface wavelength
n	the number of periods, or cycles, since ripples first appeared on a flat bed, or since the start of an experiment with a bed previously rippled
N	the number of turns of a nut setting the stroke of the pistons and, hence, a measure of the amplitude of the water motion ($a = 0.4576$ N centimeters)
r	a dimensionless measure of the grain size, defined by equation (2)
T	period of the sinusoidal water motion
T_c	T for the initiation of grain motion on a flat bed
T_r	T for the initiation of ripples on a flat bed
U	amplitude, or greatest magnitude, of the water velocity above the boundary layer
U_c	U for the initiation of grain motion on a flat bed
U_r	U for the initiation of ripples on a flat bed
X_2	dimensionless parameter defined by equation (7)
η	ripple height (see Fig. 1)

SYMBOLS AND DEFINITIONS--Continued

λ ripple length (see Fig. 1)

λ_i initial length of ripples newly formed on a flat bed

λ_n natural or unstrained ripple length

ν kinematic viscosity of water

ρ density of water

ρ_s density of sand grains

τ bottom stress

τ_c τ for the initiation of grain motion on a flat bed

ϕ dimensionless measure of the intensity of sand motion, defined by equation (1)

ϕ_c ϕ for the initiation of grain motion on a flat bed

ϕ_r ϕ for the initiation of ripples on a flat bed

ϕ_s ϕ for the onset of sheet flow

Ψ Shields parameter, defined by equation (21)

ω angular frequency, $= 2\pi/T$

SAND RIPPLE GROWTH IN AN OSCILLATORY-FLOW WATER TUNNEL

by

Karl E.B. Lofquist

I. BACKGROUND

1. Introduction.

Oscillatory surface waves commonly produce ripples on a sandy seabed. These ripples, on the one hand, increase the roughness of the bed and so increase the bottom stress and the rate of energy loss from the waves which produced them. On the other hand, they enhance the agitation of the sand and so are an essential part of the mechanism of sand transport. When the oscillatory water motion over the bed is able to move sand grains along the bottom or to lift them above it, if only during a part of the cycle, a superimposed steady current, even though weak, is able to move sand consistently in one direction. Ripples enhance the movement and lifting of sand grains, particularly near their crests where water velocities are amplified and where the sharp curvature of the profile serves to separate the flow and the moving grains from the bottom.

The involvement of these effects in coastal engineering has enhanced interest in oscillatory-flow ripples, which have claimed much study. Nevertheless, these ripples remain poorly understood. This is in large part because observations remain inadequate to define the roles of the many factors involved. Also, the import of observations is sometimes obscured by diversities in technique and, less often, by apparent discrepancies. This study describes a series of laboratory experiments. Its purpose is to add to available observations with special attention to ripple initiation and growth.

Observations and discussions of ripples usually concern two-dimensional bed forms and one or another of several stages in ripple growth from an initially level bed. These stages are:

(a) Initiation of grain motion;

(b) possible regimes of rolling grains or "rolling-grain" ripples;

(c) emergence of "vortex" ripples, spontaneously or from rolling-grain ripples;

(d) subsequent growth of these vortex ripples;

(e) attainment of stable equilibrium form; and

(f) erosion and ultimate disappearance of bed forms at high water velocities.

This experimental study deals with all these stages in varying degree, as have the previous investigations which are discussed in Section I,3.

Sketches of regular and irregular ripple profiles with definitions of their dimensions are shown in Figure 1.

2. Dimensionless Variables.

Interpretation of ripple observations is made easier by the use of dimensionless variables. This study adopts, with slight modification, the system advanced by Yalin and Russell (1962). The four independent dimensionless variables are:

$$\frac{a}{D}\ ,\ \frac{\rho_s}{\rho}$$

$$\phi \equiv \frac{U^2}{g(\frac{\rho_s}{\rho} - 1)D} \qquad (1)$$

$$r \equiv \left[\frac{g(\frac{\rho_s}{\rho} - 1)D^3}{\nu^2}\right]^{1/2} \qquad (2)$$

where

$2a$ = orbital diameter of the fluid motion

D = average grain diameter

ρ_s, ρ = densities of sand and fluid

g = acceleration due to gravity

U = maximum velocity of the fluid

ν = kinematic viscosity of the fluid

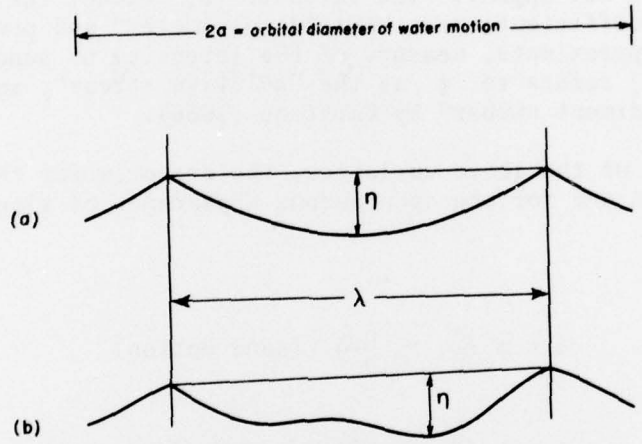

Figure 1. Definition sketches for ripple dimensions, showing the measurement of η for regular (a) and irregular (b) profiles.

It is convenient to express the effects of viscosity in terms of r rather than by the more usual grain-size Reynolds number, UD/ν, equal to $r\phi^{1/2}$, because r depends only on the materials used and is typically a constant during a series of experiments. When the materials involved are quartz sand and water and ρ_s/ρ and ν can be regarded as constant, r serves as a measure of D. Also, r^2 is proportional to a Reynolds number based on the Stokes fall velocity of the grains and their mean diameter D. Not included in the above are parameters describing the effects of grain-size distribution and grain shape and the degree of packing of the sand surface. Thus, the angle of repose does not appear. The variable ϕ, except for the absence of the drag coefficient, is a "Shields parameter" and provides a convenient, if approximate, measure of the intensity of sand motion. Dingler (1975) refers to ϕ as the "relative stress", and $\phi^{1/2}$ has been named the "sediment number" by Carstens (1966).

In terms of the above variables, the criteria for the initiation of sand motion and for the spontaneous appearance of ripples can be expressed as

$$\phi = \phi_c\left(\frac{a}{D},\ r,\ \frac{\rho_s}{\rho}\right) \quad \text{(sand motion)} \tag{3}$$

$$\phi = \phi_r\left(\frac{a}{D},\ r,\ \frac{\rho_s}{\rho}\right) \quad \text{(ripple formation)} \tag{4}$$

and, for example, the dependent equilibrium ripple length λ can be expressed as

$$\frac{\lambda}{D} = \frac{\lambda}{D}\left(\phi,\ \frac{a}{D},\ r,\ \frac{\rho_s}{\rho}\right) . \tag{5}$$

Thus, the criteria for the initiation of sand motion, and of ripple formation, are described by dimensionless plots without distinguishing whether the boundary layer, or stress, is laminar or turbulent. Such distinction has been attempted by Komar and Miller (1973) and others. The degree of turbulence can be defined by the character of the stress coefficient which is itself some function of the above variables.

3. Previous Observations.

a. Facilities. Results of previous investigations may best be introduced by a brief evaluation of facilities used in the investigations most often cited. Bagnold (1946) and Manohar (1955) used sediment-filled trays oscillating in still water. This device conveniently provided wide ranges of period and amplitude, but subjected

the grains to unnatural (though possibly negligible) accelerations. Stationary beds are provided by wave tanks and oscillatory-flow water tunnels. Inman and Bowen (1962), Kennedy and Falcon (1965) and Yalin and Russell (1962) used wave tanks. Although the mechanics of sand movement by waves in tanks are that of the prototype, limitations in tank size and wavelength keep wave periods rather small, typically less than 3 seconds. Oscillatory-flow water tunnels may or may not be limited in period. Carstens, Neilson, and Altinbilek (1969) used a tunnel with a rather wide cross section well adapted to observe three-dimensional bed forms but which was restricted to a single period of oscillation (3.56 seconds). Mogridge and Kamphuis (1972) and Rance and Warren (1968) had the use of large tunnels without restriction on period. The tunnel of Chan, Baird, and Round (1972) was limited in its range of period and by a circular cross section only 5 centimeters in diameter, but was suitable for use with fluids other than water. Inman (1957) and, later, Dingler (1975) observed ripples on the seabed itself. The seabed lacks all the usual laboratory restrictions of size and scale, but it is out of the observer's control so that the cause of an effect may be obscured. Both Inman (1957) and Dingler (1975) discussed the problem of defining an amplitude and a frequency for the bottom water motion for field conditions where the wave spectra have many components.

b. Initiation of Grain Motion. The first stage of ripple development, the initiation of grain motion, has been the most studied. Silvester (1974) provides references to 13 separate criteria, to which may be added others of Komar and Miller (1973; 1975), Chan, Baird, and Round (1972), Sternberg and Larsen (1975), and Dingler (1975). Of the assembled criteria, 14 can be put in the dimensionless form,

$$\phi_c = \text{const.}\ r^{\alpha}\left(\frac{a}{D}\right)^{\beta} \quad . \tag{6}$$

This particular form of equation (3) is the usual result of fitting data, over a limited range, with a straight line on a log-log plot. Some of the criteria apply specifically to laminar or turbulent boundary layers. Criteria which can be defined by the data of Bagnold (1946) and Manohar (1955) have been discussed by Komar and Miller (1973).

However, taken altogether, the available data do not clearly define the function $\phi_c(a/D,\ r,\ \rho_s/\rho)$. Among the 14 formulas represented in equation (6), β varies between zero and 2/3, while α varies between -2/5 and +38/45, leaving it open to question whether an increase in r causes ϕ_c to decrease or increase. In contrast, the effects of a/D are relatively clear and trends of the data of various observers are shown in Figure 2 by plots of ϕ_c as function of a/D. Included in the figure are trends from the frequently cited Bagnold (1946) and Manohar (1955) with three data points from Carstens, Neilson, and Altinbilek (1969). To extend the range of r in the data, trends have been added from

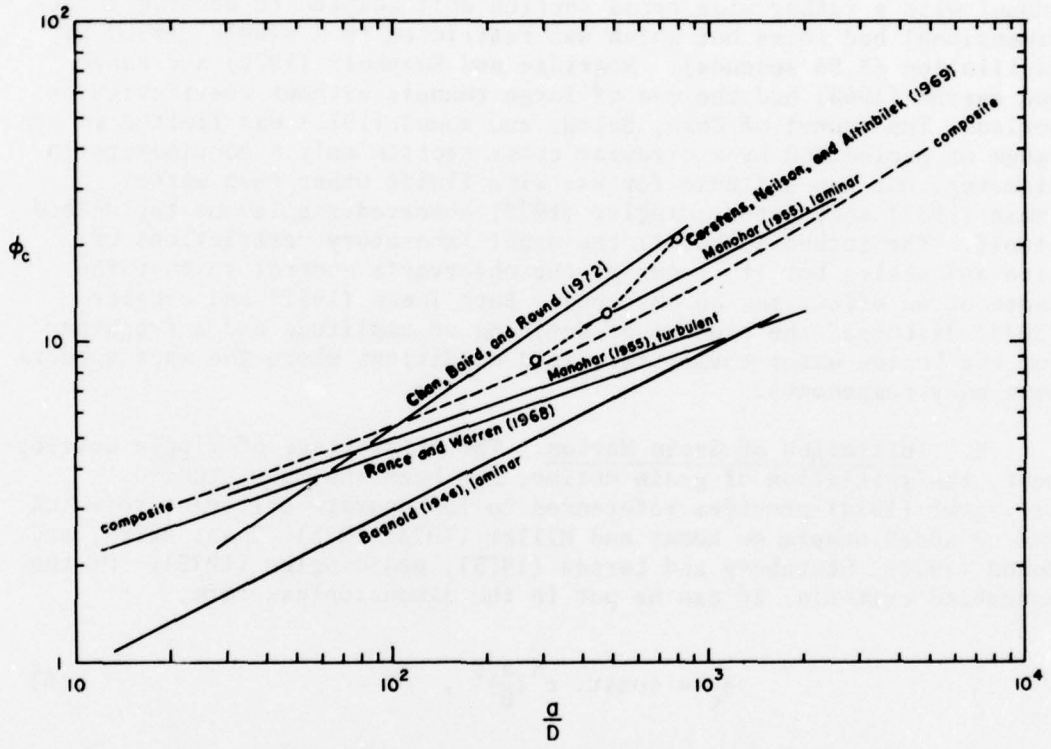

Figure 2. Trends of ϕ_c as function of a/D, from various observers.

Rance and Warren (1968) who, using a large water tunnel and limestone chips, attained values of $r > 10^4$; and from Chan, Baird, and Round (1972) who, using a small pipe but with various viscous liquids, attained values of $r < 0.2$. The various trends reflect a considerable scatter in the data, on the order of ± 40 percent. Some of this scatter may derive from the neglected effects of grain-size distribution and grain shape which, as Collins and Chesnutt (1976) describe, can be significant in the evolution of beach profiles or from the degree of compaction of the sand surface. However, most of the scatter can be attributed to the subjective element in determining the condition of incipient grain motion. The definition and determination of U_c and ϕ_c are discussed in Section III,1. Generally, the data represented in Figure 2 show a weak correlation of larger values of ϕ_c with smaller values of r. For convenient reference, a single composite curve, for all values of r, has been drawn through the trends shown in the figure. For small a/D, this curve becomes parallel to the trend of Rance and Warren (1968), with ϕ_c proportional to $(a/D)^{1/3}$; for large a/D, the curve makes ϕ_c proportional to $(a/D)^{2/3}$, a behavior suggested by the known stress on a smooth bed combined with a Shields criterion, as defined in Section III,4.

c. Early Stages of Ripple Development. Observations of ripple development following the initiation of sand motion as reported by various investigators are summarized below. Bagnold (1946) identified a "rolling-grain" type of ripple stable over the range $U_c < U < 2U_c$ with ripple length and height, for constant a, increasing with ω. At $U \approx 2U_c$ these ripples rather suddenly change character and become "vortex-type" ripples, with vortices developing behind the ripple crests and over the troughs. The vortex ripple length is independent of ω and is proportional to a, for small a, and constant for larger a. Bagnold states that these ripples can form "from any sufficiently large surface feature" at values of U even below U_c. He describes artificial generation of ripples for $U < U_c$ (also described in more detail by Carstens, Neilson, and Altinbilek, 1969). Manohar (1955) describes stable regimes of rolling-grain motion and "first-stage" ripples very similar to the rolling-grain ripples of Bagnold. He also describes "second-stage" ripples which appear to be the vortex ripples of Bagnold. Throughout the process of ripple formation, Manohar finds, for given a, stable ripples at each value of ω, and ripple length increasing with ω. He provides data for the "initiation of ripples" which occurs, on the average, at a value of U which exceeds the values for "initial" and "general" motion of "sediment in the turbulent boundary layer" by 24 and 13 percent. Presumably, this refers to the initiation of second-stage or vortex ripples. Kennedy and Falcon (1965) provide no data on the inception of either sand motion or ripple formation, but observe that, when there is "general motion of the upper layers" of the bed particles, ripples appear simultaneously and "once they grow to a certain height, vortices are shed from the ripple crests." They state that, in their experiments, the rolling-grain ripples described by Bagnold (1946) did not appear with quartz sand but did

appear with plastic (opalon) beads. They also report that "the equilibrium ripple wavelength was observed to form at an early stage of ripple growth for all sediment materials used" and that the ripple length increased with both a and ω. Carstens, Neilson, and Altinbilek (1969) describe an (apparently) unstable progression from rolling grains through a stage of rolling-grain ripples and into the stage of vortex ripples, which attain an equilibrium length, approximately proportional to a. They find a "small lag" between incipient motion and the spontaneous formation of ripples which, by an average of their three observations, occurs around $U = 1.16\ U_c$.

d. Equilibrium Two-Dimensional Ripples. The preceding descriptions include references to the stable forms which ripple profiles attain. The primary source of information on two-dimensional equilibrium ripple forms is the study of Mogridge and Kamphuis (1972), obtained with a large oscillatory-flow water tunnel and using three types of plastic grains and a single quartz sand (with $D = 0.36$ millimeters). Observations of the equilibrium ripple length and height are summarized by curves in Figures 17 and 18 of their report. These figures give λ/D and η/D as functions of $2a/D$ for selected values of the parameter,

$$X_2 \equiv \frac{D}{g\left(\frac{\rho_s}{\rho} - 1\right)T^2} = \frac{\phi}{\pi^2}\left(\frac{D}{2a}\right)^2 . \qquad (7)$$

Figure 17 of Mogridge and Kamphuis (1972) is reproduced in Figure 3 with the addition of lines of constant ϕ drawn according to equation (7). The figure shows that, over wide ranges of a/D and ϕ, lines of constant ϕ are approximately straight with a slope of plus one. Thus, along each such line, λ/a is approximately constant and independent of a/D. That is,

$$\frac{\lambda}{a} \approx f(\phi) . \qquad (8)$$

As ϕ increases, λ/a ultimately decreases while its dependence upon a/D increases gradually. In particular,

$$\frac{\lambda}{a} \approx \frac{4}{3} \qquad \begin{matrix} 10^2 < \frac{a}{D} < 5\times10^3 \\ 0 < \phi < 30 . \end{matrix} \qquad (9)$$

Equation (9), remarkably, states that λ/a is nearly constant and independent of U or T over a wide range of ϕ, which (as this study confirms)

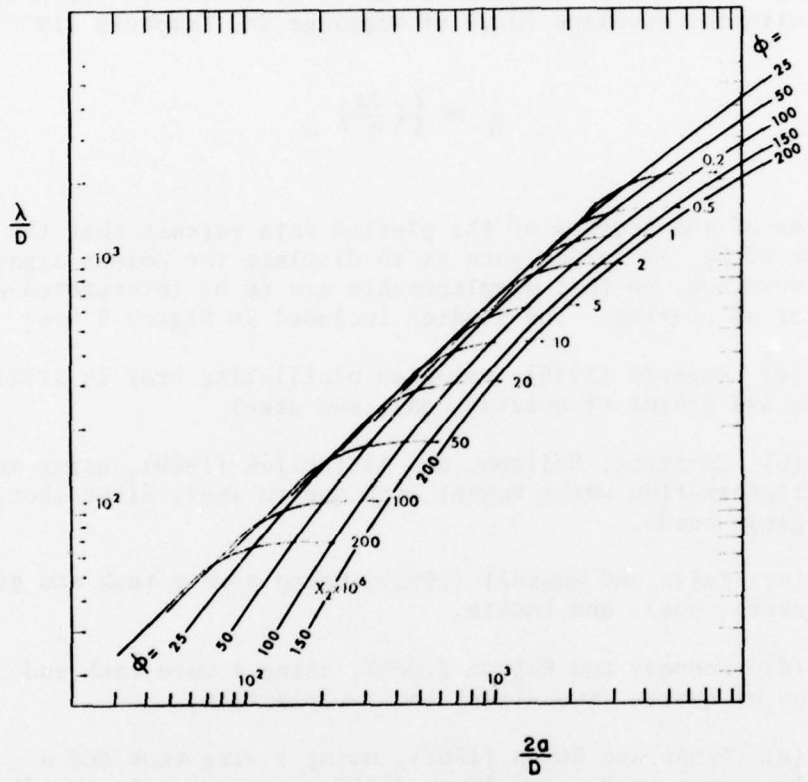

Figure 3. Design curves for equilibrium bed-form wavelength. λ/D is given as function of $2a/D$ and X_2 by Mogridge and Kamphuis (1972), and curves of constant ϕ have been added. ϕ and X_2 are defined by equations (1) and (7).

extends to high rates of scour and high degrees of sand agitation. Similarly, Figure 18 of Mogridge and Kamphuis (1972) is reproduced in Figure 4 with lines of constant ϕ added. Again, for small values of ϕ, η/a is approximately constant, but, as ϕ increases, η/a decreases and its dependence upon a/D, increases, both relatively rapidly. As ϕ increases, η/a decreases more rapidly than does λ/a, so that the ripple steepness, η/λ decreases.

In Figure 5, λ/D as function of 2a/D, from several studies, is compared with the envelope curve of Mogridge and Kamphuis (1972).

$$\frac{\lambda}{D} \approx \frac{2}{3}\left(\frac{2a}{D}\right) . \qquad (10)$$

Examination of the sources of the plotted data reveals that the effect of ϕ, or of X_2, is seldom such as to displace the points significantly from the envelope, so that displacements are to be interpreted as disagreement or as scatter. The studies included in Figure 5 are:

(a) Bagnold (1946), using an oscillating tray in still water and grains of quartz, coal, and steel.

(b) Carstens, Neilson, and Altinbilek (1969), using an oscillatory-flow water tunnel with quartz sand, flint shot, and glass beads.

(c) Yalin and Russell (1962), using a wave tank and grains of quartz, coal, and Lucite.

(d) Kennedy and Falcon (1965), using a wave tank and grains of quartz (two sizes) and two plastics.

(e) Inman and Bowen (1962), using a wave tank and a single quartz sand; also Inman (1957), observing in the field.

(f) Dingler (1975), using a wave tank and quartz sand (two sizes) and observing in the field.

Dingler (1975) discusses most of these studies and presents plots similar to those in Figure 5.

In general, for $2a/D < 2\times10^3$, the data in Figure 5 agree with the curves of Mogridge and Kamphuis (1972) as reduced to equation (9) or (10). An exception is the leveling off of the curves of Bagnold (1946) in Figure 5(a). Since laboratory observations in Figure 5 for $2a/D < 2\times10^3$ include grains of quartz over a wide range of sizes, and grains of other materials, they extend as well as confirm the results of Mogridge and Kamphuis (1972).

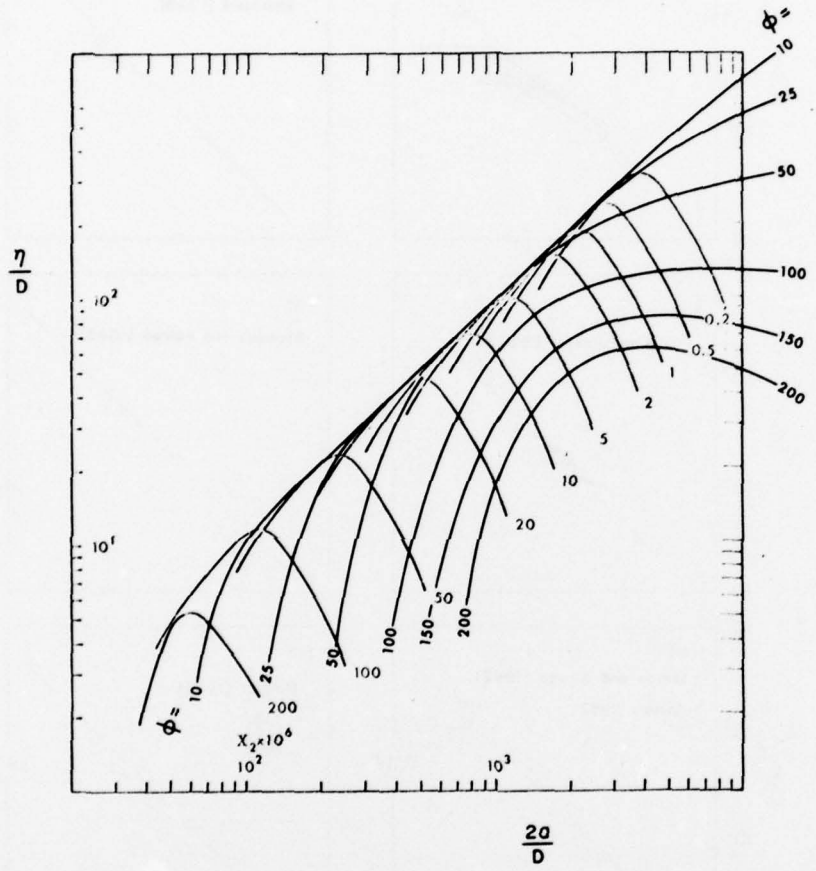

Figure 4. Design curves for equilibrium bed-form height. η/D is given as function of 2a/D and X_2 by Mogridge and Kamphuis (1972), and curves of constant ϕ have been added. ϕ and X_2 are defined by equations (1) and (7).

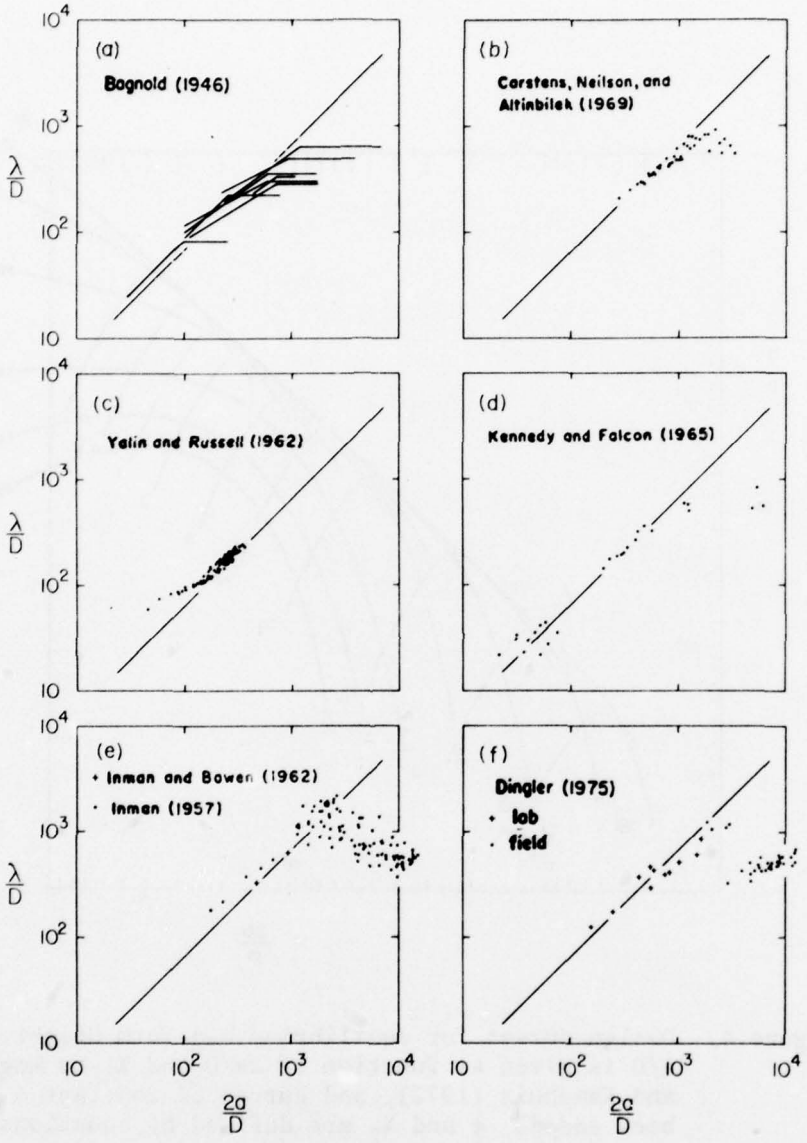

Figure 5. λ/D as function of 2a/D, from various observers. The straight line in each plot is given by equation (10).

However, for $2a/D > 2\times10^3$, the data in Figure 5 show a tendency for λ/D and λ/a to fall below values according to equations (10) and (9). This tendency appears in the laboratory observations in Figure 5(b and d) and, more strongly, in the field observations in Figure 5(e and f). Circumstances, especially in the field, appear to favor a positive correlation between the "independent" variables $2a/D$ and ϕ, so that their effects are not readily separated. This problem is discussed further in Section VII,6. The data falling below the envelope curve of Mogridge and Kamphuis (1972) in Figure 5 include large values of ϕ, between 50 and 200, which can account for some of this deviation. However, the reductions in λ/D thus accounted for are a rather small part of those actually found, and substantial reductions are found also with small values of ϕ. Thus, the data, with their scatter, reveal no clear effect of ϕ upon λ/D. Dingler's (1975) data, unlike those of Inman (1957), form two separate clusters, despite fairly continuous distributions of $2a/D$ and ϕ. Small values of λ/a appear to be characteristic of small sand grains, and values of $\lambda/a < 1/2$ are most often associated with values of $D < 0.2$ millimeters. This would suggest an effect of grain size, or of r, not included in the curves of Mogridge and Kamphuis (1972). In their experiments, r remained within the rather narrow range $28 < r < 43$, so that its possible effects were hardly explored.

Nielsen (1977) has suggested that λ/a should be a function of U/w, where w is the fall velocity of the sand grains, and has plotted data from various sources in this form. His curve drawn through the data shows an accelerating decline in λ/a with increasing U/w similar to that with ϕ in equation (8). U/w can be written as $\phi^{1/2}f(r)$, where the function $f(r)$ depends on the variation of the drag coefficient of the grains with Reynolds number. Over the range of practical interest, $f(r)$ decreases with r almost as rapidly as $1/r$. Then, a reduction in r, as well as an increase in ϕ, increases U/w and so, by Nielsen's curve, reduces λ/a. Such a behavior seems appropriate for a modification of the curves of Mogridge and Kamphuis (1972) with $(U/w)^2$ replacing ϕ. A rather large degree of scatter in the data of Nielsen's plot obscures to what extent separate effects of ϕ and r combine into the single effect of U/w. However, Nielsen (1977) has identified U/w as a variable likely to be useful in analyses of ripple forms.

Several studies (not included in Fig. 5) report behavior of λ quite different from the results of Mogridge and Kamphuis (1972). Manohar (1955), using an oscillating tray in still water, found λ/D to be almost independent of a and to be approximately proportional to U. Guided by the process of vortex shedding by cylinders, Homma and Horikawa (1962) cite the field data of Inman (1957) and their observations and those by Scott (1954) in wave tanks to show that λ/a is primarily a function of the Reynolds number Ua/ν. Horikawa and Watanabe (1967) obtained a similar result when sand was replaced with plastic pellets.

However, the data of Scott (1954), within scatter, are fairly consistent with equation (10), and the data of Inman (1957) in Figure 5(f) show increased scatter when plotted against Ua/ν. On the basis of theory and some observations, Shulyak (1969) found that

$$\lambda = C(U + U_1)T \tag{11}$$

where C and U_1 are functions of grain and fluid properties. The presence of U_1 makes this expression incompatible with equations (9) and (10).

e. Disappearance of Ripples. Observers agree that, as a, or U, or both increase, bed forms reach a maximum height and then decline and eventually disappear in a slurry, a condition Dingler (1975) calls "sheet flow." At the onset of this condition, $\phi = \phi_S$. Kennedy and Falcon (1965), using Inman's (1957) data, find this disappearance at $a/D \simeq 8{,}000$ ($UT/D \simeq 50{,}000$), while Carstens, Neilson, and Altinbilek (1969) find $a/D = 1{,}700$. Earlier, Carstens (1966) described the growth and decline of bed forms in terms of $\phi^{1/2}$ rather than a/D, with maximum size at $\phi^{1/2} = 6.5$ and disappearance at $\phi^{1/2} = \phi_S{}^{1/2} \simeq 13.0$. In any case, the tunnel in Carstens' studies was restricted to a single period (3.56 seconds), so possible separate effects of ϕ and a/D could not easily be distinguished. Mogridge and Kamphuis (1972) observe that bed forms decrease and disappear with increasing a/D, but seem to imply that T (with X_2) is here held constant, so that U increases with a. In Figure 4, as ϕ increases η/D decreases and can reasonably be extrapolated to zero. Manohar (1955) (with Figure 23 in his report) provides a criterion for the disappearance of bed forms which can be written

$$\phi_S{}^{1/2} r^{1/5} = 20.9 \ .$$

For each grain material (value of r), Manohar (1955) obtained U_S by averaging all observations, each at a given value of a, and thereby obscured any dependence of ϕ_S on a/D. With all observations plotted, the data (in Manohar's Table 9) show U_S clearly increasing with a for eight grain materials, with scatter obscuring the trend in the single remaining case of the lightest plastic. For glass beads and quartz sand ($2.5 < \rho_S/\rho < 2.65$), the data are closely approximated by

$$\phi_S{}^{1/2} = 20.2\ r^{-1/4} + 0.33\times10^{-3}\ r^{1/2}(a/D) \ . \tag{12}$$

The remaining observations, with two types of plastic beads (ρ_s/ρ = 1.28, 1.05), give values of ϕ_s somewhat higher, presumably due to an effect of smaller ρ_s/ρ. In Manohar's (1955) experiments, r varied over the range, $14 < r < 356$. The condition for sheet flow observed by Chan, Baird, and Round (1972) is given by their equation (iii) which can be written,

$$\phi_s = 23.2\, r^{-1/3}(a/D)^{1/3} . \tag{13}$$

In their experiments, using various fluids and granular materials, ρ_s/ρ and r varied over the ranges, $1.04 < \rho_s/\rho < 5.1$ and $0.16 < r < 160$. Based on observations on the seabed, Dingler (1975) concluded that the ripple steepness η/λ begins a decline at ϕ around 40 and that ripples disappear at ϕ around 240, or

$$\phi_s \simeq 240 . \tag{14}$$

This value is not greatly larger than Carsten's (1966) earlier proposal of around 169 (i.e., around 13^2).

f. Three-Dimensional Bed Forms. Several of the studies cited above contain references to three-dimensional bed forms. Bagnold (1946) discovered a small regular "brick pattern" when a was reduced to about $\lambda/6$. Manohar (1955) observed a similar pattern at "very short strokes" as ω increased "almost to the point of ripple disappearance." Kennedy and Falcon (1965) also report brick patterns but at relatively large periods and orbital diameters, with $2a/\lambda \approx 10$. In contrast, Carstens, Neilson, and Altinbilek (1969) describe three-dimensional bed forms which, unlike the brick patterns, were irregular and were often observed. They found that, with increasing a/D, two-dimensional ripples, having attained maximum size at a/D = 775, gave way to three-dimensional forms which persisted until their disappearance at a/D = 1,700. Inman (1957) has defined the degree of two and three dimensionality in terms of three categories which he includes with his observations. Outside references to three-dimensional forms are found; therefore, it must be presumed that the bed forms under discussion are two dimensional.

g. Limitations of Time and Space. Except for Carstens, Neilson, and Altinbilek (1969) discussion of the evolution of a duned bed and for occasional descriptions of the early spread of ripples over a flat bed, the bed forms described in the references are presumed to be in equilibrium with their environment, not changing with time and requiring increments in a or U to induce further change. The presumption of stability is sometimes stated and sometimes implied. Inman (1957) remarks that for ripples in coarse sand the condition of equilibrium is made less certain by their slow response to changes in the environment, but that ripples in fine sand are more rapidly modified. Dingler (1957) observes that following sheet-flow ripples can reform within a few cycles. In any case, references to duration or rate of processes are rare.

Some of the discrepancies in the preceding survey invite speculation that stable states had not in fact been established, particularly in cases where the growth of λ and η stopped short of the values predicted by equation (9) and related curves of Mogridge and Kamphuis (1972). For example, Bagnold (1946) took his equilibrium ripple length to be that of three adjacent ripples which had grown to equal size from an initial local disturbance, not discussing the possibility that they might continue to grow, perhaps at a reduced rate. Again, the unusual growth of λ with increasing ω (rather than a) observed by Manohar (1955) suggests a continuing response to an earlier selection of a. If the increases in ω were fairly continuous, an effect on the concurrent growth of λ might be unduly inferred. In general, rates of change might be so small as to remain undetected and yet persist to produce significant effects.

These discrepancies also suggest a closer examination of limitations in the experimental facilities and of their possible effects; in particular, end effects combined with the shortness of the sand bed. At the ends of the sand beds or trays there is a tendency for local scour, which is sensitive to the local geometry of the rigid container. The local scour tends to define a ripple trough and so to inhibit motions which may accompany the normal development of the ripple profile. The effect of both ends of the bed acting as permanent ripple troughs is to permit only those ripples for which λ is equal to the length of the bed divided by some integer. It would appear that end effects become more serious as the bed becomes shorter. Surprisingly, end geometries and effects are seldom mentioned in the studies referred to above.

h. Emerging Questions. The preceding discussion shows that more information is needed to provide a satisfactory description of ripples and their development. Areas where new observations may be most useful include:

(a) Whether and to what extent, on a flat bed, the criteria for the initiation of sand motion and for the spontaneous generation of ripples are distinct;

(b) whether a stable rolling-grain type ripple precedes the appearance of the usual vortex-type ripple;

(c) the rate of ripple growth, which is needed to define and predict the onset of ripple equilibrium with the imposed flow;

(d) extension or modification of the results of Mogridge and Kamphuis (1972) on stable ripple dimensions, especially for natural sands with larger prototype values of a and T;

(e) conditions of two- and three-dimensional bed forms; and

(f) conditions for the disappearance of bed forms.

Also of interest is what, if any, increase in the water velocity is needed for transition from one state of ripple development to the next, and how the process is modified if the bed is initially disturbed, by objects or by previous ripples.

II. EXPERIMENTAL PROGRAM AND PROCEDURES

1. Nature and Scope of the Experiments.

The experiments described in this study were designed to provide additional observations of ripple development with special attention to those aspects just enumerated. A further aim was to make the observations under near-prototype conditions. This end was served by the use of three natural sands in an oscillatory water tunnel able to provide values of a and T over wide ranges. There were 104 experiments of which 24 began from a level bed. In these 24 experiments the entire ripple development from initiation of grain motion to equilibrium profiles was observed. The other 80 experiments began with profiles previously established and with a or T, or both, changed from the previous values. Here the response of the old profiles to the new values of a and T was observed. Leveling the bed required that most of the water be temporarily drained from the tunnel and that the top of the test section be removed. In proceeding to a new experiment with a previously rippled bed, these procedures were unnecessary. The amplitude a, which in any case could not be changed during operation, was always selected before an experiment. With previously rippled beds the period was also selected, but when starting an experiment with a leveled bed, T was gradually reduced until the onset of grain motion or spontaneous ripples was observed, defining T_c or T_r. After ripples had begun to grow, development was allowed to proceed to the final equilibrium bed form without further change in T. In most cases, experiments continued long enough to ensure that equilibrium conditions had been established. Some experiments were interrupted and continued on the following day. Bed forms and their development were recorded with frequent photos supplemented with written notes.

The water tunnel used in these experiments has been described by Lofquist (1977). Essentially, the tunnel is a U-tube with the middle horizontal part comprising the test section. The water is moved sinusoidally back and forth over the sand by the positive displacement of tight-fitting pistons. The amplitude a, which can be changed only when the apparatus is at rest, and the period T, which is continually adjustable, can both be selected within wide limits. These limits contain most of the normal prototype range. The test section and the sand bed which fills its lower part are 253 centimeters long and 20.8 centimeters wide, with a normal depth of flow over the (undisturbed) sand bed of 29.8 centimeters. At either end of the test section the flow continues horizontally through smooth-bottomed "spools" for 41 centimeters before beginning its upward curve.

In this study, even the largest ripples were too low to reveal any flattening of their crests by the presence of the top of the test section. Thus, it is assumed that effects of the top were generally negligible. Possible effects of the sidewalls on three-dimensional bed forms are discussed in Section VII,4.

Because of the probable significance of "end effects," the geometry of the ends of the test section and of the sand bed deserves special attention. A drawing of a longitudinal section through one of the spools and the adjacent end of the test section is shown in Figure 6. The sand bed is bounded by a curved ramp, of 10.2 centimeters (4 inches) radius, which is flush with the floor of the spool. This curvature reduces local scour. Once disturbed, the sand surface might end either against the curved ramp or at some point on the floor of the spool, possibly even reaching the nearer screen. This screen is 31 centimeters from the crest of the ramp and has openings of 0.15 millimeters; the farther screen at the back of the spool has openings of 0.25 millimeters. The first screen serves to contain the sand while both together act to make the oncoming flow more nearly uniform. To inhibit premature grain motion and scour at the ends of the sand bed the flow velocity near the ends was lowered relative to that over the major part of the bed by placing a scow-shaped constriction against the top of the tank. This constriction, which was made of Lucite, with a maximum thickness of 4.6 centimeters, reduced the depth of flow over the level of the undisturbed sand bed to 25.2 centimeters. Its shape is shown in Figure 6. The curved transition at either end of the scow extends for 32 centimeters.

To define conditions for the initiation of grain motion or for spontaneous ripples on a flat bed requires that the surface itself be first well defined. To this end a special device leveled the submerged bed while giving it a nearly constant and repeatable degree of compaction. This was a scraper held in a motor-driven carriage which ran along a track and the tops of the tank walls with the top of the tank removed.

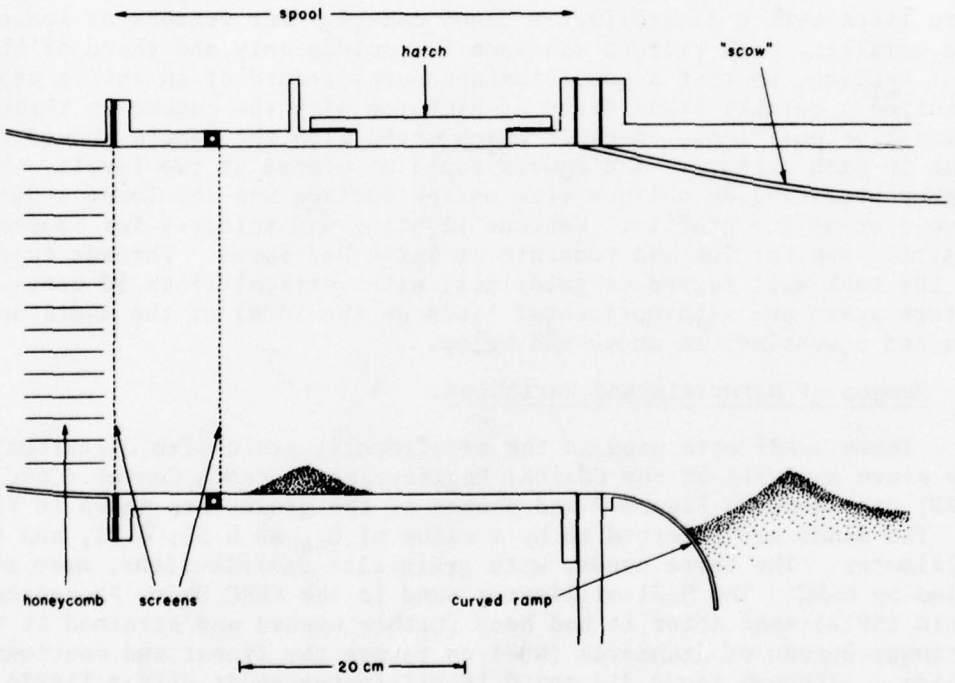

Figure 6. Longitudinal section through spool and the adjacent end of the test section.

The speed of the carriage held fairly steady between 2 and 3 centimeters per second and on the final pass a "standard" accumulation of sand, about 2 centimeters high, was pushed along by the scraper. Flexible plastic "wings" attached to the sides of the scraper pressed against the channel walls and removed any "meniscus" of sand. The motor-driven scraper could not reach within 3 or 4 centimeters of the ends of the bed and these areas were leveled afterward by a hand-operated scraper held against the floors of the spools.

Pictures of the surface of the sand bed and of ripple profiles were taken with a 35-millimeter Canon camera. For reasons of space and parallax, each picture was made to include only one third of the test section, so that a quasi-instantaneous record of an entire profile required a quickly taken triad of pictures with the camera in three successive positions. A clock which moved with the camera showed the time in each picture. The camera could be placed at two levels, the higher providing an oblique view of the surface and the lower a direct side view of the profile. Various lighting was selected for camera position and for low and moderate or large bed forms. Threads taped to the tank wall served as gridlines, with vertical lines 10 centimeters apart and with horizontal lines at the level of the undisturbed bed and 5 centimeters above and below.

2. Ranges of Materials and Variables.

Three sands were used in the experiments; grain-size distributions (by sieve analysis at the Coastal Engineering Research Center (CERC) in 1977) are shown in Figure 7 and photos of the grains are shown in Figure 8. The sands are referred to by a value of D_{50} as 0.55, 0.21, and 0.18 millimeter. The three sands, with grain-size distributions, were supplied by CERC. The 0.21-millimeter sand is the CERC Shore Processes Test Basin (SPTB) sand after it had been further washed and strained at the National Bureau of Standards (NBS) to remove the finest and coarsest grains. Although the 0.21- and 0.18-millimeter sands differ little in average grain diameters, the distribution of the 0.21-millimeter sand is relatively broad and contains grains of a "medium" size. The specific gravities of the three sands (measured at NBS) were found to lie in the range 2.650 ± 0.004, and all have been rounded to 2.65, the usual value for quartz.

In Tables A-1, A-2, and A-3 in Appendix A, the experiments are numbered and listed chronologically with their conditions and with selected observed quantities (one table for each sand). The water temperature remained fairly constant throughout the experiments, with readings all within 4° Celsius and over half within 1° Celsius of the average (21.2° Celsius). Therefore, ν has been regarded as constant (at 10^{-2} centimeter squared per second) and r takes on the constant values: 52.39, 13.25, and 9.81 for the 0.55-, 0.21-, and 0.18-millimeter sands, respectively. The independent variable a is conveniently determined by N, which is simply the number of turns of a nut setting the stroke of the pistons such that,

$$a = 0.4576\ N \text{ centimeters} . \qquad (15)$$

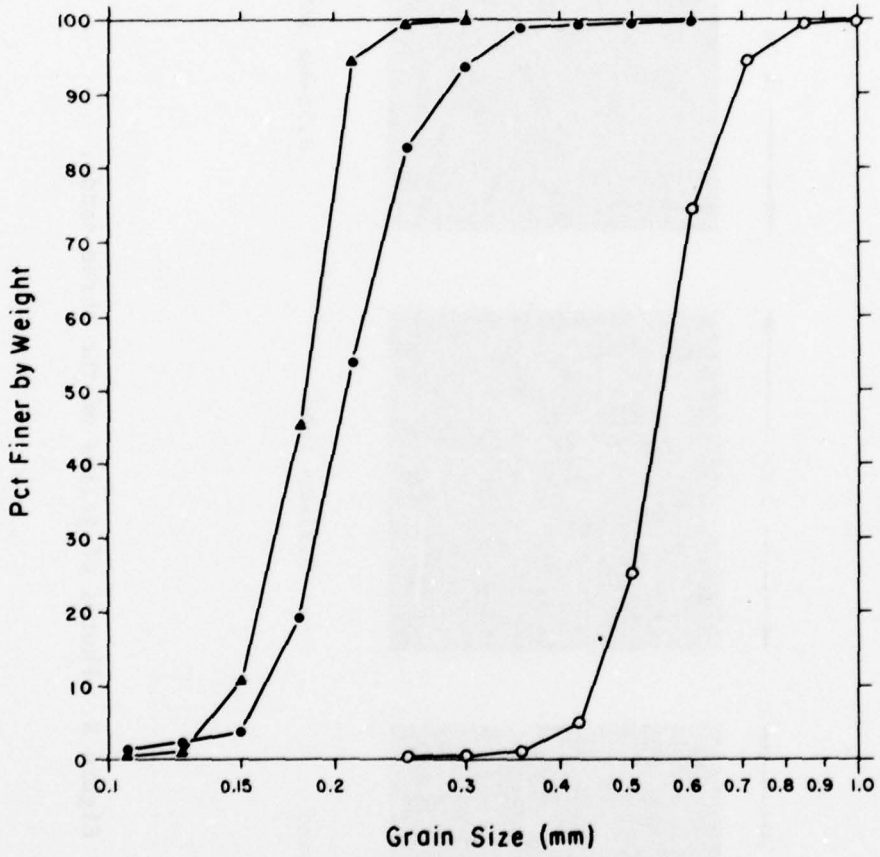

Figure 7. Grain-size distributions for the three sands.

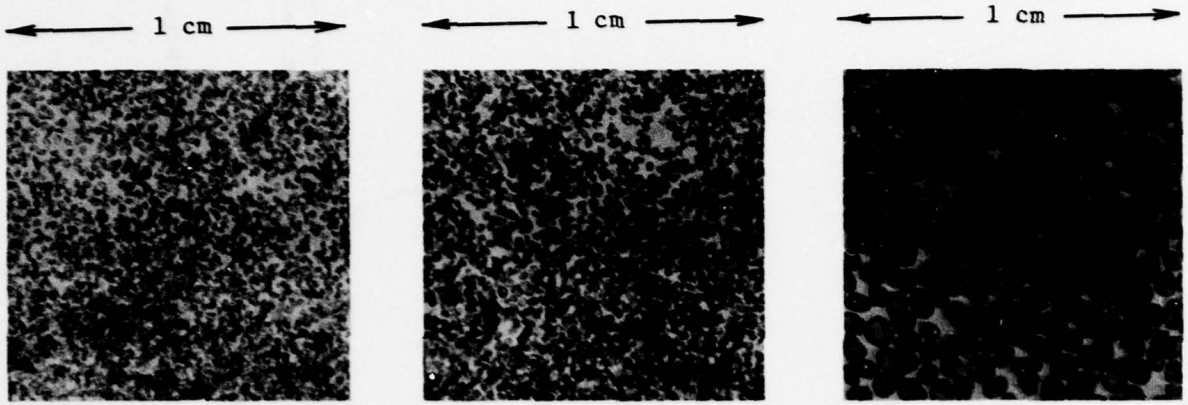

Figure 8. Photos of grains of the three sands.

The period T, when not independently chosen, is denoted T_c or T_r, for conditions of initiation of grain motion or of spontaneous ripple formation. The maximum horizontal velocity is simply

$$U = \frac{2\pi a}{T} \tag{16}$$

and ϕ is given by equation (1). The tables in Appendix A include observed values of ripple length and height which are discussed in Sections IV,4 and V,3. The chronological sequence of the experiments in the tables is emphasized because the final bed form of one experiment was often the initial bed form of the next, and because in a known sequence of combinations of a and T the return to an earlier combination permits observation of any hysteresis. The duration of each experiment is given to help assess the steadiness of final conditions. Experiments with smaller ϕ and less intense sand motion tend naturally to be longer. In a few cases steady conditions were probably not attained.

Appendix A shows that the ranges of a, T, and U were:

$$9.15 \text{ centimeters} < a < 45.8 \text{ centimeters}$$

$$1.60 \text{ seconds} < T < 16.0 \text{ seconds}$$

$$18.0 \text{ centimeters per second} < U < 77.1 \text{ centimeters per second}$$

The upper limit on U was found necessary to forestall damage to the screens by the flow forces which increased rapidly as the screens became clogged by sand carried in suspension.

Table 1 contains symbols for the experiments which show their values of D and N, and, hence, a/D. Increasing a/D is shown by a clockwise progression of a flag on each symbol.

In Figures 9, 10, and 11 (one for each sand) N has been plotted against T with the number of each experiment. An asterisk denotes an experiment with the bed initially leveled. These plots serve to clarify the range and sequence of the experiments. On these logarithmic plots, lines of constant U have a slope of plus one, and two such lines, for values of U encompassing all the points, are drawn on each plot. Curves show the observed T_c as function of a. It should be remembered that, except when T is T_c or T_r, Figures 9, 10, and 11 merely display a pattern of independent variables.

Table 1. Symbols used to denote combinations of D and N. The third independent variable, T, is not denoted.

N, identification	D = 0.55 mm		D = 0.18 mm		D = 0.21 mm	
	a/D	symbol	a/D	symbol	a/D	symbol
20			508	◀		
25			636	▶	545	●
26	216	⊖				
30	250	⊖	763	◀	653	●
33	275	⊖				
40	333	⊖	1017	▼	872	●
50	416	⊖	1271	▶		
52	433	⊖				
60	500	⊖	1525	◀	1307	●
80	666	⊖			1743	●
100	832	⊖	2542	▲		
compressed surface	500	□ ⊟				
expts. 37-47	various	◇				

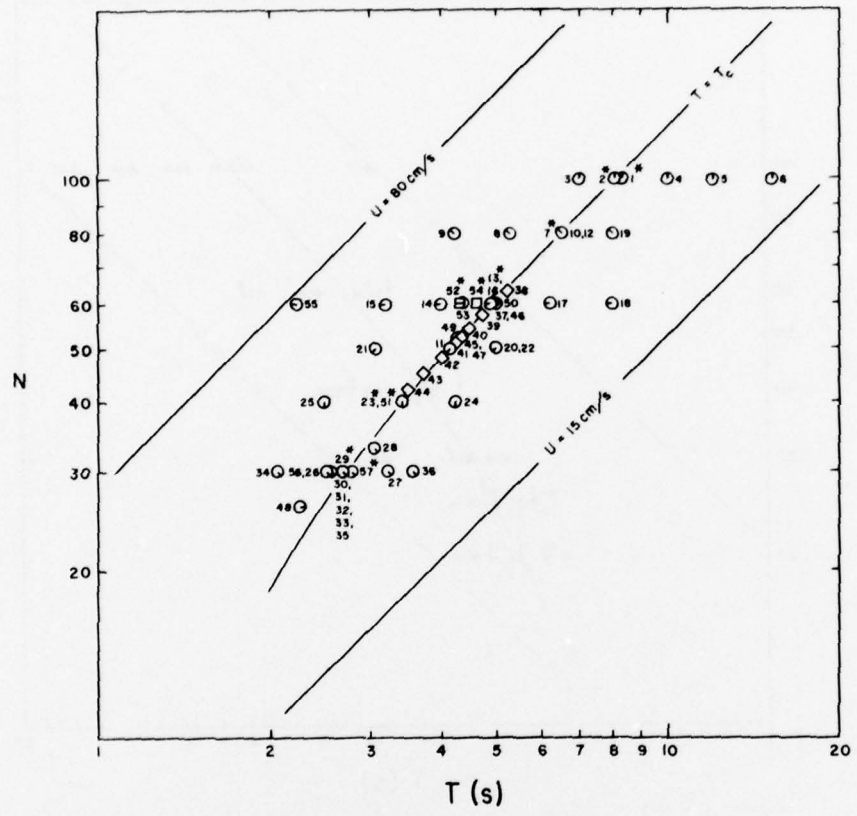

Figure 9. Distribution of N and T for experiments 1 to 57 with the 0.55-millimeter sand. Asterisks denote experiments with the bed initially leveled. Symbols are defined in Table 1. (a = 0.4576 N centimeters.)

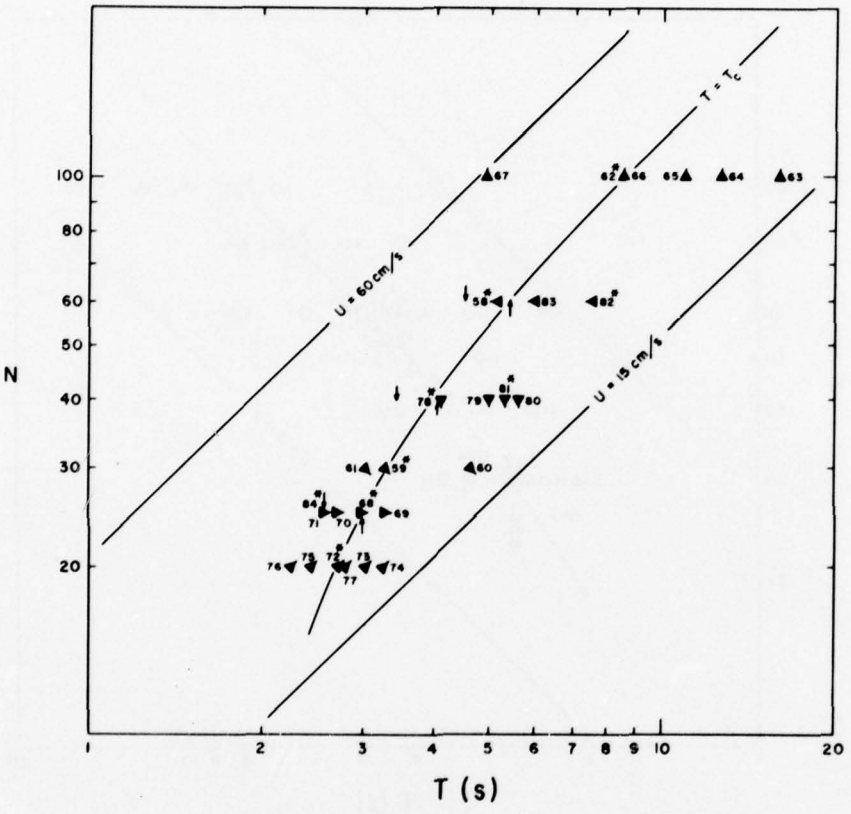

Figure 10. Distribution of N and T for experiments 58 to 84 with the 0.18-millimeter sand. Asterisks denote experiments with the bed initially leveled. Symbols are defined in Table 1. Arrows point downward to observations of T_r and upward to supplementary observations of T_c. (a = 0.4576 N centimeters.)

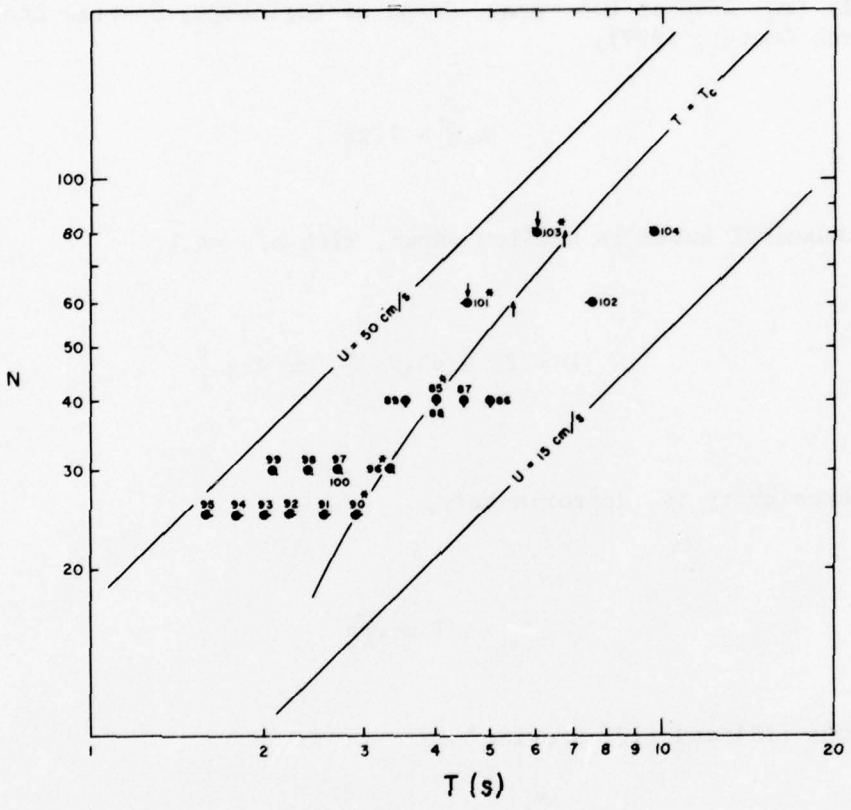

Figure 11. Distribution of N and T for experiments 84 to 104 with the 0.21-millimeter sand. Asterisks denote experiments with the bed initially leveled. Symbols are defined in Table 1. Arrows point downward to observations of T_r and upward to supplementary observations of T_c. (a ≈ 0.4576 N centimeters.)

3. Referral to Prototype Conditions.

Sinusoidal flow at values of a, T selected in the laboratory is approximated at the seabed under various combinations of wave height (H) and length (L) and depth of water (h), providing that the waves do not break. The condition that shallow-water waves be nonbreaking is, approximately (eq. 2-90 in U.S. Army, Corps of Engineers, Coastal Engineering Research Center, 1977),

$$h/H > 1.28 \ . \tag{17}$$

For sinusoidal waves in shallow water, with $h/L << 1$,

$$H = 2a \sinh\left(2\pi \frac{h}{L}\right) \simeq 4\pi a \frac{h}{L} \tag{18}$$

and the celerity is, approximately,

$$L/T \simeq \sqrt{gh} \ . \tag{19}$$

Equations (18) and (19) provide

$$h/H \simeq \frac{\sqrt{gh}\ T}{4\pi\ a}$$

so that, with equation (17), for nonbreaking waves,

$$\sqrt{gh} \gtrsim (2.56)\ 2\pi \frac{a}{T} = 2.56\ U \ . \tag{20}$$

With U less than 77.1 centimeters per second, as in these experiments, any value of h greater than 40 centimeters ensures nonbreaking waves.

III. INITIATION OF GRAIN MOTION

1. Determination of the Condition.

The 24 experiments starting with a leveled bed yielded 24 observations of the initiation of grain motion, the first stage in the development of ripples. These observations, as do others of the type in the literature, have a somewhat subjective character. Determination of the condition of incipient motion is a perception of some combination of the number of grains moving and how far they move. As U is increased slowly and steadily, eventually a few sand grains are seen to rock or tumble from their nests, twice each period, presumably near times of maximum stress. As U continues to increase, grain motion intensifies, more or less steadily, until all the surface grains are in motion. Between these stages U typically increases around 20 to 40 percent. The determination of "incipient motion" is made somewhere in this range, and is seldom further defined. Manohar (1955) identifies conditions of "initial" and "general" grain motion, in laminar and turbulent boundary layers, separated by increments in U of about 13 and 10 percent. Carstens, Neilson, and Altinbilek (1969) identify incipient motion with the motion of 10 percent of the surface grains. In this study, incipient motion is defined by the motion of from 10 to 20 grains per square centimeter combined with a perception of rapid intensification of grain motion with increasing U. Since moving grains dislodge other grains and set them in motion and may progressively loosen the surface, a long slow rate of increase in U may produce a greater intensity of grain motion, at a given U, than does a short quick rate. Possibilities for personal bias are obvious, and may produce significant differences between observers. However, the observations of a single observer following set procedures should be repeatable enough to reveal trends.

2. Effects of Surface Compression.

A different, impersonal, possible source of scatter in observations of incipient motion is the degree of compaction of the surface grains. Experiments 52 and 54 with the 0.55-millimeter sand (Table A-1) were designed to test this effect. A tamper 13 by 32 centimeters, was fixed to a rigid frame such that with the frame resting on the tops of the channel walls the tamper rested on the sand bed surface as usually leveled. Before each of the two compression experiments, the scraper of the leveler was elevated a small distance, δ, which left the surface of the sand bed δ above its usual level. The tamper was then carefully placed upon the submerged leveled sand surface leaving a gap δ between its frame and the tops of the channel walls. Forcing the frame down to make contact pressed the sand surface down a distance δ and so defined a compaction of the surface grains. Since the tamper was small,

this procedure had to be repeated about 20 times to compress the bed for one experiment. The edge of the tamper, where it touched the walls of the tank, was made square, while the other three edges were tapered and rounded to provide smooth overlaps. In experiments 52 and 54, δ was 1.51 and 0.83 millimeters, respectively. The pressures needed for these compressions were considerable, requiring in the first case the full weight of a man standing on the tamper frame. Resulting increases in U_c over the U_c for the usual uncompressed bed, represented by experiment 13, are 6.1 percent for δ = 0.83 millimeters and 12.9 percent for δ = 1.51 millimeters (Table A-1). Considering the severity of the compressions, these associated increases in U_c seem small and suggest that compression effects are generally unimportant.

3. Results for the Three Sands.

The 24 observations of the initiation of grain motion are shown in Figure 12, where ϕ_c is plotted against a/D and r, as in equation (3). The figure shows that the data fall along separate curves for each sand (value of r) with points for the two compressed surfaces falling above the curve for the 0.55-millimeter sand. For comparison with previous observations, the composite curve in Figure 2 has been transcribed. The trends of the data have curvatures opposed to that of the transcribed composite. Also, it is seen that the present data lie somewhat above the composite though not outside the range of earlier data (Fig. 2). Much of the apparent discrepancies probably stem from personal bias as described in Section III,1.

4. Applicability of a Shields Criterion.

Madsen and Grant (1975; 1976) have stated that a Shields criterion proven useful in unidirectional flow can also be applied in oscillatory flow. By this criterion, grain motion begins when the bottom stress reaches a critical value, τ_c, satisfying

$$\Psi \equiv \frac{\tau_c}{g(\rho_s-\rho)D} = \Psi\left(\sqrt{\frac{\tau_c}{\rho}}\,\frac{D}{\nu}\right) \tag{21}$$

where the function Ψ, first sketched by Shields (1936), is fairly constant over much of its useful range. As pointed out by Madsen and Grant (1976),

$$\sqrt{\frac{\tau_c}{\rho}}\,\frac{D}{\nu} \equiv r\Psi^{\frac{1}{2}} \tag{22}$$

so that Ψ can be replotted more conveniently as function of r alone.

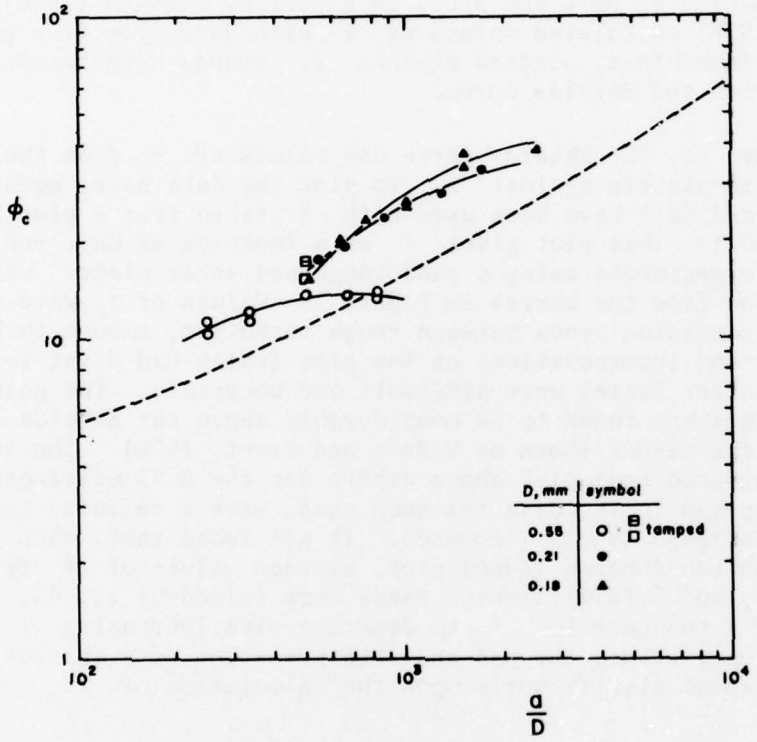

Figure 12. Observed ϕ_c as a function of a/D and r (or D). The dashline is the composite curve from Figure 2.

Using the friction factor

$$f = \frac{2\tau}{\rho U^2} \tag{23}$$

given as function of Ua/ν and a/D_{50} in a plot by Jonsson (1966), Madsen and Grant (1976) calculated values of Ψ with data from five previous studies and found that, plotted against r, trends were reasonably compatible with the Shields curve.

In Figure 13, the Shields curve and values of Ψ from the data in this study are plotted against r. To plot the data here, equations (21), (22), and (23) have been used with f taken from a plot by Kamphuis (1975). That plot gives f as a function of Ua/ν and a/D_{90} from recent experiments using a sand-roughened shear plate. Values of D_{90} were taken from the curves in Figure 7. Values of τ_c were found to lie in the transition zones between rough turbulent, smooth turbulent and laminar, and interpolations on the plot (which had first to be redrawn on a larger scale) were difficult and uncertain. The points for the three sands are found to be considerably above the Shields curve (as most of the trends shown by Madsen and Grant, 1976). The two points for the compressed beds plot above others for the 0.55-millimeter sand. There is a spread in the data for each sand, with a definite tendency for Ψ to decrease as T increases. It was found that, when recalculated with f from the Jonsson (1966) plot, average values of Ψ for the 0.55-, 0.21-, and 0.18-millimeter sands were raised by 25, 45, and 41 percent, and a tendency for Ψ to decrease with increasing T was no longer apparent. Thus, the use and interpretation of a Shields criterion appears to depend significantly upon the calculation of f.

Carstens, Neilson, and Altinbilek (1969) have offered a semi-empirical derivation of a $\Psi(r)$ based on the concept of a critical velocity u_c at some elevation in the boundary layer such that the relevant force on a surface grain is proportional to $D^2\rho u_c^2$ times a (free fall) drag coefficient which is a given function of $u_c D/\nu$. From three observations (Fig. 2 in this study) they found that u_c is best evaluated at an elevation 0.6 D where, for laminar (thick) and turbulent (thin) boundary layers, u_c is taken to be $0.6\, D\tau_c/\rho\nu$ and $7.22\sqrt{\tau_c/\rho}$. On this basis, Carstens, Neilson, and Albinbilek (1969) derive the curves for Ψ shown in Figure 21 of their study and again in Figure 13 of this study. (Their equation 39 is clearly in error, but the curve so labeled in their Figure 21 was computed correctly.) Their curve for $\Psi(r)$, which remains undefined in a transition zone between its two branches, fits the finer sands of this study rather well (Fig. 13). This is not surprising in view of the agreement between values of ϕ_c from Carstens, Neilson, and Altinbilek (1969) and from this study (Figs. 2 and 12).

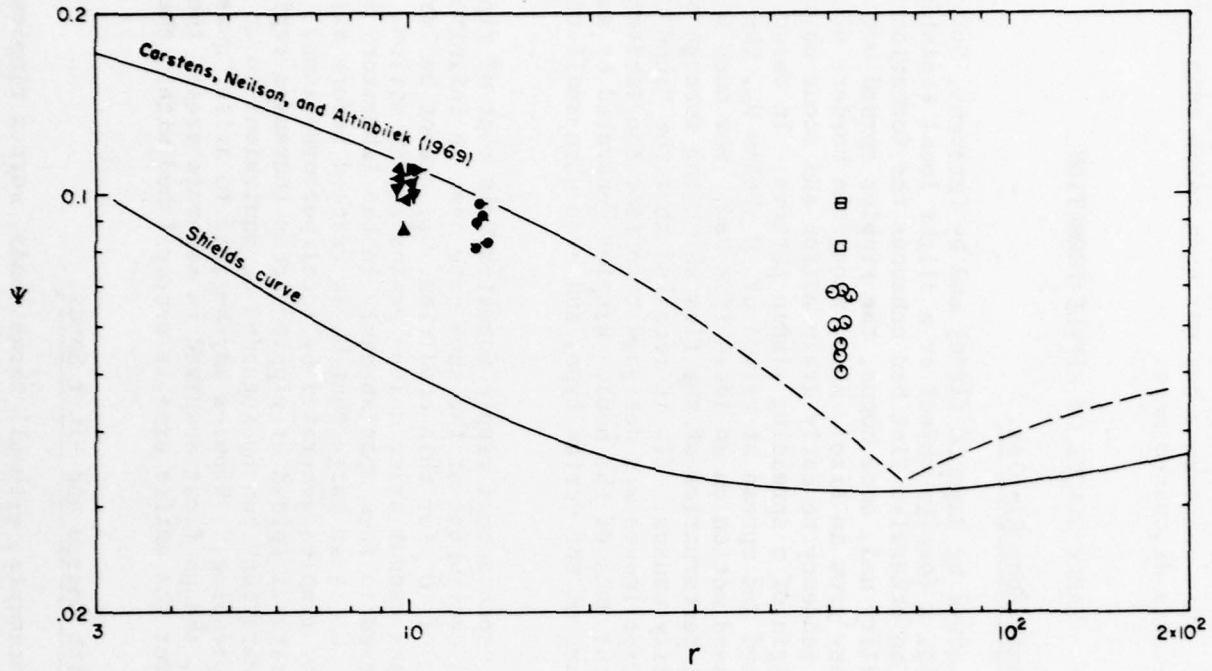

Figure 13. Comparison of Ψ computed from the data of this study with Shields curve for steady flow and a modified curve of Carstens, Neilson, and Altinbilek (1969). Symbols are defined in Table 1.

It appears reasonable that some further modification of the Shields criterion might make it more precise in oscillatory flow. Shields (1936) interpreted the factor $\nu\sqrt{\rho/\tau_c}$ occurring in the abscissa of his plot of Ψ as a measure of the thickness of the boundary layer. In oscillatory flow, the boundary layer thickness is dependent, in part, on the period. This dependence has not been taken into account by either of the criteria discussed here.

IV. EARLY STAGES OF RIPPLE FORMATION

1. Induced and Spontaneous Ripples.

As has been observed by Bagnold (1946) and by Carstens, Neilson, and Altinbilek (1969), a foreign object or a slight local elevation of the sand surface on an otherwise flat bed enhances the formation of ripples in that locality and, once begun, the ripples spread out over the surface while they grow in size. Also, along the borders of a sand bed there is a tendency to early grain motion and scour which then becomes the origin of a spreading ripple pattern. In these ways ripples can be started and spread at values of U below U_c, the value needed to initiate sand motion on an ideal flat bed. How much below depends on the local perturbation of the flow which the foreign object or surface irregularity causes. (It is recalled that the "scow" constriction in these experiments was designed to offset the tendency to premature scour at the ends of the bed). Ripples generated by such local disturbances are of the vortex type, and even when small they have sharp crests.

The concept of "spontaneous ripple formation" is that of ripples arising suddenly and everywhere at the same rate over an infinite flat bed. The value of U for this condition, U_r, cannot be less than U_c, since ripples cannot arise unless grains are in motion. Ripples can be observed to form spontaneously in the laboratory if the rate of increase of U is so large that U_r is reached before all of the bed is overrun by ripples generated by local perturbations. As U approaches U_r, the rate of spread of rippled areas increases rapidly, and "spontaneous generation" can be regarded as equivalent to an "infinite rate of spreading." Ripples may be said to arise "quasi-spontaneously" when, though first observed in separate areas, their subsequent spread over the entire area is accomplished within the time of a few periods.

2. Observations with Coarse and Finer Sands.

In all the experiments, with all three sands, vortex ripples were found to begin, either quasi-spontaneously or at some point on the boundary, at values of U near to or somewhat below U_c. Thus, in most experiments with a previously leveled bed, ripple development was

allowed to proceed with U left equal to U_c, though in a few cases U was increased to establish U_r. Early ripple development with the 0.18- and 0.21-millimeter sands differed somewhat from that with the 0.55-millimeter sand.

With the 0.55-millimeter sand, the scow proved effective and the ends of the bed were the last areas to become rippled. At $U \approx U_c$, ripples formed either spontaneously or first along the walls. Slight increases in U beyond U_c, made in experiments 2, 29, and 57, were found to cause the rate of spreading to increase rapidly. The difference between U_r and U_c appeared to be very slight, probably less than 5 percent and within the uncertainty of U_c itself. No ripples resembling the rolling-grain type described by Bagnold (1946) were observed to form in advance of the spreading vortex ripples.

With the 0.18- and 0.21-millimeter sands, the scow was ineffective, and the vortex ripples originated along the end of the sand bed at the top of the curved ramps and particularly near the wall in one corner; presumably, this was due to an irregularity. Conditions for spontaneous ripples and initiation of grain motion were distinct, and in three experiments (81, 82, and 84) with the 0.18-millimeter sand and in two experiments (101 and 103) with the 0.21-millimeter sand, U was increased beyond U_c to determine U_r. Average ratios of U_r/U_c were 1.182 with the 0.18-millimeter sand and 1.156 with the 0.21-millimeter sand. These ratios are fairly close to the 1.16 found by Carstens, Neilson, and Albinbilek (1969), and much less than the factor of about 2 cited by Bagnold (1946).

3. Rolling-Grain Ripples.

With the 0.18- and 0.21-millimeter sands, unlike with the 0.55-millimeter sand, a distinct bed form resembling the rolling-grain ripples of Bagnold (1946) did appear. At $U = U_c$, soon after grain motion began, rolling grains associated in bands normal to the flow. These bands were not very straight; the length along their crests and the spacing between them were rather uneven, and they tended to be distributed in irregular patches over the sand bed. Their overall appearance was more like a "rash" than a regular ripple pattern (see Fig. 14). The figure shows the irregular bands covering the left half of the bed while vortex ripples are advancing from the right. These bands were quite stable and, even as U was increased above U_c, showed little tendency to become more regular, or to intensify or spread. Surprisingly, the rolling-grain bands were observed to take no part in vortex ripple formation. A band more than a few ripple lengths ahead of an advancing pattern of vortex ripples would never independently grow into a vortex crest and would remain unaffected by the advancing pattern until the foremost crest had approached within a ripple length or two. At this point the band would aline itself to merge with the crest. This passive behavior is quite different from the more active role described by Bagnold (1946) and Manohar (1955), and it might be doubted that the bands of this study are rolling-grain ripples as

Figure 14. Rolling-grain ripples (left) and vortex ripples (right).
The three photos cover the entire test section in experiment 59.

defined by Bagnold. However, the similarity of the photos in Figure 14 and in Figure 7 of Bagnold (1946) make the identity clear.

4. Initial Ripple Length.

The length of the vortex ripples at about the time they had spread over most of the bed was measured from the photographic record. Such ripples are shown in Appendix B which contains photos of the initial and final ripples in all 24 experiments started with a leveled bed. This initial ripple length is an approximate average value, because the ripples leading the advance are smaller than the older ripples nearer the point of origin of the train, and because three-dimensional areas were excluded from the averaging. The initial ripple length (λ_i) is shown in Figure 15 in the form of λ_i/D plotted against a/D. For each sand, values of λ_i are remarkably independent of a. Average values of λ_i for the 0.18-, 0.21-, and 0.55-millimeter sands are 4.5, 5.4, and 8.5 centimeters respectively.

V. GROWTH AND VARIABILITY OF EQUILIBRIUM RIPPLES

1. Two- and Three-Dimensional Forms.

As mentioned earlier, in the experiments with previously leveled beds, ripple development was left to proceed at $U = U_c$ or, in a few cases, at $U = U_r$. Although the small initial ripples were always two dimensional, further growth involved the suppression and coalescing of crests which often occurred first near a channel wall. That is, during growth the bed form became to some degree three dimensional. With the 0.55-millimeter sand this degree was relatively small and as the ripples approached equilibrium dimensions they became and remained two dimensional. This pattern of growth, with a transitory three-dimensional phase, is illustrated in Figure 16 by a sequence of photos from experiment 51. Two-dimensional growth involves a reduction in the number of crests per unit length of the profile. This can result from a spreading of the profile into unrippled areas or, in these experiments, into the spools. When further spreading is blocked, some crests shrink and disappear. Typically, as a crest disappears, its neighbors move toward it and it is replaced by a new trough. Less often, two neighboring crests approach each other and merge into a single crest. Growth need not begin from a leveled bed, and occurs more generally in response to an increase in a. Also, when a is reduced, the process just described is reversed, new crests arise, and λ shrinks. Two-dimensional processes of shrinkage and growth are shown in Figures 17 and 18 by sequences of photos from experiments 48 and 49. These record the successive responses of a profile when, first, the amplitude was reduced by one-half and then doubled to its original value. In these two experiments, the profiles were contained between rigid end crests, as described in Section V,5.

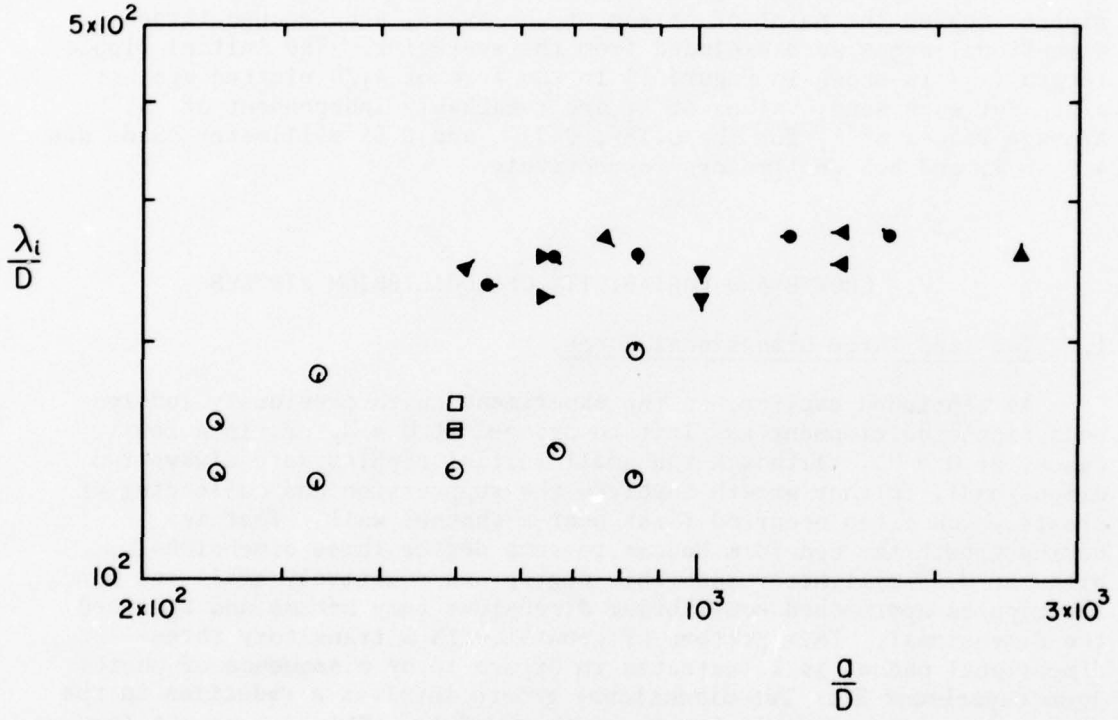

Figure 15. Initial ripple length, independent of a. Symbols are defined in Table 1.

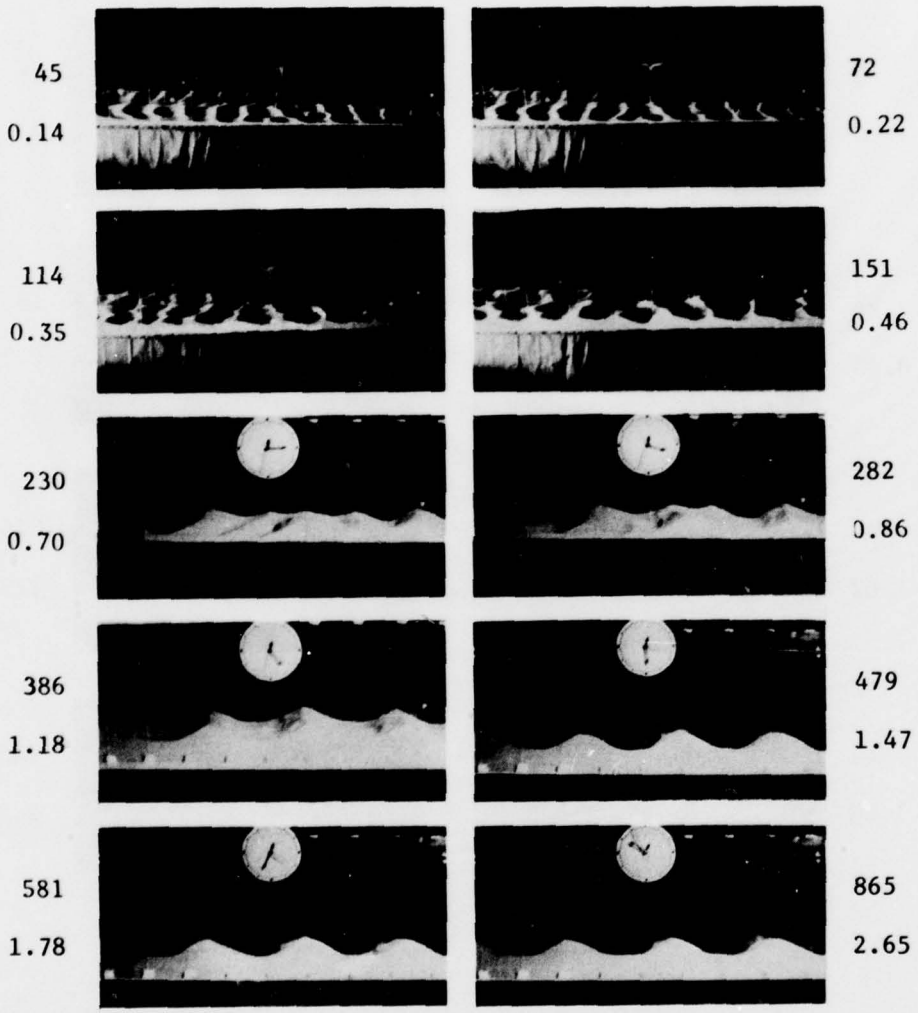

Figure 16. A three-dimensional phase during growth (the mid-third of test section in experiment 51). Upper and lower numbers by each photo give n and (D/a)n, where n is the number of cycles since the start of ripple growth.

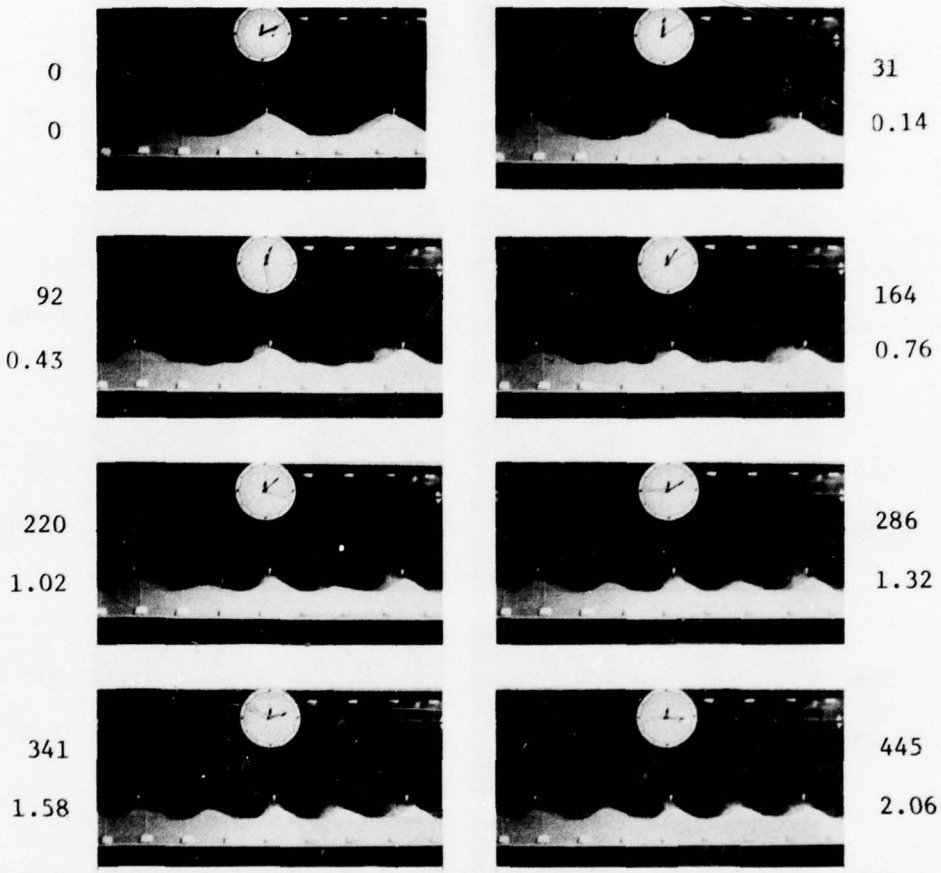

Figure 17. Response of a bed form to a reduction in a (the mid-third of test section in experiment 48). Here N = 26, following experiment 47 where N = 52. Upper and lower numbers by each photo give N and (D/a)n, where n is the number of cycles since the beginning of the experiment.

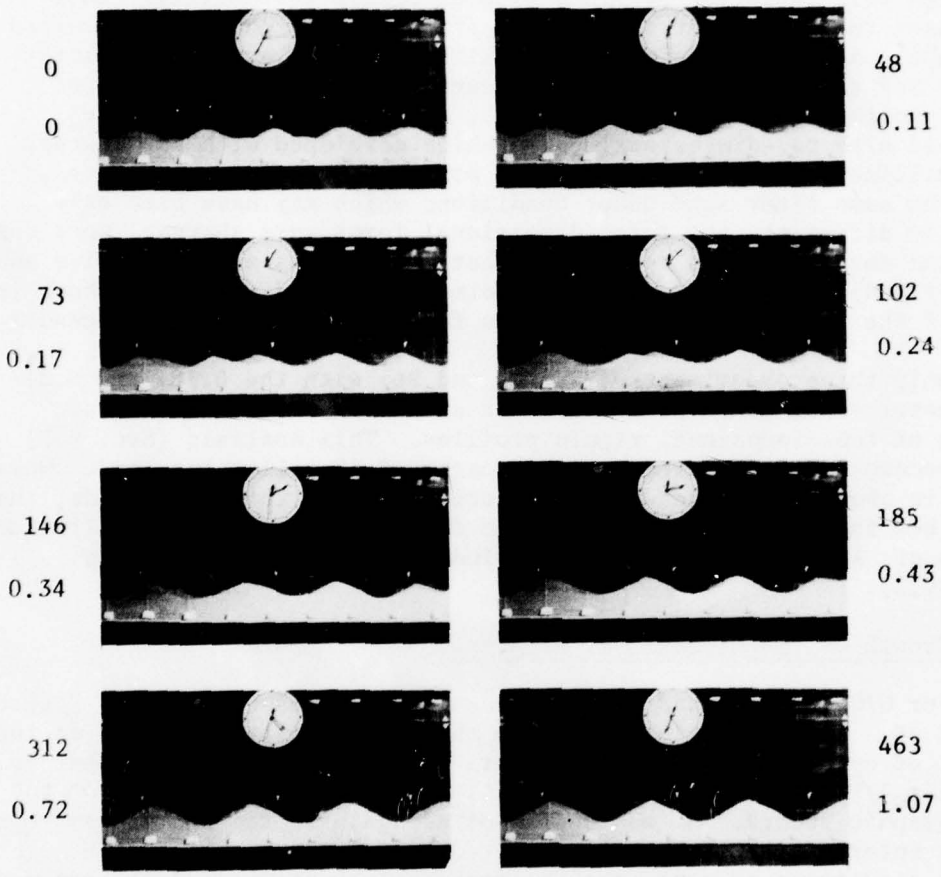

Figure 18. Response of a bed form to an increase in a (the mid-third of test section in experiment 49). Here N = 52, following experiment 48 where N = 26. Upper and lower numbers by each photo give n and (D/a)n, where n is the number of cycles since the beginning of the experiment.

With the 0.18- and 0.21-millimeter sands, the degree of three dimensionality during growth was relatively large and in many cases, the bed forms remained more or less three dimensional even when fully developed. Sometimes with these finer sands a profile, or a part of it, would evolve through two- and three-dimensional phases and on occasion this evolution seemed a type of cyclic instability. In a few cases the attainment of a steady state and its character remained in doubt. Although attaining an equilibrium as to average characteristics and an unchanging overall appearance, three-dimensional bed forms, unlike two-dimensional ripples, never became static. When compared with two-dimensional forms which developed with the coarser 0.55-millimeter sand under otherwise similar conditions or, indeed, with the same finer sand under conditions which may have been only slightly different, the three-dimensional forms were sharper, more complex and smaller (it is recognized that these terms are subjective and ill defined). Characteristic three-dimensional bed forms are shown in most of the photos of final bed forms for the finer sands in Appendix B.

Only three experiments (72, 90, and 96) with the 0.18- and 0.21-millimeter sands could be included in an analysis of the rates of growth of two-dimensional ripple profiles. This analysis (Sec. V,2) thus becomes almost limited to the coarser 0.55-millimeter sand. However, in about two-thirds of the experiments with the finer sands, the final bed forms were sufficiently two dimensional to yield equilibrium values of λ and η, which are included in a subsequent analysis (Sec. V,3).

2. Growth of Two-Dimensional Ripples.

For $U/U_c \approx 1$, η/a and λ/a are shown as functions of time in Figures 19 and 20. The time is expressed in the form $(D/a)n$, where n is the number of cycles since the time of origin of the ripples, t_o; that is, $n = (t-t_o)/T$. For each experiment, η, λ, and t were taken from the photographic record. η was then plotted against t, and t_o was read at the intersection of the extrapolated curve and the axis $\eta = 0$. During conditions of rapid growth, measurements of η and λ are made less precise by the partially three-dimensional character of the profiles. However, all the data from the experiments with the 0.55-millimeter sand with untamped beds lie near a single curve, showing that η/a is approximately a function of $(D/a)n$, and that any further dependence upon a/D is relatively minor. Points from the experiments with tamped beds plot somewhat above this curve, and points for the finer sands lie along a separate (dotted) curve. As time increases, these curves approach asymptotes of about $\eta/a = 0.24$ for the 0.55-millimeter sand and $\eta/a = 0.18$ for the finer sands. The difference between these curves indicates a slight effect of grain size or of r. Using the values of t_o and n already determined, λ/a has been plotted as function of $(D/a)n$ in Figure 20. In this case reduction to a single curve is not possible since, unlike η, λ does not become zero at $t = t_o$ (as shown in Fig. 15). Even so, the separate curves for different a/D with the coarse 0.55-millimeter sand appear to approach a single asymptote, of about $\lambda/a = 4/3$

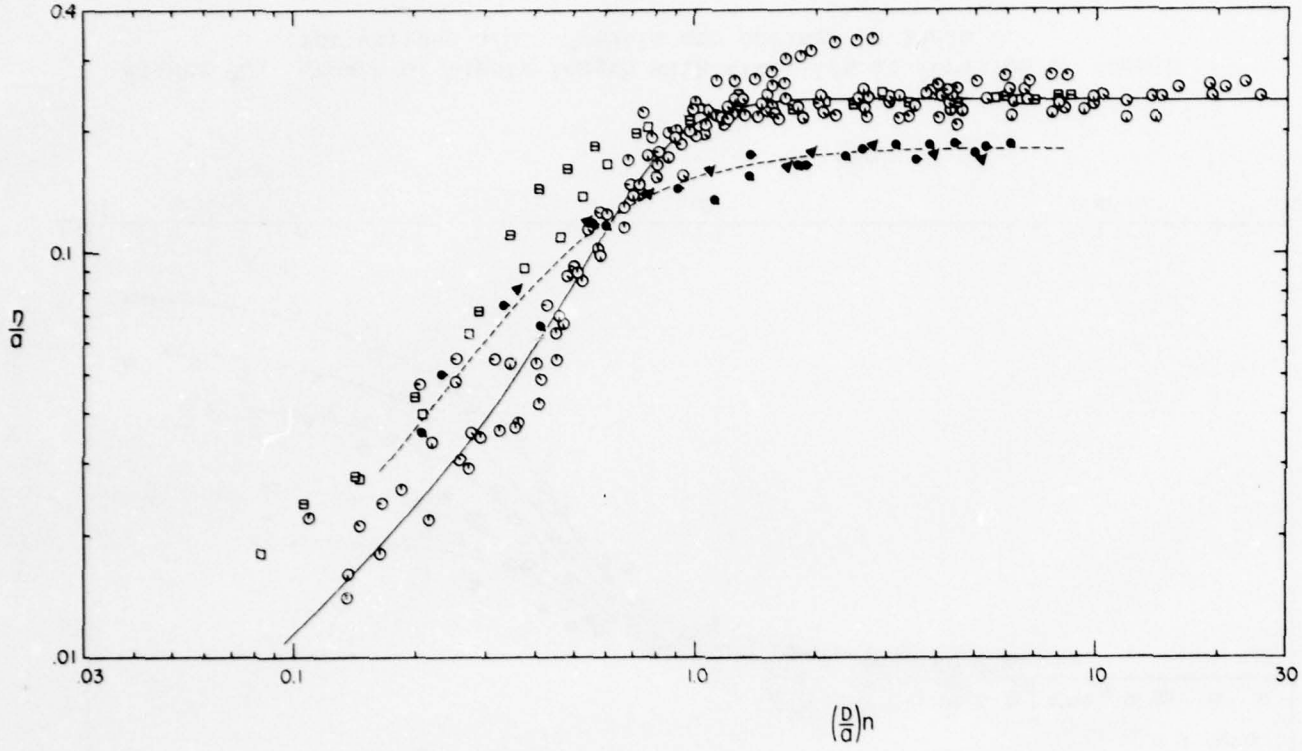

Figure 19. Growth of ripple height with time, η/a as function of (D/a)n. Symbols are defined in Table 1.

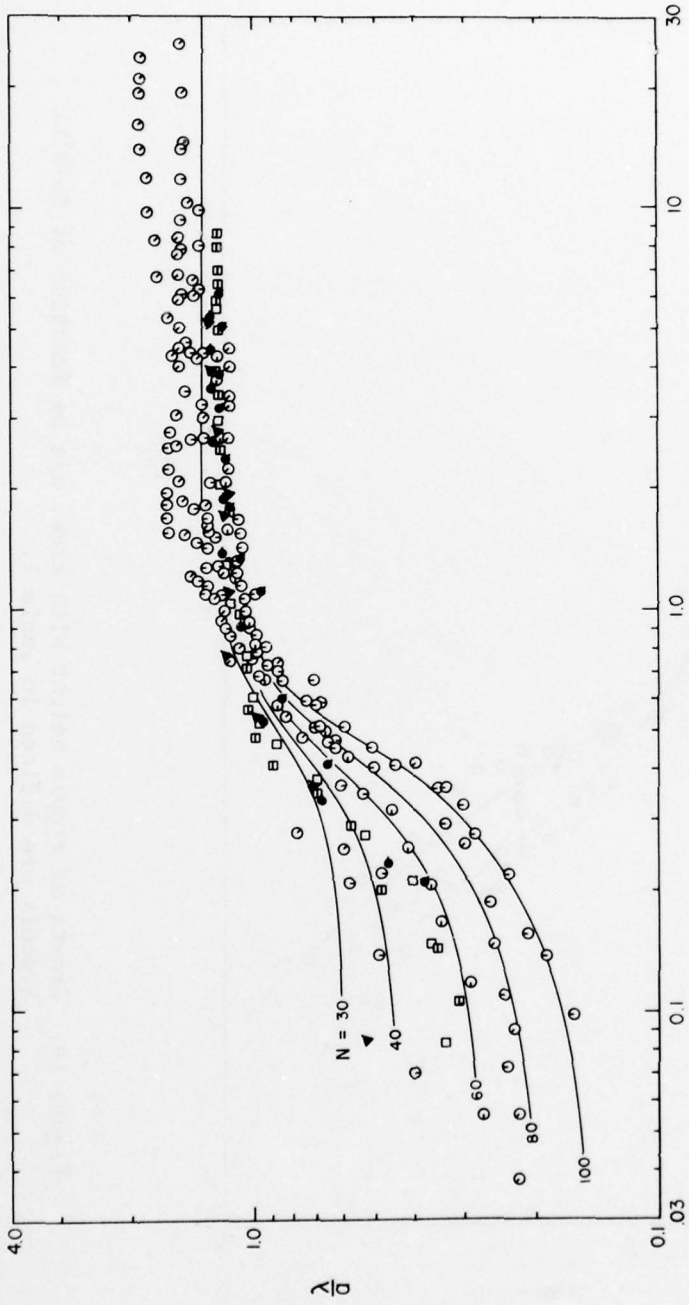

Figure 20. Growth of ripple length with time, λ/a as function of (D/a)n for various a/D. Symbols are defined in Table 1.

as given by equation (9); the curve for the finer sands has a somewhat lower asymptote around $\lambda/a = 1.25$.

The curves show that the growth of both η and λ is fairly complete by the time $(D/a)n$ equals 1. This suggests the simple criterion that, with $U/U_c \approx 1$, the ripples are mature if $n > a/D$. Other stages of ripple growth can be defined in similar terms. Such criteria, which make the time of development proportional to $(a/D)T$, appear to be in conflict with Inman's (1957) comment that ripples in fine sand are more rapidly modified than ripples in coarse sand. It is not clear under what conditions or restrictions, if any, this comparison applies. In any case, U need not approximate U_c as in Figures 19 and 20. Only three experiments with the finer sands are included in these figures and some further dependence upon grain size (r) may well exist.

Along the asymptotes in Figures 19 and 20, the data show considerable scatter which is largely due to end effects (discussed in Sec. V,4). Sudden and substantial increases in λ and η result when a shrinking crest finally ceases to be counted. These increases result from averaging over the limited number of ripples in the test section and do not imply actual abrupt changes in the profile.

3. Equilibrium Two-Dimensional Ripple Profiles.

Photos of the final equilibrium profiles for all the experiments started from a leveled bed are contained in Appendix B. The two-dimensional profiles differ widely in scale, but are rather similar in shape, with variations of types discussed below. The photos reveal a variety of configurations at the ends of the profiles. The scour sometimes appearing at the curved ramp acting as a persistent trough, may serve to "anchor" the end of the profile.

Final equilibrium values of λ/D are plotted against $2a/D$ in Figure 21. Included in the data are all the experiments with the 0.55-millimeter sand, and 33 experiments with the 0.18- and 0.21-millimeter sands which were sufficiently two dimensional to permit analysis. In this form, the data can be compared directly with the previous observations in Figure 5, by their relation to equation (10) which is the straight line common to both Figures 5 and 21. The data of this study (Fig. 21) follow this line reasonably well, though their trend shows λ/D to increase, nearly, with the three-fourths power of $2a/D$, rather than with the first power. Deviations of the data from equation (10) are not accounted for by the regular and relatively minor effect of ϕ. However, the deviations are within the range of inherent scatter and end effects discussed in Section V,4. Also, values of λ/D falling below the line for the four highest values of $2a/D$ may be the beginning of the trend for λ/a to decline with $2a/D$, which was found in several of the plots in Figure 5, and discussed in Section I,3,d. Here, as

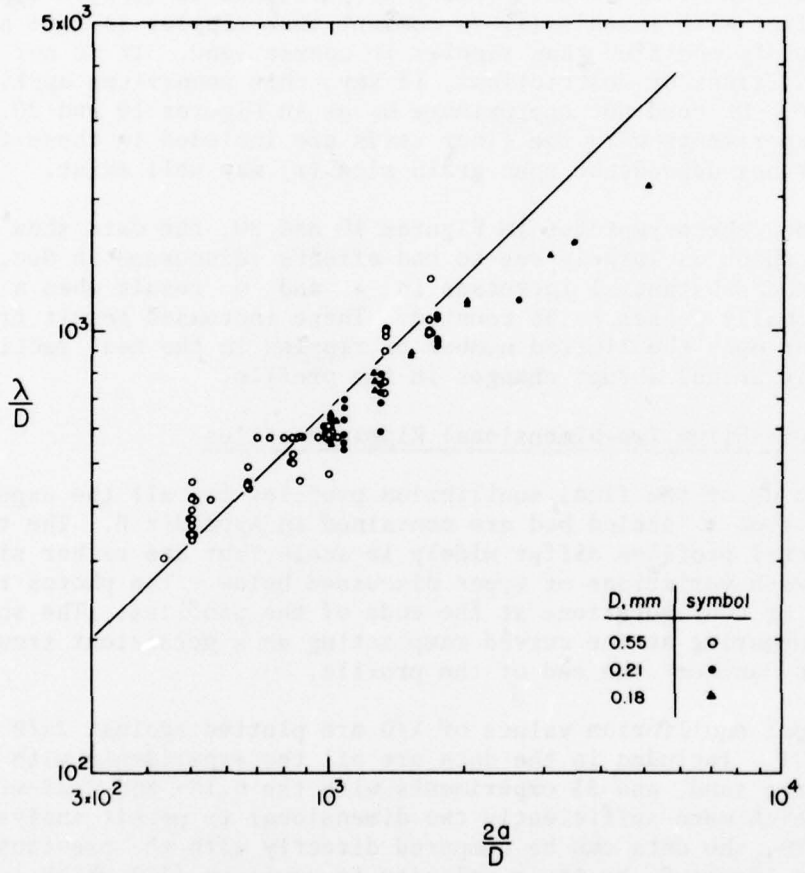

Figure 21. Equilibrium λ/D as function of 2a/D.
The straight line is given by equation (10).

in those cases, sands with small grain sizes are involved. Further, these four experiments were among those with profiles showing some three dimensionality, which is characterized by smaller bed forms, and in two of them (experiments 64 and 82 with the 0.18-millimeter sand) an occasional recurrence of three-dimensional bed forms may have prevented attainment of two-dimensional equilibrium. With these considerations and the previous observations (Fig. 5), the data in this study are regarded as agreeing with equation (10) reasonably well, rather than as indicating a three-fourths power law.

To observe the effects of ϕ, which were not revealed in Figure 21, the same data have been replotted in Figure 22 to give λ/a as function of ϕ. Flags have been added to the plotted symbols to give values of N (or a/D) as shown in Table 1. The curve in Figure 22 is another replot of Figure 17 in Mogridge and Kamphuis (1972). This curve indicates that in the experiments of this study the effect of ϕ upon λ/a remains slight but still dominates that of a/D which equations (8) and (9) show to be negligible.

Final equilibrium values of η/a are plotted against ϕ in Figure 23. Included experiments (with values of ϕ and symbols) are the same as in Figure 22. The curves for constant values of a/D in Figure 23 are a replot of Figure 18 in Mogridge and Kamphuis (1972). In this case, over the range of the data, the effects of varying a/D are noticeable, and separate curves have been drawn. However, the curves form a rather narrow band, and do not serve to reduce the scatter. The data do not follow the curves as closely as in Figure 22, with points for the coarse sand falling above and points for the finer sands falling below. These moderately separate trends indicate a noticeable dependence on r not contained in Figure 18 of Mogridge and Kamphuis (1972).

4. End Effects.

Figures 19 to 23 show a considerable degree of scatter, attributable to variations in the effects of the ends of the channel on the average ripple length. Assuming that the particular geometry of the ends somehow tends to hold crests in certain fixed positions near the ends (as does the local scour before a ramp), two such crests, one at either end of the channel, will be "fixed" a distance S apart. To be stable, the profile between must have an average ripple length $\lambda = S/m$ where m is some integer. There is usually no integer which makes λ equal to λ_n, the "natural" ripple length which, for the given a and T, would form on an unbounded bed. If $\lambda_n > \lambda$ the profile will tend to press the end crests outward or, if $\lambda_n < \lambda$, to pull them inward, increasing or decreasing S, and in either case acting against the end effect tending to hold the crests in place. Thus, the resulting displacement of the crests is limited and leaves λ still unequal to λ_n. Preferably then, the ends should be indifferent to the position of the end crests and, if space had allowed, long gently sloping ramps might have been preferable to the

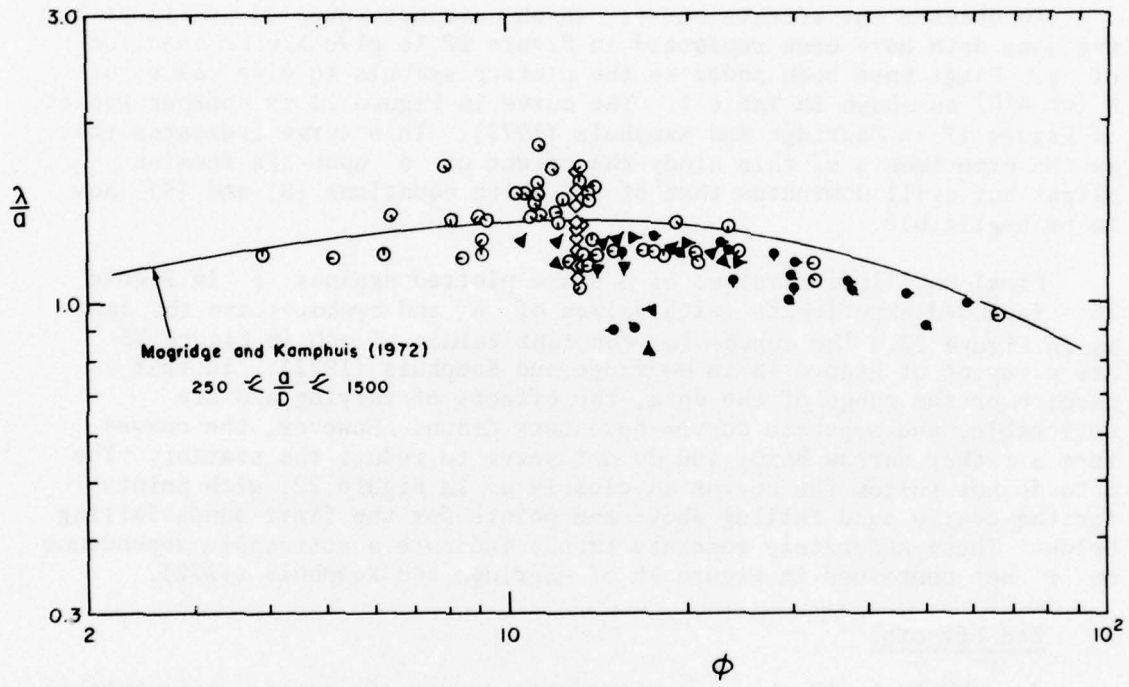

Figure 22. Equilibrium λ/a as function of ϕ. The data are in general agreement with Mogridge and Kamphuis (1972). Symbols are defined in Table 1.

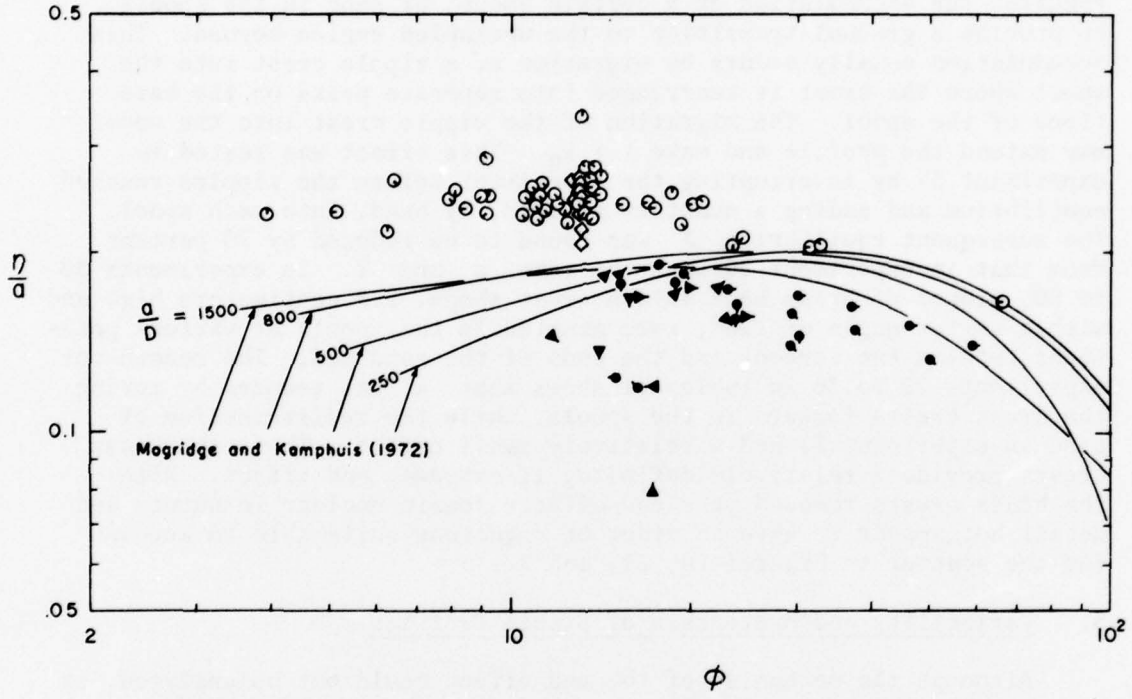

Figure 23. Equilibrium η/a as function of ϕ and a/D. The data indicate an apparent effect of grain size not found in Mogridge and Kamphuis (1972). Symbols are defined in Table 1.

short curved ones actually used (Fig. 6). In present circumstances, not only the ramps with scoured troughs and crestlike summits, but the screens in the spools act to position and hold crests, since the sand which cannot pass through a screen tends to accumulate a short distance in front of the screen, in the form of a crest (Fig. 6). Such crests are liable to move, and cases of cyclic instabilities of sand crests within the spools, with an otherwise stable profile, were observed. Finally, it seems that a stable profile cannot end abruptly, but requires the accumulation of a certain amount of sand in the spools to provide a gradual transition to the unrippled region beyond. This accumulation usually occurs by migration of a ripple crest into the spool where the crest is rearranged into separate peaks on the bare floor of the spool. The migration of the ripple crest into the spool may extend the profile and make $\lambda > \lambda_n$. This effect was tested in experiment 57 by interrupting the experiment before the ripples reached equilibrium and adding a quantity of sand, by hand, into each spool. The subsequent equilibrium λ was found to be reduced by 20 percent from that in experiment 29 with the same a and T. In experiments 30 to 50, pieces of brass bent into a crest shape, 2.8 centimeters high and with a vertex angle of 120°, were mounted in the spools at various positions between the screens and the ends of the sand bed. The record for experiments 29 to 36 in Table A-1 shows that λ was reduced by moving the brass crests forward in the spools, while the redistribution of sand in experiment 31 had a relatively small effect. Thus, the brass crests provide a relatively definite, if extreme, end effect. With the brass crests removed, the end effects remain unclear in nature and detail but appear to have an order of magnitude quite able to account for the scatter in Figures 20, 21, and 22.

5. Variability and Hysteresis of Stable Profiles.

Although the mechanism of the end effect could not be analyzed, it was possible to measure its limits. A series of experiments (37 to 47) with the 0.55-millimeter sand was performed to determine over what range of λ/a a profile could remain stable and how the profile shape varied with λ/a. The brass crests were mounted atop the ramps 254 centimeters apart with seven sand crests between. Since the brass crests fixed the ends of the profile, the average ripple length, λ, remained constant in this series (equal to 254/8 = 31.8 centimeters) as long as the number of sand crests remained unchanged. As in equation (9), λ_n is approximately proportional to a, with λ/λ_n proportional to λ/a. Each experiment of this series had a different value of a (and hence λ/a) and T was adjusted to keep U approximately constant at 34.5 centimeters per second $\simeq U_c$. The variable η was observed. Photos of the center third of the final profiles for these experiments are shown in Figure 24. Figure 25 is a plot of final η/λ as function of λ/a including the numbers of the consecutive experiments. The series begins at experiment 37 with a low λ/a; that is, a compressed profile. In experiment 38, with λ/a further reduced to about 1.1, signs of instability appeared (note the incipient shrinking of the center crest in Fig. 24) and the experiment was quickly stopped. Previous experiments had shown that, if the

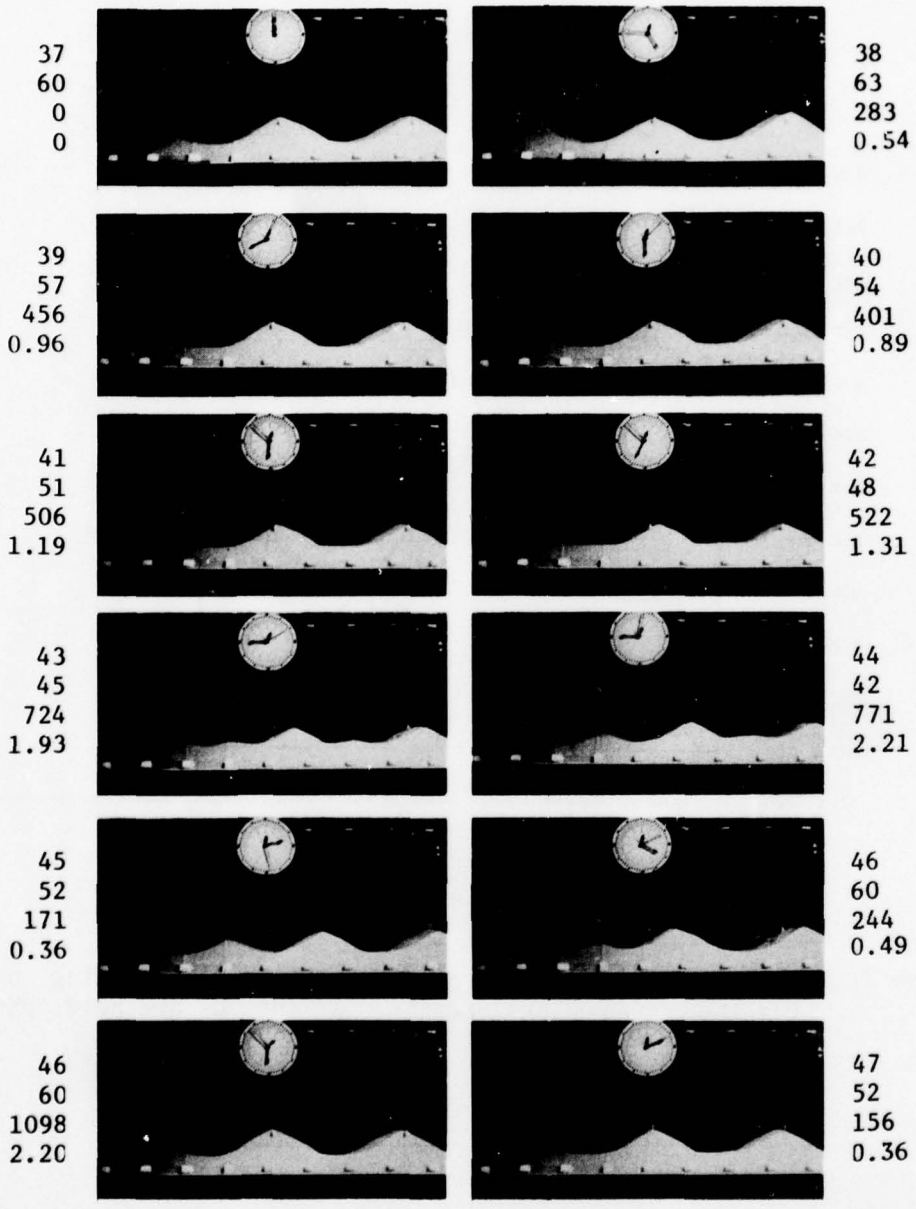

Figure 24. Response of a profile to varying strain (the mid-third of test section in experiments 37 to 47). Numbers by each photo give (in descending order) the experiment number; N; the number of cycles since the beginning of the experiment (n); and (D/a)n. (D = 0.55 millimeters.)

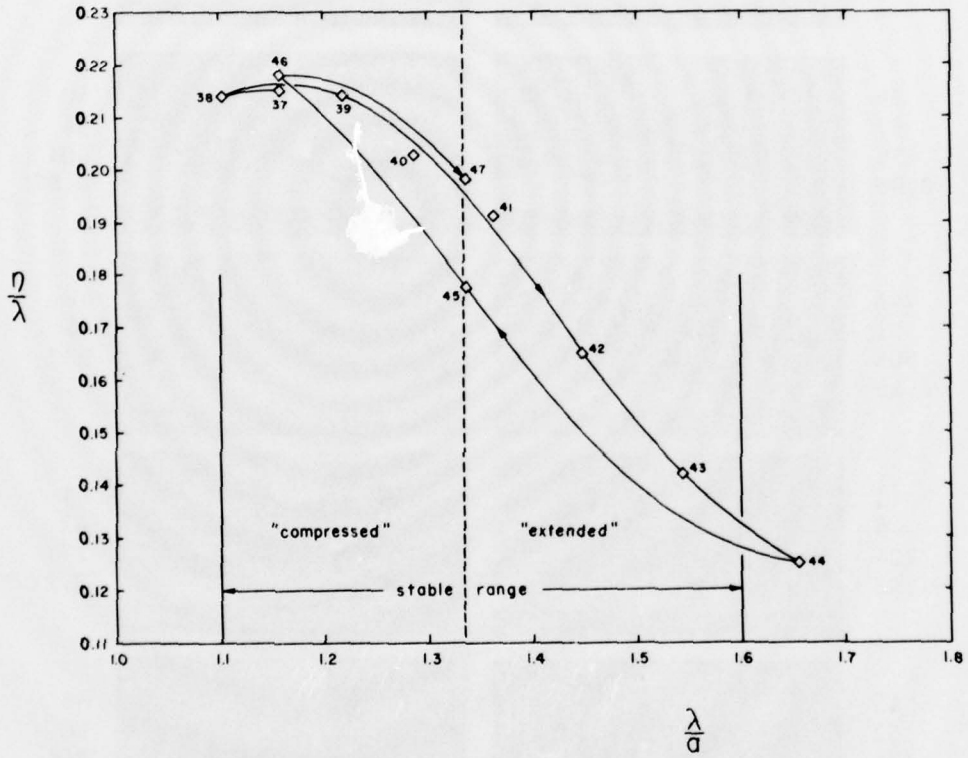

Figure 25. Final η/λ for strained profiles obtained by varying a. For the numbered experiments, λ and U are held constant. (D = 0.55 millimeters.)

experiment were continued, one crest of the compressed profile would shrink and disappear (and thereby increase λ). In following experiments, λ/a was successively increased, and the observed η/λ successively decreased. The troughs became longer and shallower, and each eventually developed a gentle "rise", characteristic of an extended profile. In experiment 44 one of the trough rises began to grow. The experiment was stopped but apparently not soon enough; in the following experiment 45, even with λ/a reduced to 4/3, this growth, though slower, continued. Not until experiment 46, with λ/a in the compressed range, did the new crest shrink and disappear. The number of sand crests was still counted as seven and λ unchanged in determining λ/a and η/λ for experiments 45 and 46. The appearance and disappearance of this incipient crest (Fig. 24) give the curves in Figure 25 a hysteresis which would not have occurred had λ/a been kept below some value between that for experiments 43 and 44 and the new crest not allowed to start. Following experiment 46, λ/a was again increased, and the point for experiment 47 falls on the former descending curve. On the basis of these observations, the stable ranges of λ/a and η/λ are taken to be, approximately,

$$1.1 < \lambda/a < 1.6 \qquad (24)$$

(stable)

$$0.22 > \eta/\lambda > 0.125 \qquad (25)$$

The middle of the range of λ/a in equation (24) is near 4/3, so that λ_n can be identified as the ripple length predicted by equation (9). In Figure 25 the profile has been described as "compressed" or "extended" as λ/a is less than or greater than 4/3. The points from this series of experiments with their variations in λ/a and η/a, are identified by the diamond symbol in Figures 22 and 23. It is seen that their ranges are about the same as the ranges of the scatter. Therefore, the scatter is probably associated with various degrees of profile strain.

Characteristics of "strained" profiles are shown in Figure 26. As in experiments 37 to 47, λ is constant and, from top to bottom, λ/a increases as a decreases.

Based on the information summarized in Figures 25 and 26, the following implications for equilibrium ripple shape are drawn. When the end crests of a two-dimensional profile are fixed, the conditions of strain imply that changes in λ responding to variations in a must show hysteresis. As a increases, such a profile becomes compressed and, as crests disappear, λ increases in steps such that $\lambda > 1.1a$ (eq. 24). As a decreases, the profile becomes extended and as new crests appear, λ decreases in steps such that $\lambda < 1.6a$. Thus, λ depends, in part, on whether a has been increasing or decreasing and must show hysteresis as a is varied from and returned to its original value, provided that the variation in a was large enough to eliminate an old crest or create a new one. The photos in Figures 17 and 18 show a

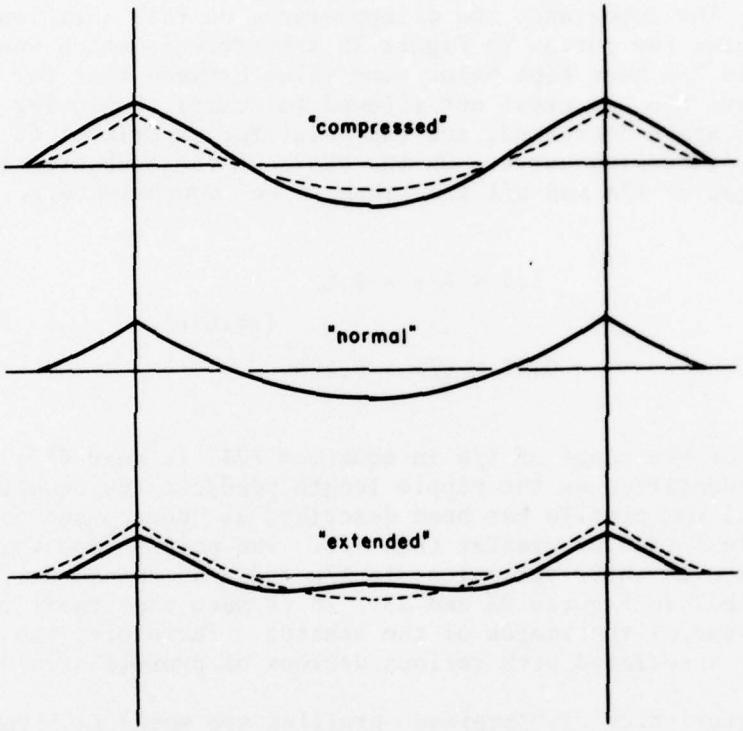

Figure 26. Compressed, normal, and extended profiles. From top to bottom, λ/a increases as a is decreased. The dashed curves are the "normal" profiles redrawn for comparison.

hysteresis in the differences between the profiles at the start of experiment 48 (following experiment 47) where λ = 31.8 centimeters, and at the end of experiment 49, where λ = 25.4 centimeters. As the record in Table A-1 shows, both profiles are in equilibrium with the same combination of a and T, but in experiment 48, a was half the value of experiment 47, and in experiment 49 a was returned to the original value of experiment 47. The first profile in Figure 17 (resulting from experiment 47) is unstrained with seven crests on the bed. The last profile in Figure 18 (resulting from experiments 48 and 49 in sequence) is compressed with nine crests. For the same variation in a, the hysteresis, or net change in λ, would have been more had the first profile of Figure 17 been extended with only six sand crests on the bed. In the few possible cases where hysteresis might have occurred with the brass end crests removed, its observation is obscured by scatter in the data in Table A-1.

VI. CONDITIONS FOR TWO- AND THREE-DIMENSIONAL BED FORMS

1. Approach.

As described in Section V,1, with the 0.55-millimeter sand the final bed forms were always two dimensional, but with the 0.18- and 0.21-millimeter sands the final bed forms were either two or three dimensional or even some combination of both. Although experiments with the finer sands yielded data for the preceding descriptions of two- and quasi two-dimensional profiles, they were also intended to identify the conditions for two- and three-dimensional final bed forms. To this end, the experiments were located again on plots of N and T, as in Figures 10 and 11, with symbols denoting the two- or three-dimensional character of the final bed forms. As before, N is a measure of amplitude a (a = 0.4576 N centimeters). The symbols and definitions are listed in Table 2. Although the definitions are subjective, it is expected that, after the symbols are plotted, a curve can be drawn separating two-dimensional from three-dimensional bed forms.

2. Results.

Symbols showing the character of the final bed forms of the experiments with the 0.18- and 0.21-millimeter sands have been plotted in Figures 27 and 28 at the points (T,N) which define the experiments. These points are the same as in Figures 10 and 11 from which the number of each experiment can easily be obtained.

In Figure 27, regions of predominantly two- and three-dimensional final bed forms can be separated by the straight line U = 25.2 centimeters per second, with two- and three-dimensional forms on the sides of

Table 2. Symbols showing degrees of two and three dimensionality.

Final bed form	Symbol
2D	
Trend to 2D	
Mostly 2D	
2D,3D	
Mostly 3D	
Trend to 3D	
3D	

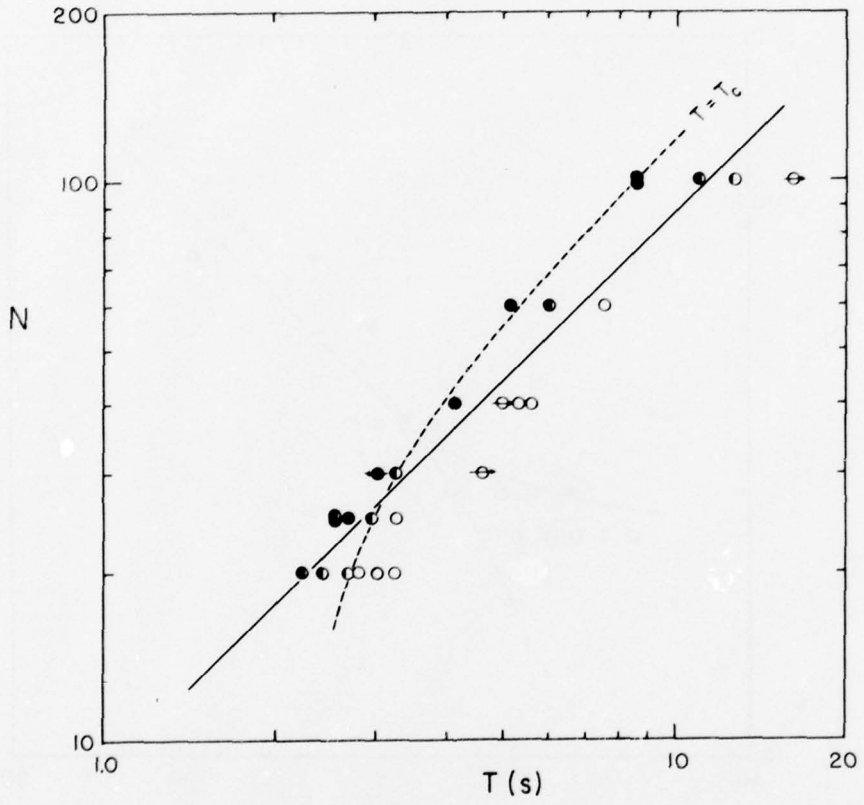

Figure 27. Occurrence of two- and three-dimensional bed forms with the 0.18-millimeter sand. Three-dimensional forms occur above the solid line, given by $\phi = 21.3$ or U = 25.2 centimeters per second. Symbols are defined in Table 2.

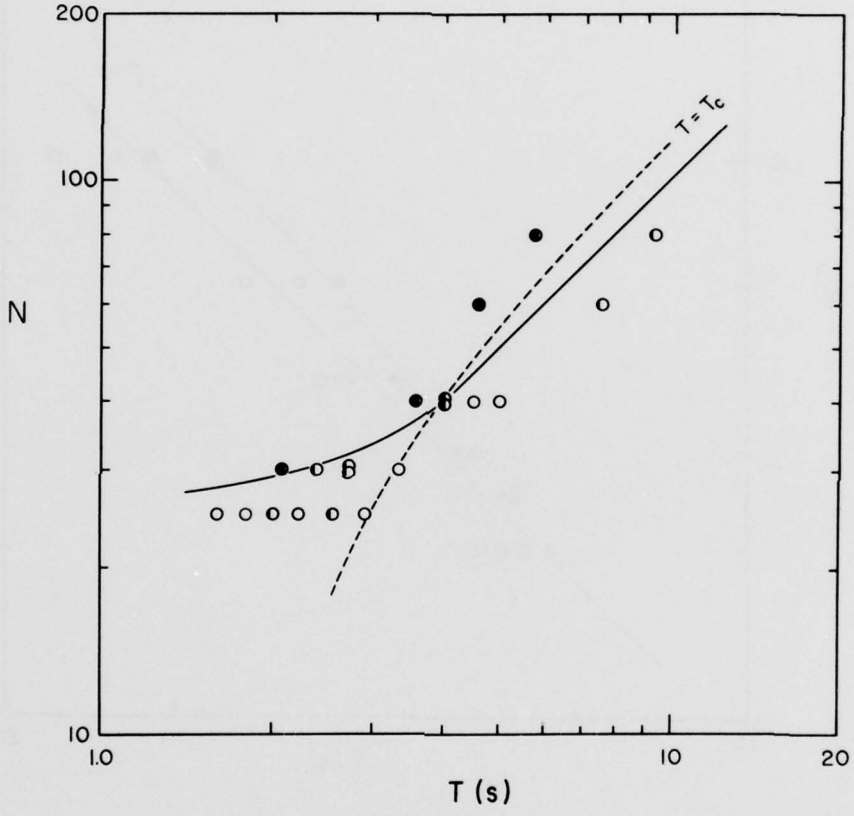

Figure 28. Occurrence of two- and three-dimensional bed forms with the 0.21-millimeter sand. Three-dimensional forms occur above the solid line. Symbols are defined in Table 2.

smaller and larger U. With D = 0.18 millimeters, this line can also be defined as $a/D = (222\ sec^{-1})T$, or as $\phi = 21.3$. The first definition confirms the observation of Carstens, Neilson, and Altinbilek (1969) that bed forms are two or three dimensional as a/D is less than or greater than 775, when T = 3.56 seconds (the period in their experiments), but conflicts with their criterion as stated in terms of a/D alone. The second definition conforms generally, though only roughly, with Carsten's (1966) earlier criterion that two- and three-dimensional forms occur as $\phi^{\frac{1}{2}}$ is less than or greater than approximately 6.5.

In Figure 28, with the 0.21-millimeter sand, a line of constant ϕ again appears to separate two- and three-dimensional regions for moderate and large values of a, but it cannot be extended to small values of a, where a two-dimensional character seems dominant at all values of T. In this case, for small values of a/D, the criterion of Carstens, Neilson, and Altinbilek (1969) seems to apply. A curve separating two- and three-dimensional regions has been attempted in Figure 28, but its contorted character warns of uncertainty. Why, at small values of a, two- dimensional bed forms should occur at small values of T with the 0.21-millimeter sand and not with the 0.18-millimeter sand is difficult to say. It can only be suggested that the relatively broad grain-size distribution of the 0.21-millimeter sand (Fig. 7) makes the dependence of bed form upon grain size less precise, and that the larger grains act to place the 0.21-millimeter sand in an unstable transition zone between the 0.18- and 0.55-millimeter sands. For the 0.55-millimeter sand, all final bed forms were two dimensional.

Photos of final bed forms in four experiments with the 0.18-millimeter sand are shown in Figure 29. The experiments have been selected in two widely separated pairs at large and small values of a (at N = 100,25). Each pair straddles the line of constant ϕ which separates the regions of two- and three-dimensional bed forms in Figure 27. The photos show that in each case the character of the bed form confirms the choice of the symbol plotted in Figure 27 and that the line of separation splits each pair.

3. Results with Inman's (1957) Sea Floor Data.

An attempt was made to establish conditions for the occurrence of two- and three-dimensional ripples on the sea floor based on the observations and definitions of Inman (1957). As mentioned earlier, he defined the ripple pattern according to whether the length of the ripple crests was greater than 8λ (long-crested), between 3λ and 8λ, or less than 3λ (short-crested). Symbols for these patterns have been plotted by values of a/D and ϕ which, for 95 observations, could be obtained from the data in Inman's tables (see Fig. 30). In general, the three patterns are found to be mixed together over the $(a/D,\phi)$ field of

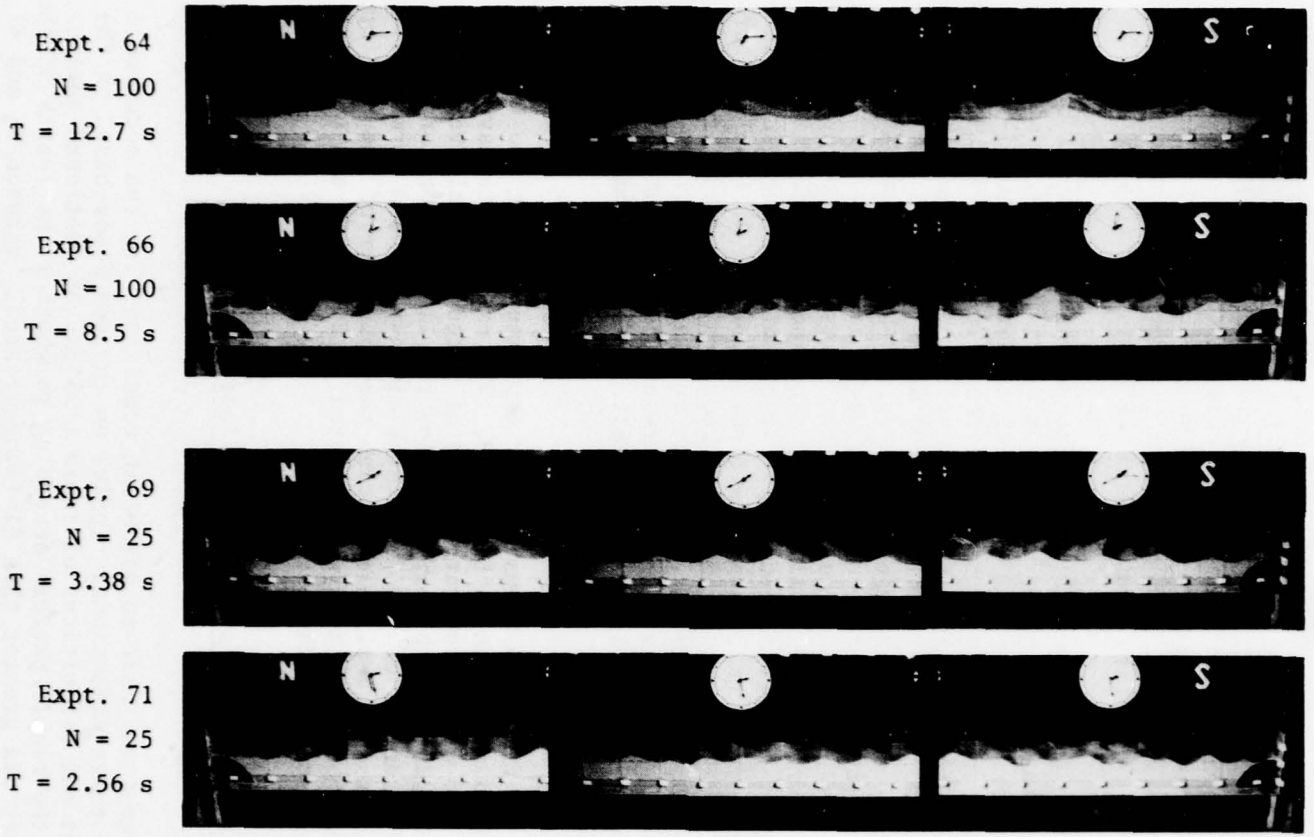

Figure 29. Pairs of final two- and three-dimensional bed forms at large and small N. (D = 0.18 millimeters; a = 0.4576 N centimeters.)

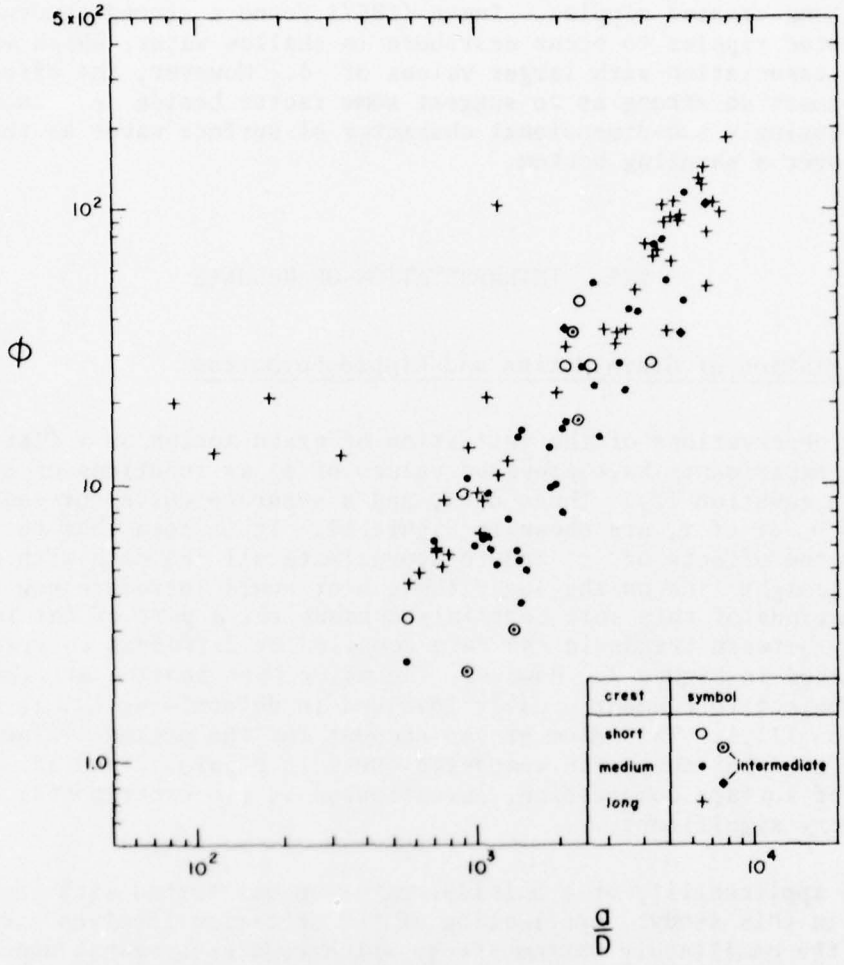

Figure 30. Occurrence of two- and three-dimensional ripples on the seabed (data from Inman, 1957).

the data, which were obtained mostly in exposed coastal waters. However, there appears to be some tendency for longer crested ripples to associate with larger values of ϕ and a/D. Of the 5 observations for $\phi < 4$, none is long crested; of the 27 observations for $\phi > 46$, none is short crested, and all of the 4 observations for $\phi > 110$ are long crested. Also five observations for conditions of limited fetch, with $T < 3.5$ seconds, form a separate group displaced, at given ϕ, toward smaller a/D. These are all long-crested ripples. Inman (1957) found a strong tendency for long-crested ripples to occur nearshore in shallow water, which would imply an association with larger values of ϕ. However, the effect of depth appears so strong as to suggest some factor beside ϕ, such as the increasingly two-dimensional character of surface waves as they advance over a shoaling bottom.

VII. INTERPRETATION OF RESULTS

1. Initiation of Grain Motion and Ripple Formation.

The observations of the initiation of grain motion on a flat bed in these experiments have provided values of ϕ_c as functions of a/D and r, as in equation (3). These data, and a separate curve for each value of D, or of r, are shown in Figure 12. It is seen that to suppress the effects of r and to approximate all the data with a single straight line on the logarithmic plot would introduce new scatter. Approximations of this sort certainly account for a part of the large disparity between trends in the data compiled by different observers, as indicated in Figure 2. However, the major part remains attributable to the subjective element usually involved in determining ϕ_c, as discussed in Section III,1. This element can account for the present values of ϕ_c plotting somewhat above the composite curve in Figures 2 and 12. The effects of surface compression, investigated in two experiments, do not appear very significant.

The applicability of a Shields criterion was tested with the observations in this study. Application of the criterion involves a computation of the oscillatory bottom stress which remains somewhat uncertain. Although the successful use of a Shields criterion does provide insight into the mechanics of incipient motion, the prediction of incipient motion can be approached directly, and perhaps more easily, by the empirical determination of ϕ_c as a function of a/D and r.

Carstens (1966) has stated that the concept of incipient grain motion on a flat bed is of doubtful relevance in the formation of ripples, since the seabed is seldom flat, and he would suggest a study of the minimum conditions for the stimulation of ripples by foreign objects and it may be added here, by relict bed forms. However, the innumerability of foreign objects able to stimulate ripples, including

their dependence on orientation and exposure to the flow, makes such a study infeasible. Also, a distinction must be made between setting sand in motion at points on a relict bed form and establishing a new bed form. A new oscillatory flow may at first move sand on sharp relict ripple crests, but such flow may merely round the crests until the sand ceases to move. In predicting stable bed forms, it is more pertinent to determine the minimum conditions of flow required to sustain them, assuming that any stimuli which may be needed to initiate their development will always be present. Minimum conditions to sustain a rippled bed can reasonably be sought in terms of a minimum value of ϕ. Lofquist (1975) found that an oscillatory flow, combined with an effect of permeability, became unable to sustain ripple migration at a value of ϕ around one-fourth ϕ_c. Carstens, Neilson, and Altinbilek (1969), for a/D = 139 (in their experiment 62), identified a minimum $\phi = 2.15$ needed to continue the growth and spread of small ripples initiated by a foreign object. A reduced ϕ could possibly have maintained the ripples in equilibrium after they had attained full size.

It was found that the conditions required to initiate grain motion on a leveled bed in these experiments were also sufficient to initiate vortex ripples, though, for the finer sands, these ripples always started at some point at the ends of the test bed. However, it appeared that if the test bed were boundless the criteria for grain motion and ripple formation would indeed be distinct. The difference between ϕ_r and ϕ_c appears to be small, negligible for coarse sand, but increasing as the grain size (r) decreases.

In these experiments, the rolling-grain ripples of Bagnold (1946), were observed with the 0.18- and 0.21-millimeter sands but not with the 0.55-millimeter sand. Such an unpredictable occurrence is characteristic of previous observations. Despite their persistence, these ripples appeared to play no part in the development of vortex ripples. This passive behavior contrasts with the more active role described by Bagnold (1946), Manohar (1955), and Carstens, Neilson, and Altinbilek (1969), and suggests that rolling-grain ripples are not an essential part of ripple development.

2. Growth of Ripples.

The profiles were always initially two dimensional when the ripples were small, but during the subsequent period of rapid growth they became, in varying degree, three dimensional. Following this period, as the profiles approached equilibrium, the ripples either became again two dimensional or remained more or less three dimensional.

The dimensionless initial ripple length, λ_i/D, was found to be approximately constant for each sand, to increase moderately as r decreased, and to be independent of a/D. That λ_i is independent of a

provides insight into the mechanics of ripple initiation, and suggests the involvement of stress and the distances grains move over the flat bed, rather than the action of a disturbance in the water, which would move with amplitude a. However, Carstens and Neilson (1967) mention vortices in the water just over the bed and perpendicular to the flow, apparently, before ripples appear. Also, Folk (1976), cites many examples to show that bed forms are the result, rather than the cause, of vortices in the flow.

Observations of growing ripples suggest that η/a and λ/a depend primarily on $(D/a)n$, where n is the number of cycles since the ripples first appeared. These $(D/a)n$ observations are restricted to the condition that $U/U_c \approx 1$ and, except for three experiments, to the use of the 0.55-millimeter sand. The maturity of ripple profiles has been found to depend on $(D/a)n$, involving an interval of time proportional to $(a/D)T$. The period of rapid, and partly three-dimensional, ripple growth may have been lengthened by the presence of the channel walls. On an unbounded bed, the development of a partly three-dimensional bed form might be hastened by lateral spreading of more nearly stable forms from wherever they occur.

3. Size and Shape of Stable Ripples.

Observations of λ/D (Fig. 21) and of λ/a and η/a (Figs. 22 and 23) in this study are in general agreement with most of the previous studies summarized in Figure 5. Despite minor differences, the observations have confirmed the results of Mogridge and Kamphuis (1972), and extended them to sands of different sizes at large a and T. The observations have thereby supported the validity of the approximate equation (9) which states that λ is proportional to a, and that, with a held constant, λ is relatively insensitive to changes in T and to the associated changes in U. These remarkable results deserve further study and explanation.

Occasional failures of laboratory observations to follow the curves of Mogridge and Kamphuis (1972) in Figure 5 might be explained as the effects of boundaries, by failure to achieve a steady state, or, possibly, as distortions associated with oscillating trays. However, field and some laboratory observations of λ/D follow a trend below and away from these curves as a/D increases to large values. This trend was discussed in Section I,3,d and was identified with fine sands. It was then suggested that the plots of Mogridge and Kamphuis (1972) might require modification for smaller values of r.

Whatever the effects of r, observed values of λ/D should fall progressively below the curves of Mogridge and Kamphuis (1972) as a/D increases to large values. Continued adherence to equation (10) would produce comparably large values of λ/D. As a becomes infinite, the oscillatory ripples cannot grow to infinite size but rather must turn

into ripples characteristic of steady flow. Such ripples are of limited length. Yalin (1977) cites the approximation,

$$\frac{\lambda}{D} \approx 1{,}000 \quad \text{(steady flow)} \tag{26}$$

(and replaces the constant, 1,000, with a function of Reynolds number. Yalin's data have an average λ/D of around 800). A relation of the form of equation (26), with the constant lowered, moderately, to between 500 and 600, is consistent with the trends of the observations of Inman (1957) and Dingler (1975) for large a/D (see Fig. 5,e and f). Then, for oscillatory ripples, if ϕ is held constant and both a and T become large, λ/a must ultimately become small. Such behavior is not found in the plots of Mogridge and Kamphuis (1972) which, as T becomes infinite and X_2 (eq. 7) approaches zero, require λ/a to remain, approximately, constant, as in equation (8).

The transition from oscillatory to steady-flow ripples suggests an analogy with the transition from laminar to turbulent flow in a rough pipe. This analogy is illustrated by schematic plots in Figure 31. For pipe flow (Fig. 31a), as the Reynolds number, R, increases, a friction coefficient, C_f, breaks away from its laminar asymptote at the onset of turbulence ultimately to approach a constant value depending on the wall roughness defined by a parameter, k. For ripples (Fig. 31b), as a/D increases, λ/D diverges from its oscillatory asymptote, ultimately to approach the constant value for steady flow. The transition has been presumed to depend on some function $\kappa(\phi,r)$ which combines the effects of ϕ and r (possibly like U/w as discussed in Section I,3,d) and is analogous to the parameter k in pipe flow.

In the case of pipe flow, transition to turbulent flow is enhanced and shifted to lower values of R by disturbances in the incoming flow such as slight turbulence or swirl. Extending the analogy, transition from oscillatory to steady-flow ripples might be enhanced and shifted to lower values of a/D by deviations from pure sinusoidal two-dimensional flow over the bed. The analogy then suggests that, for given a/D, ϕ, r, values of λ/D would tend to be larger (closer to eq. 10) in a water tunnel, which provides a sinusoidal two-dimensional flow, and smaller (closer to eq. 26) on the sea bed where the flow is perturbed, tendencies which were observed in Figure 5 and discussed in Section I,3,d. Effects of perturbations in the flow might also account for some of the scatter found in plots of λ/D and λ/a, particularly from field observations.

Results of this study (summarized in App. A) show that two-dimensional profiles, developing under the same given values of a and T and with minimum end constraints, attain nearly identical final forms, even when the initial bed forms were very different. This indicates that unconstrained equilibrium profiles are independent of

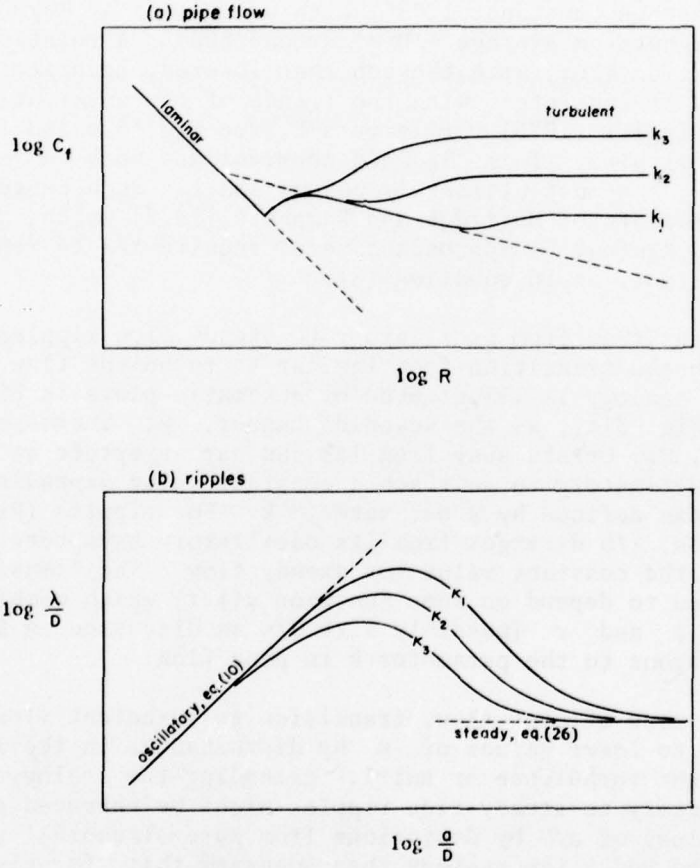

Figure 31. Analogy between (a) transition from laminar to turbulent flow in a rough pipe, and (b) transition from oscillatory-flow to steady-flow ripples.

their histories. However, in experiments 37 to 49 with fixed end crests (Fig. 25), there was a variety of ripple forms, corresponding to different values of a with a fixed value of λ, within the limits of equations (24) and (25). In addition, when the profiles were strained beyond these limits, a hysteresis resulted (discussion of Figs. 17 and 18 in Sec. V,5). On the unbounded seabed, ripples might be expected to show strain while still adjusting to previous changes in a, though, presumably, the time of adjustment, and with it the maximum strain encountered, would be reduced by the freedom of the profile to extend and contract longitudinally. A quicker adjustment might result from the opportunity for lateral motions combined with deviations of the bed forms from two dimensionality. On the seabed examples where a crestline stops or branches into two are common. The lateral movement of such features into or out of an area could change the average ripple length almost continuously. This mechanism was alluded to in Section VII,2 in regard to the growth of ripples.

4. Two- and Three-Dimensional Bed Forms.

Equilibrium bed forms were always two dimensional with the 0.55-millimeter sand but both two and three dimensional with the two finer sands. Attempts to further define the conditions for two- and three-dimensional forms are inconclusive. With the 0.18-millimeter sand, two- or three-dimensional forms were observed, with fair consistency, as ϕ was less than or greater than 21.3 (U = 25.2 centimeters per second; Fig. 27). With the 0.21-millimeter sand the separation of two- and three-dimensional forms was not so simple. A suggestion for this difference in behavior between the two finer sands, based on grain-size distribution, was offered in Section VI,2. Generally, irregularities in the occurrence of two- and three-dimensional forms might stem from limitations of time and space. It was noted in Section V,1 that profiles are prone to become three dimensional during periods of growth and that, with the finer sands, during slow or imperceptible growth, recurrence of two and three dimensionality was not uncommon. There remains then a possibility that some of the observed final bed forms might have modified or changed character if the experiments had been prolonged. Although the channel walls clearly suppress large three-dimensional motions, they also initiate small ones, since at a wall the vorticity vector of the flow must be parallel to the wall, rather than normal to it as in strictly two-dimensional flow. Once established, symmetrical slightly three-dimensional flows and associated bed forms might become unstable, lose symmetry and become increasingly three dimensional. Since such wall effects on the transition from two- to three-dimensional bed forms in these experiments are not known to be negligible, the curves in Figures 27 and 28 must be used with caution. After transition, the effects of the walls on the further development of three-dimensional bed forms must be presumed significant, and for this reason their final characteristics have not been described in detail.

Although a three-dimensional character of the bed form might be initiated and then conditioned by the presence of channel walls, such constraints are by no means its only possible source. This is shown by the three-dimensional ripples observed by Inman (1957) on the unbounded seabed. A likely source here are the lateral perturbations in the flow over the bottom which must be found under surface waves which are themselves not two dimensional. This supposition is consistent with the irregular occurrence of long-, medium-, and short-crested ripples (Fig. 30). It is further supported by the observed tendencies for long-crested ripples to occur in shallow water under shoaling waves and in protected areas where the fetch is short--both conditions likely to favor more regular and two-dimensional surface waves. However, the observations at short fetch are also at smaller values of a/D. It has already been noted that oscillatory ripples should become more like steady-flow ripples as a and T become large. Raudkivi (1976; pp. 62-65) describes steady-flow ripples as typically three dimensional. These considerations are consistent with a tendency for oscillatory ripples to become more three dimensional with increasing a/D.

5. Disappearance of Ripples.

To forestall damage to the screens (Table A-2, experiment 67) in these experiments, ϕ had to be limited to values unable to produce sheet flow. Therefore, this section only discusses the criteria of Manohar (1955), Chan, Baird, and Round (1972), and Dingler (1975), given by equations (12), (13), and (14), respectively. In equations (12) and (13), ϕ_S depends on both a/D and r; in equation (14) this dependence is absent, perhaps due to relatively small ranges of a/D and r in Dingler's (1975) observations of sheet flow, with a/D between 5×10^3 and 10^4 and with D between 0.128 and 0.158 millimeters, corresponding to $r \simeq 5.8$ and 8.0. Curves of $\phi = \phi_S$, given by equations (12) and (13) for $r = 5$, 10 and by equation (14), are plotted against a/D in Figure 32 (discussed in Sec. VII,6). The curves in Figure 32 are solid where supported by observations and dashed where extrapolated. In the region of Dingler's (1975) observations of sheet flow, the criteria are in remarkable agreement, considering their diverse derivations and the distortions to which equations (12) and (13) are ostensibly subject. Unnatural accelerations of the oscillating tray may have reduced the ϕ_S observed by Manohar (1955), especially at smaller values of a/D. Effects of confinement in the pipe test section of Chan, Baird, and Round (1972) are clearly severe on bed forms with height comparable to the pipe diameter (5.1 centimeters), but may have lessened as the bed flattened to approach sheet flow. (However, in experiment 55 ϕ exceeded ϕ_S by eq. 13 without attaining sheet flow.) Taken together, equations (12), (13), and (14) suggest a ϕ_S as a modification of equation (14) to allow for relatively slight effects of a/D and r. These effects are not yet established, but ϕ_S appears to increase with increasing a/D and, usually, with decreasing r, though perhaps not always, as suggested by the crossing extrapolations of equation (12) for $r = 5$ and 10.

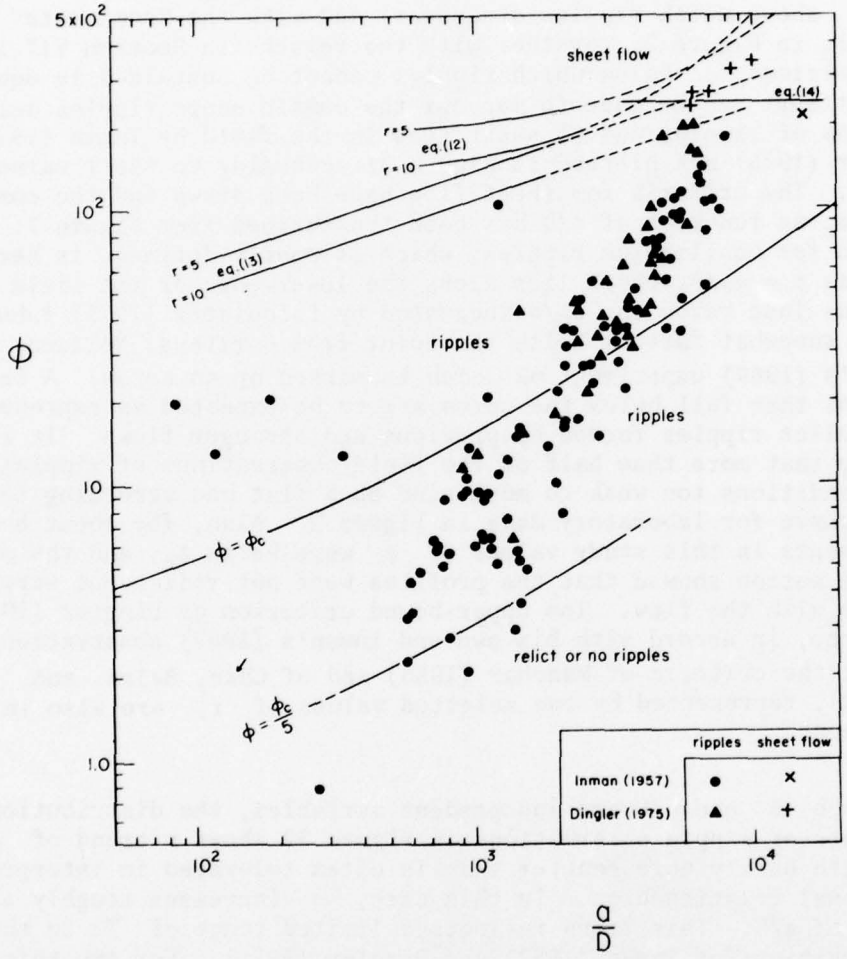

Figure 32. Limits to the occurrence of ripples on the seabed (data from Inman, 1957, and Dingler, 1975).

6. Occurrence of Ripples.

With the criteria of Manohar (1955) and Dingler (1975) providing a maximum ϕ above which ripples disappear, and with the "composite" curve for ϕ_c in Figure 2, together with the remarks in Section VII,1 regarding a minimum ϕ below which ripples cannot be sustained in equilibrium, an attempt may be made to map out the domain where ripples occur. Observations of ripples and of sheet flow in the field by Inman (1957) and Dingler (1975) are plotted in Figure 32 according to their values of a/D and ϕ. The criteria for sheet flow have been drawn and the composite curve for ϕ_c as function of a/D has been transcribed from Figure 2. A lower bound for equilibrium ripples, which is poorly defined, is here suggested as $\phi = \phi_c/5$, which lies along the lower edge of the field observations just below the $\phi_c/4$ suggested by Lofquist's (1975) laboratory study, and somewhat farther below the point from Carstens, Neilson, and Altinbilek's (1969) experiment 62 which is marked by an arrow. A few observations that fall below the curve are to be expected as representing cases of relict ripples formed by previous and stronger flows. It is interesting that more than half of the field observations of ripples are for flow conditions too weak to move sand on a flat bed according to the composite curve for laboratory data in Figure 2. Also, for about half of the experiments in this study values of ϕ were below ϕ_c, and the observed sand motion showed that the profiles were not relict but were in equilibrium with the flow. The upper-bound criterion of Dingler (1975) is, of course, in accord with his own and Inman's (1957) observations of sheet flow; the criteria of Manohar (1955) and of Chan, Baird and Round (1972), represented by two selected values of r, are also in fair agreement.

Although ϕ and a/D are independent variables, the distribution of the points of ripple observations in Figure 32 shows a trend of ϕ with a/D with hardly more scatter than is often tolerated in interpreting functional relationships. In this case, ϕ increases roughly as the square of a/D. This trend reflects a limited range of T in the field observations of Inman (1957) and Dingler (1975). For two-thirds of these observations, T fell in the range from 8 to 12 seconds. This range is characteristic of the California coast and may not appear elsewhere. The observed trend of ϕ with a/D is then not a functional relationship but a circumstantial correlation. It makes separation of the effects of ϕ and a/D upon λ/D or η/D very difficult.

With ρ_s/ρ regarded as constant for natural sands, the occurrence of ripples, as well as other of their characteristics, depends on the three independent variables a/D, ϕ, and r. The choice of a/D, rather than r, as abscissa in Figure 32 owes much to the fact that the trend of ϕ_c with a/D is fairly clear while the effects of r on ϕ_c remain contradictory and obscure. (In field data, r depends primarily on D.) Similarly, λ/D and η/D have been found to depend more

strongly and clearly on a/D than on either ϕ or r. Figure 32 may be compared with Figure 9 in Inman (1957) which attempts to show the domain of ripple occurrence on a field of U versus D. With the present dimensionless variables, this is roughly equivalent to $\phi^{\frac{1}{2}}$ versus $r^{2/3}$. In Inman's plot the effects of a/D (or of T) are not indicated; in Figure 32 r is absent, except as a parameter in the criteria for sheet flow of Manohar (1955) and Chan, Baird, and Round (1972).

VIII. SUMMARY

This study has discussed observations of ripples from a series of laboratory experiments, without any attempt at theoretical models; the direct results of these observations are summarized in this section. A guide to this summary is provided by the list of "emerging questions" in Section I,3,h. These questions and related findings are put in two groups.

The first group of findings relates to the initiation of grain motion and ripples on a flat bed. Their primary application is in support of physical models of ripple development:

(a) ϕ_c has been found to be a function of both a/D and r (Fig. 12).

(b) A prior compression of the sand surface was found to have only a small effect upon ϕ_c (Fig. 12).

(c) A Shields criterion for the initiation of grain motion under oscillatory flow was found in need of further modification (Fig. 13).

(d) ϕ_r was found to be distinct from ϕ_c, but the difference was small and detectable only with the finer sands (the arrows in Figs. 10 and 11).

(e) Rolling-grain ripples were observed only with the two finer sands. These ripples appeared not to play an active or necessary role in the formation of vortex ripples.

(f) The initial length of vortex ripples was found to depend slightly on D but not on a (Fig. 15). This independence suggests that vortex ripples are not caused by a prior disturbance moving with the water.

The second group of findings relates to the character of bed forms, whether in growth or in equilibrium. In large part, they confirm the design curves of Mogridge and Kamphuis (1972), while enlarging their experimental base with other sand grain sizes at moderate and large values of a and T.

Beyond this:

(g) The growth of η/a and λ/a, with time, has been found to be a function of $(D/a)n$. This function shows ripples to be mature when $n > a/D$ (Figs. 19 and 20).

(h) The variety of initial bed forms which converge into final forms depending, essentially, only on a and T has supported the conclusion that an equilibrium profile, when unconfined, is independent of its history (Figs. 21, 22, and 23).

(i) When confined at its ends, an equilibrium profile has been found to have various sizes and shapes determined by its value of λ/a, which is contained within definite limits but is otherwise determined by the history of the profile (Fig. 25).

(j) Both two- and three-dimensional final bed forms were observed. Clear criteria for these forms were not established, but a dependence on ϕ and, possibly, on a/D is apparent (Figs. 27, 28, and 29). Three dimensionality was found enhanced by a reduction in D and by growth or instability of the profile.

In this study, more than usual, discussions have involved the findings of earlier studies, and it is hoped that the attempts to relate and interpret them (e.g., Figs. 3, 4, 5, 30, and 32) have a value apart from the new laboratory observations. More work is needed to improve prediction of the rippled character of the seabed under given conditions of flow. The design curves of Mogridge and Kamphuis (1972), useful as they are, need modification at large values of a/D as shown by the field observations of Inman (1957) and Dingler (1975) and as discussed in Section VII,3. Conditions for two- and three-dimensional bed forms remain poorly defined (Secs. VI,2,3 and VII,4). Despite these reservations, the character of the seabed can even now be predicted well enough to encourage studies of the bottom stress and of the amount of sand in suspension, both of which depend on the bed forms. As described in Section I,1, results of these studies find application in coastal engineering problems of surface wave decay and of sand transport.

LITERATURE CITED

BAGNOLD, R.A., "Motion of Waves in Shallow Water, Interaction Between Waves and Sand Bottoms," *Proceedings, Royal Society of London*, Series A, Vol. 187, 1946, pp. 1-18.

CARSTENS, M.R., "Similarity Laws for Localized Scour," *Journal of the Hydraulics Division*, American Society of Civil Engineers, Vol. 92, No. HY3, May 1966, pp. 13-36.

CARSTENS, M.R., and NEILSON, F.M., "Evolution of a Duned Bed under Oscillatory Flow," *Journal of Geophysical Research*, Vol. 72, No. 12, June, 1967, pp. 3053-3059.

CARSTENS, M.R., NEILSON, F.M., and ALTINBILEK, H.D., "Bed Forms Generated in the Laboratory Under an Oscillatory Flow: Analytical and Experimental Study," TM-28, U.S. Army, Corps of Engineers, Coastal Engineering Research Center, Washington, D.C., June 1969.

CHAN, K.W., BAIRD, M.H.I., and ROUND, G.F., "Behaviour of Beds of Dense Particles in a Horizontally Oscillating Liquid," *Proceedings, Royal Society of London*, Series A, Vol. 330, 1972, pp. 537-559.

COLLINS, J.I., and CHESNUTT, C.B., "Grain Shape and Size Distribution Effects in Coastal Models," TP 76-11, U.S. Army, Corps of Engineers, Coastal Engineering Research Center, Fort Belvoir, Va., July 1976.

DINGLER, J.R., "Wave-Formed Ripples in Nearshore Sands," Ph.D. Dissertation, Department of Oceanography, University of California, San Diego, Calif., 1975.

FOLK, R.L., "Rollers and Ripples in Sand, Streams and Sky: Rhythmic Alteration of Transverse and Longitudinal Vortices in Three Orders," *Sedimentology*, No. 23, Oct., 1976, pp. 649-669.

HOMMA, M., and HORIKAWA, K., "Suspended Sediment due to Wave Action," *Proceedings of the Eighth Coastal Engineering Conference*, 1962, pp. 168-193.

HORIKAWA, K., and WATANABE, A., "A Study on Sand Movement due to Wave Action," *Coastal Engineering in Japan*, Vol. 10, 1967, pp. 39-57.

INMAN, D.L., "Wave-Generated Ripples in Nearshore Sands," TM-100, U.S. Army, Corps of Engineers, Beach Erosion Board, Washington D.C., Oct. 1957.

INMAN, D.L., and BOWEN, A.J., "Flume Experiments on Sand Transport by Waves and Currents," *Proceedings of the Eighth Coastal Engineering Conference*, 1962, pp. 137-150.

JONSSON, I.G., "Wave Boundary Layers and Friction Factors," *Proceedings of the 10th Coastal Engineering Conference*, American Society of Civil Engineers, 1966, pp. 127-148.

KAMPHUIS, J.W., "Friction Factor under Oscillatory Waves," *Journal of the Waterways, Harbors and Coastal Engineering Division*, American Society of Civil Engineers, Vol. 101, No. WW2, May 1975, pp. 135-144

KENNEDY, J.F., and FALCON, M., "Wave Generated Sediment Ripples," Report No. 86, Department of Civil Engineering, Hydrodynamics Laboratory, Massachusetts Institute of Technology, Cambridge, Mass., Aug. 1965.

KOMAR, P.D., and MILLER, M.C., "The Threshold of Sediment Movement Under Oscillatory Water Waves," *Journal of Sedimentary Petrology*, Vol. 43, No. 4, Dec. 1973, pp. 1101-1110.

KOMAR, P.D., and MILLER, M.C., "The Initiation of Oscillatory Ripple Marks and the Development of Plane-Bed at High Shear Stresses under Waves," *Journal of Sedimentary Petrology*, Vol. 45, No. 3, Sept. 1975, pp. 697-703.

LOFQUIST, K.E.B., "An Effect of Permeability on Sand Transport by Waves," TM-62, U.S. Army, Corps of Engineers, Coastal Engineering Research Center, Fort Belvoir, Va., Dec. 1975.

LOFQUIST, K.E.B., "A Positive Displacement Oscillatory Water Tunnel," MR 77-1, U.S. Army, Corps of Engineers, Coastal Engineering Research Center, Fort Belvoir, Va., Feb. 1977.

MADSEN, O.S., and GRANT, W.D., "The Threshold of Sediment Movement Under Oscillatory Waves: A Discussion," *Journal of Sedimentary Petrology*, Vol. 45, No. 1, Mar. 1975, pp. 359-367.

MADSEN, O.S., and GRANT, W.D., "Sediment Transport in the Coastal Environment," Report No. 209, Department of Civil Engineering, Hydrodynamics Laboratory, Massachusetts Institute of Technology, Cambridge, Mass., Jan. 1976.

MANOHAR, V., "Mechanics of Bottom Sediment Movement Due to Wave Action," TM-75, U.S. Army, Corps of Engineers, Beach Erosion Board, Washington, D.C., June 1955.

MOGRIDGE, G.R., and KAMPHUIS, J.W., "Experiments on Bed Forms Generated by Wave Action," *Proceedings of the 13th Coastal Engineering Conference*, Vol. II, 1972, pp. 1123-1142.

NIELSEN, P., " A Note on Wave Ripple Geometry," Progress Report No. 43, Institute of Hydrodynamics and Hydraulic Engineering (ISVA), Technical University of Denmark, Aug. 1977, pp. 17-22.

RANCE, P.J., and WARREN, N.F., "The Threshold of Movement of Coarse Material in Oscillatory Flow," *Proceedings of the 11th Coastal Engineering Conference*, American Society of Civil Engineers, 1968, pp. 487-491.

RAUDKIVI, A.J., *Loose Boundary Hydraulics*, 2d ed., Pergamon Press, Elmsford, N.Y., 1976.

SCOTT, T.S., "Sand Movement by Waves," TM-48, U.S. Army, Corps of Engineers, Beach Erosion Board, Washington D.C., Aug. 1954.

SHIELDS, A., "Application of Similarity Principles and Turbulence Research to Bed-Load Movement," translated from "Anwendung der Aenlichkeitsmechanik und der Turbulenz forschung auf die Geschiebebewegung," Mitt. d. Preuss. Versuchsanstalt f. Wasserbau u. Schiffbau, Berlin, Heft 26, 1936, by W.P. Ott and J.C. van Uchelen, U.S. Dept. of Agriculture, Soil Conservation Service Cooperative Laboratory, California Institute of Technology, Pasadena, Calif., 1936.

SHULYAK, B.A., "Certain Aspects of the Interaction Between Wave Flow and a Deformable Bottom at Low Velocities," *Dynamics and Morphology of Sea Coasts*, translation of *Dinamika i Morphologiya Morskikh Beregov*, Moskva, 1961, available at National Technical Information Service, Springfield, Va., 1969, pp. 218-283.

SILVESTER, R., *Coastal Engineering*, Vol. 2, Elsevier, Amsterdam, 1974.

STERNBERG, R.W., and LARSEN, L.H., "Threshold of Sediment Movement by Open Ocean Waves: Observations," *Deep-Sea Research*, Vol. 22, 1975, pp. 299-309.

U.S. ARMY CORPS OF ENGINEERS, COASTAL ENGINEERING RESEARCH CENTER, *Shore Protection Manual*, 3d ed., Vols. I, II, and III, Stock No. 008-022-00113-1, U.S. Government Printing Office, Washington, D.C., 1977, 1,262 pp.

YALIN, M.S., "On the Determination of Ripple Length," *Journal of the Hydraulics Division*, American Society of Civil Engineers, Vol. 103, No. HY4, Apr. 1977, pp. 439-442.

YALIN, M.S. and RUSSELL, R.C.H., "Similarity in Sediment Transport due to Waves," *Proceedings of the Eighth Coastal Engineering Conference*, 1962, pp. 151-167.

APPENDIX A

DATA FROM 104 EXPERIMENTS ON RIPPLE GROWTH AND EQUILIBRIUM FORMS

Tables A-1, A-2, and A-3 contain data and notes for experiments with the 0.55-, 0.18-, and 0.21-millimeter sands. The experiments are listed chronologically. Special measures carried out between experiments are noted in proper sequence. The value of N shows the stroke for each experiment. Experiments with the bed initially leveled are identified by footnotes and by observations of λ_i, which pertain only to these experiments. Absence of values for λ,η indicates a final bed form too three dimensional for λ,η to be defined. Included with some experiments are notes on their progress or outcome. These refer mostly to the two- or three-dimensional character of final bed forms with the 0.18- and 0.21-millimeter sands. (With the 0.55-millimeter sand, final bed forms are all two dimensional.) When more than one of the three T, T_c, T_r are entered, the first listed is that at which the ripple profile was allowed to develop.

$$a = 0.4576\ N \text{ centimeters}$$

$$U = 2.87\ N/T \text{ centimeters per second}$$

Table A-1. Data and notes for experiments with the 0.55-millimeter sand (r = 52.39).

Expt. No.	N	a (cm)	T, T_c (s)	λ_i (cm)	λ (cm)	η (cm)	U, U_c (cm/s)	ϕ, ϕ_c	Duration (hr:min)
1[1]	100	45.8	8.30(c)	10.7	72.5	15.50	34.6(c)	13.22(c)	6:19
2[1]	100	45.8	8.08(c)	7.35	58.3	12.33	35.6(c)	13.95(c)	3:10
3	100	45.8	7.01		55.0	11.50	41.0	18.54	1:53
4	100	45.8	10.00		55.0	11.42	28.8	9.11	2:11
5	100	45.8	12.08		55.0	10.03	23.8	6.24	1:31
6	100	45.8	15.26		55.0	10.64	18.8	3.91	1:50
7[1]	80	36.6	6.53(c)	8.0	55.6	10.14	35.2(c)	13.68(c)	1:00
8	80	36.6	5.30		42.7	8.90	43.4	20.76	3:37
9	80	36.6	4.23		40.0	7.54	54.4	32.59	2:13
10	80	36.6	6.51		56.0	9.83	35.3	13.75	5:53
11	50	22.9	4.16		27.8	5.38	34.6	13.16	2:07
12	80	36.6	6.51		54.0	10.14	35.3	13.75	5:58
13[1]	60	27.5	4.90(c)	7.5	33.6	7.17	35.2(c)	13.66(c)	3:33
14	60	27.5	4.00		33.3	6.64	43.1	20.50	1:56
15	60	27.5	3.20		32.0	5.61	53.9	32.04	1:30
16	60	27.5	4.90		32.0	6.67	35.2	13.66	1:16
17	60	27.5	6.24		32.6	6.56	27.7	8.42	1:47
18	60	27.5	7.99		32.1	6.50	21.6	5.14	2:42
19	80	36.6	8.00		50.0	10.58	28.8	9.11	13.49
20	50[1]	22.9	5.00		31.8	5.33	28.8	9.11	7:19
21	50	22.9	3.07		27.7	4.86	46.8	24.17	1:00
22	50	22.9	5.00		29.1	5.71	28.8	9.11	2:07
23[1]	40	18.3	3.45(c)	10.0	24.8	4.37	33.3(c)	12.25(c)	3:47
24	40	18.3	4.25		25.2	4.70	27.1	8.07	2:30
25	40	18.3	2.50		24.4	3.78	46.0	23.32	1:27
26	30	13.7	2.51		23.1	3.30	34.4	13.01	1:47
27	30	13.7	3.23		23.1	3.40	26.7	7.86	1:02
28	33	15.1	3.06		22.9	3.52	31.0	10.60	1:36
29[1]	30	13.7	2.69(c)	7.5	25.2	3.63	32.1(c)	11.33(c)	4:39
Brass crests mounted in spools 15 cm from screens									
30	30	13.7	2.70		21.6	3.27	32.0	11.25	4:59
Sand in one spool redistributed manually									
31	30	13.7	2.69		20.7	3.22	32.1	11.33	1:15
Brass crests in spools shifted to 22 cm from screens									
32	30	13.7	2.70		20.0	3.23	32.0	11.25	1:04

[1]Experiments with bed initially leveled.

Table A-1. Data and notes for experiments with the 0.55-millimeter sand (r = 52.39).-Continued.

Expt. No.	N	a (cm)	T, T_c (s)	λ_i (cm)	λ (cm)	η (cm)	U, U_c (cm/s)	ϕ, ϕ_c	Duration (hr:min)
Brass crests mounted at ends of sand bed atop the curved ramps									
33	30	13.7	2.69		19.2	3.42	32.1	11.33	1:12
34	30	13.7	2.07		18.6	3.06	41.7	19.13	1:11
35	30	13.7	2.71		19.1	3.45	31.8	11.16	1:24
36	30	13.7	3.58		19.2	3.64	24.1	6.40	1:07
37	60	27.5	5.00		31.8	6.83	34.5	13.12	2:37
38	63	28.8	5.25		31.8	6.81	34.5	13.12	0:45
39	57	26.1	4.75		31.8	6.81	34.5	13.12	0:50
40	54	24.7	4.50		31.8	6.44	34.5	13.12	0:35
41	51	23.3	4.25		31.8	6.08	34.5	13.11	0:44
42	48	22.0	4.01		31.8	5.25	34.4	13.05	0:38
43	45	20.6	3.74		31.8	4.50	34.6	13.18	0:49
44	42	19.2	3.50		31.8	3.98	34.5	13.12	0:47
45	52	23.8	4.33		31.8	5.69	34.5	13.15	0:15
46	60	27.5	4.97		31.8	6.92	34.7	13.28	1:29
47	52	23.8	4.32		31.8	6.30	34.6	13.21	0:11
48	26	11.9	2.26		16.9	2.83	33.1	12.06	0.35
49	52	23.8	4.33		25.4	5.50	34.5	13.15	0:34
50	60	27.5	4.99		31.8	6.83	34.6	13.18	1:13
Brass crests removed									
51[1]	40	18.3	3.42 3.58(c)	7.3	27.3	4.13	33.6 32.1(c)	12.46 11.37(c)	3:30
Surface leveled and compressed 1.5 mm									
52[1]	60	27.5	4.34(c)	8.5	33.6	6.56	39.8(c)	17.41(c)	5:14
Sand in one spool reduced and redistributed									
53	60	27.5	4.35		33.6	6.62	39.7	17.33	5:02
Sand redistribution has small effect									
Surface leveled and compressed 0.83 mm									
54[1]	60	27.5	4.62(c)	9.2	33.6	6.61	37.4(c)	15.37	3:38
55	60	27.5	2.24		26.2	4.53	77.0	65.38	1:00
T reduced in steps from 4.61 s to 2.24 s									
56	30	13.7	2.63		22.9	3.41	32.8	11.85	2:31
57[1]	30	13.7	2.78 2.81(c)	8.7	20.8	3.40	31.0 30.7(c)	10.61 10.39(c)	5:12
Experiment interrupted and sand added to spools									

[1]Experiments with bed initially leveled.

Table A-2. Data and notes for experiments with the 0.18-millimeter sand (r = 9.81).

Expt. No.	N	a (cm)	T, T_c, T_r (s)	λ_i (cm)	λ (cm)	η (cm)	U, U_c, U_r (cm/s)	ϕ, ϕ_c, ϕ_r	Duration (hr:min)
58[1]	60	27.5	5.18(c)	5.0	--[2]	--[2]	33.3(c)	37.34(c)	8:17
Final bed form: 3D									
59[1]	30	13.7	3.29(c)	4.86	16.0	2.17	26.2(c)	23.15(c)	4:01
Final bed form: 2D, 3D									
60	30	13.7	4.63		16.0	2.00	18.6	11.69	5:11
Final bed form: trend to 2D									
61	30	13.7	3.03		--[2]	--[2]	28.5	27.29	1:00
Final bed form: trend to 3D									
62[1]	100	45.8	8.51(c)	4.65	--[2]	--[2]	33.8(c)	38.44(c)	4:03
Final bed form: 3D									
63	100	45.8	16.03		--[2]	--[2]	17.9	10.84	6:02
Final bed form: trend to 2D									
64	100	45.8	12.73		3.80	3.67	22.6	17.18	7:20
Final bed form: mostly 2D									
65	100	45.8	10.99		--[2]	--[2]	26.2	23.04	3:05
Final bed form: mostly 3D									
66	100	45.8	8.53		--[2]	--[2]	33.7	38.26	2:20
Final bed form: 3D									
67	100	45.8	4.93				58.3	114.52	1:38
T reduced in steps from 7.26 s to 4.93 s where screen tears from seal. Final bed form is mostly 3D but with two large rounded crests formed by sand exchange with screens; not entered in Figure 27.									
68[1]	25	11.4	2.97(c)	4.6	14.0	2.0	24.2(c)	19.72(c)	2:11
Final bed form: 2D, 3D									
69	25	11.4	3.28		14.6	1.73	21.9	16.16	1:54
Final bed form: 2D									
70	25	11.4	2.70		13.3	1.78	26.6	23.86	1:42
Final bed form: mostly 3D									
71	25	11.4	2.56		--[2]	--[2]	28.1	26.55	0:47
Final bed form: mostly 3D									

[1]Experiments with the bed initially leveled.
[2]Final bed form too three dimensional to determine λ,n.

Table A-2. Data and notes for experiments with the 0.18-millimeter sand (r = 9.81).-Continued.

Expt. No.	N	a (cm)	T, T_c, T_r (s)	λ_i (cm)	λ (cm)	η (cm)	U, U_c, U_r (cm/s)	ϕ, ϕ_c, ϕ_r	Duration (hr:min)
72[1]	20	9.15	2.71(c)	4.45	11.5	1.69	21.2(c)	15.16(c)	3:16
Final bed form: mostly 2D									
73	20	9.15	3.03		11.5	--[2]	19.0	12.13	1:18
Final bed form, mostly 2D, with crests sloping alternately left and right									
74	20	9.15	3.25		11.5	--[2]	17.7	10.54	1:15
Final bed form: mostly 2D, with crests sloping alternately left and right									
75	20	9.15	2.44		11.3	1.56	23.6	18.71	0:51
Final bed form: 2D, 3D									
76	20	9.15	2.25		11.0	1.60	25.6	22.00	1:06
Final bed form: mostly 3D									
77	20	9.15	2.79		11.45	1.67	20.6	14.30	1:17
Final bed form: 2D									
78[1]	40	18.3	4.12(c)	4.42	--[2]	--[2]	27.9(c)	26.23(c)	3:29
Final bed form: 3D									
79	40	18.3	4.99				23.1	17.89	2:58
Final bed form: trend to 2D; readings of λ, η deferred to exp. 80									
80	40	18.3	5.63		21.0	2.52	20.4	14.05	11:54
Final bed form: 2D									
81[1]	40	18.3	5.33 4.07(c) 3.42(r)	4.10	21.1	3.08	21.6 28.3(c) 33.6(r)	15.68 26.89(c) 38.08(r)	13:47
Final bed form: 2D, following long development with sporadic 3D									
82[1]	60	27.5	7.58 5.44(c) 4.53(r)	4.51	26.8	3.30	22.8 31.7(c) 38.1(r)	17.44 33.86(c) 48.82(r)	29:19
Final bed form: 2D, following long development with sporadic 3D									
83	60	27.5	6.03		--[2]	--[2]	28.6	27.56	1:56
Final bed form: mostly 3D									
84[1]	25	11.4	2.56(r) 2.96(c)	4.11	--[2]	--[2]	28.1(r) 24.3(c)	26.55(r) 19.91(c)	1:17
Final bed form: 3D									

[1]Experiments with the bed initially leveled.
[2]Final bed form two three dimensional to determine λ, η.

Table A-3. Data and notes for experiments with the 0.21-millimeter sand (r = 13.25).

Expt. No.	N	a (cm)	T, T_c, T_r (s)	λ_i (cm)	λ (cm)	η (cm)	U, U_c, U_r (cm/s)	ϕ, ϕ_c, ϕ_r	Duration (hr:min)
85[1]	40	18.3	4.01(c)	5.41	20.0	2.85	28.7(c)	23.74(c)	10:44
Final bed form: 2D, 3D									
86	40	18.3	5.00		22.7	3.28	23.0	15.27	5:33
Final bed form: 2D									
87	40	18.3	4.50		22.6	3.22	25.6	18.85	1:54
Final bed form: 2D									
88	40	18.3	4.00		22.0	3.00	28.8	23.85	3:11
Final bed form: 2D, 3D									
89	40	18.3	3.57		19.5	2.67	32.2	29.94	2:23
Final bed form: mostly 3D									
90[1]	25	11.4	2.91(c)	4.96	14.85	2.18	24.7(c)	17.61(c)	3:51
Final bed form: 2D									
91	25	11.4	2.57		14.2	2.00	28.0	22.58	1:11
Final bed form: mostly 2D									
92	25	11.4	2.23		13.3	1.94	32.2	29.98	1:02
Final bed form: 2D									
93	25	11.4	2.01		12.3	1.86	35.8	36.91	1:55
Final bed form; mostly 2D									
94	25	11.4	1.80		11.8	1.74	39.9	46.01	1:03
Final bed form: 2D, crest ridges yaw alternately									
95	25	11.4	1.60		11.4	1.60	44.9	58.23	0:43
Final bed form: 2D									
96[1]	30	13.7	3.33(c)	5.36	16.85	2.51	25.9(c)	19.36(c)	4:02
Final bed form: 2D									
97	30	13.7	2.70		15.3	1.92	32.0	29.46	2:41
Final bed form: mostly 3D									
98	30	13.7	2.40		14.5	2.05	35.9	37.28	4:45
Final bed form: mostly 2D, following a 3D regime									
99	30	13.7	2.08		12.5	1.83	41.5	49.63	3:32
Final bed form: mostly 3D									
Sand accumulated in spools is spread over the ends of the bed									
100	30	13.7	2.71		13.9	2.19	31.8	29.24	4:34
Final bed form: mostly 2D									
101[1]	60	27.5	4.59(r) 5.50(c)	5.70	--[2]	--[2]	37.6(r) 31.4(c)	40.76(r) 28.40(c)	4:11
Final bed form: mostly 3D									
Sand accumulated in spools is spread over the ends of the bed									
102	60	27.5	7.56		24.8	3.41	22.8	15.03	6:48
Final bed form: mostly 2D									
103[1]	80	36.6	6.02(r) 6.71(c)	5.73	--[2]	--[2]	38.2(r) 34.3(c)	42.14(r) 33.91(c)	5:18
Final bed form: mostly 3D									
Sand accumulated in spools is spread over the ends of the bed									
104	80	36.6	9.66		33.2	4.38	23.8	16.36	7:23
Final bed form: mostly 2D									

[1]Experiments with the bed initially leveled.
[2]Final bed form too three dimensional to determine λ, η.

APPENDIX B

PHOTOS OF INITIAL AND FINAL BED FORMS FOR THE 24 EXPERIMENTS STARTING FROM AN INITIALLY LEVELED BED

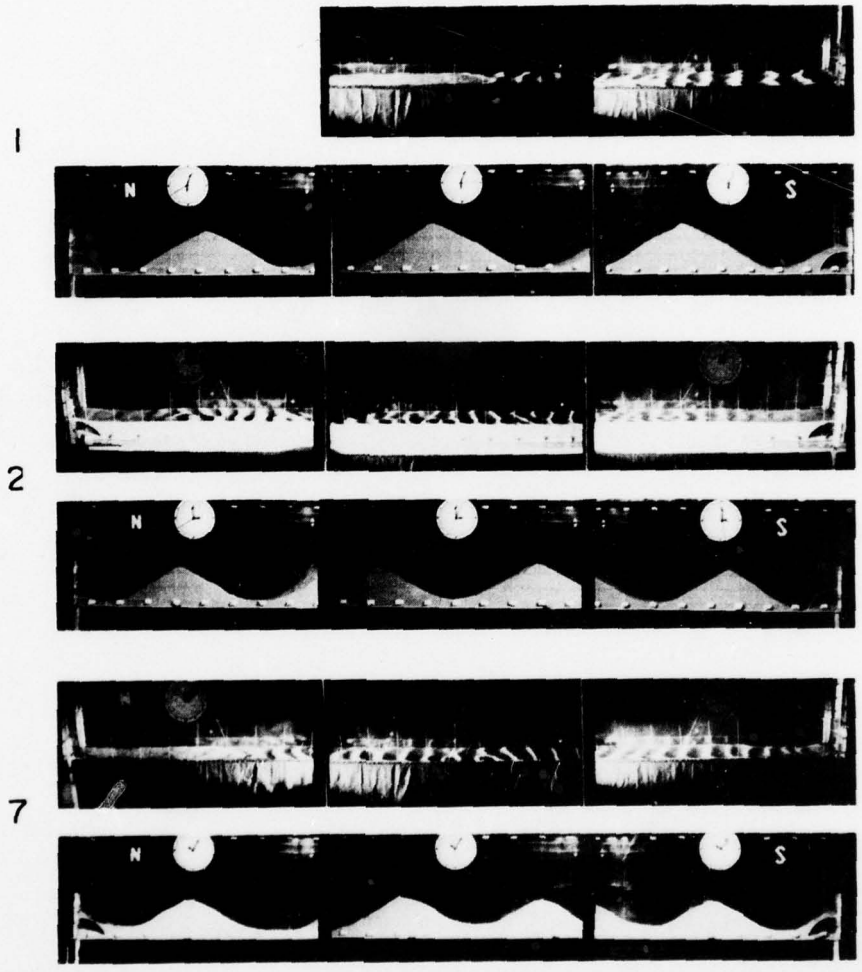

Figure B-1. Initial and final bed forms for experiments with the 0.55-millimeter sand. Experiment numbers shown at left of each pair of profiles.

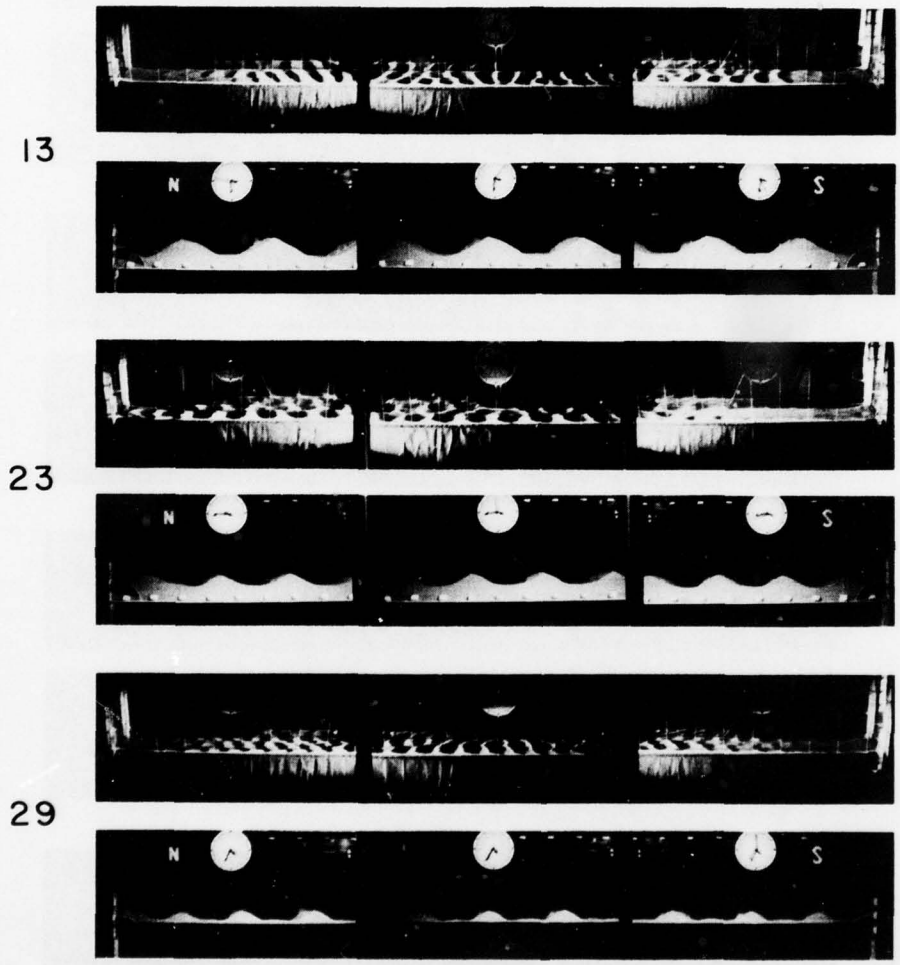

Figure B-1. Initial and final bed forms for experiments with the 0.55-millimeter sand. Experiment numbers shown at left of each pair of profiles.--Continued

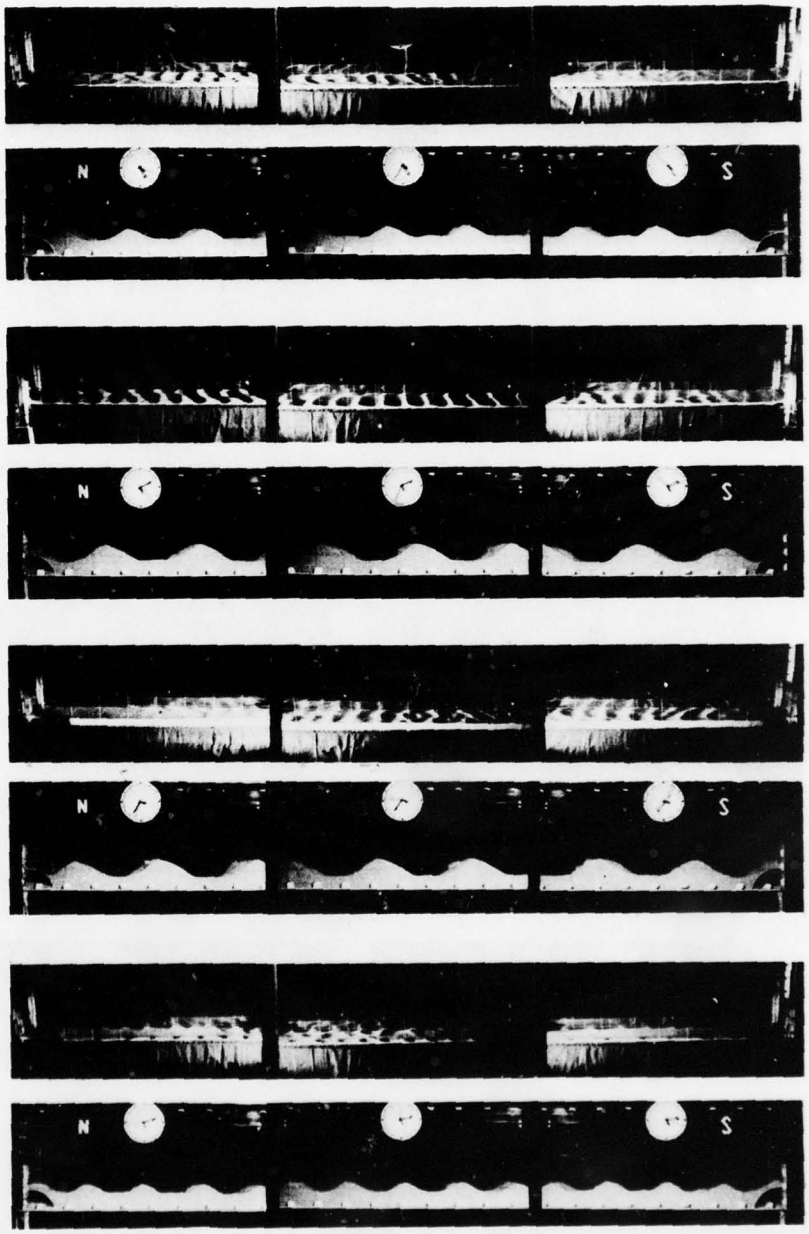

Figure B-1. Initial and final bed forms for experiments with the 0.55-millimeter sand. Experiment numbers shown at left of each pair of profiles.--Continued

AD-A060 907 COASTAL ENGINEERING RESEARCH CENTER FORT BELVOIR VA F/G 8/3
SAND RIPPLE GROWTH IN AN OSCILLATORY-FLOW WATER TUNNEL.(U)
AUG 78 K E LOFQUIST
UNCLASSIFIED CERC-TP-78-5 NL

2 OF 2
AD
A060907

END
DATE
FILMED
01-79
DDC

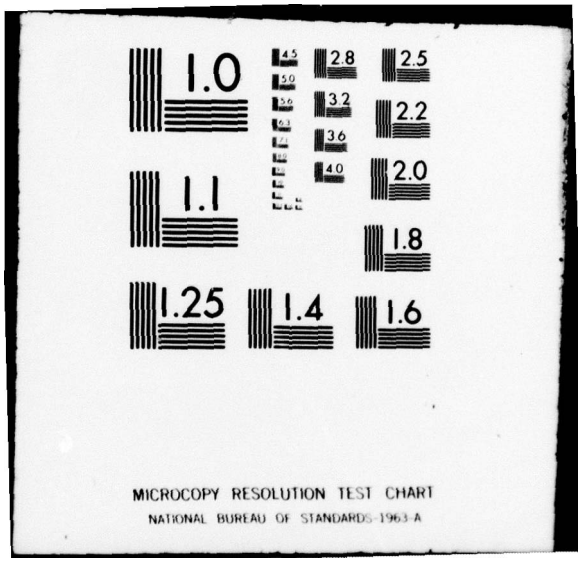
1.0
1.1
1.25
1.4
1.6
2.8
3.2
3.6
4.0
2.5
2.2
2.0
1.8
MICROCOPY RESOLUTION TEST CHART
NATIONAL BUREAU OF STANDARDS-1963-A

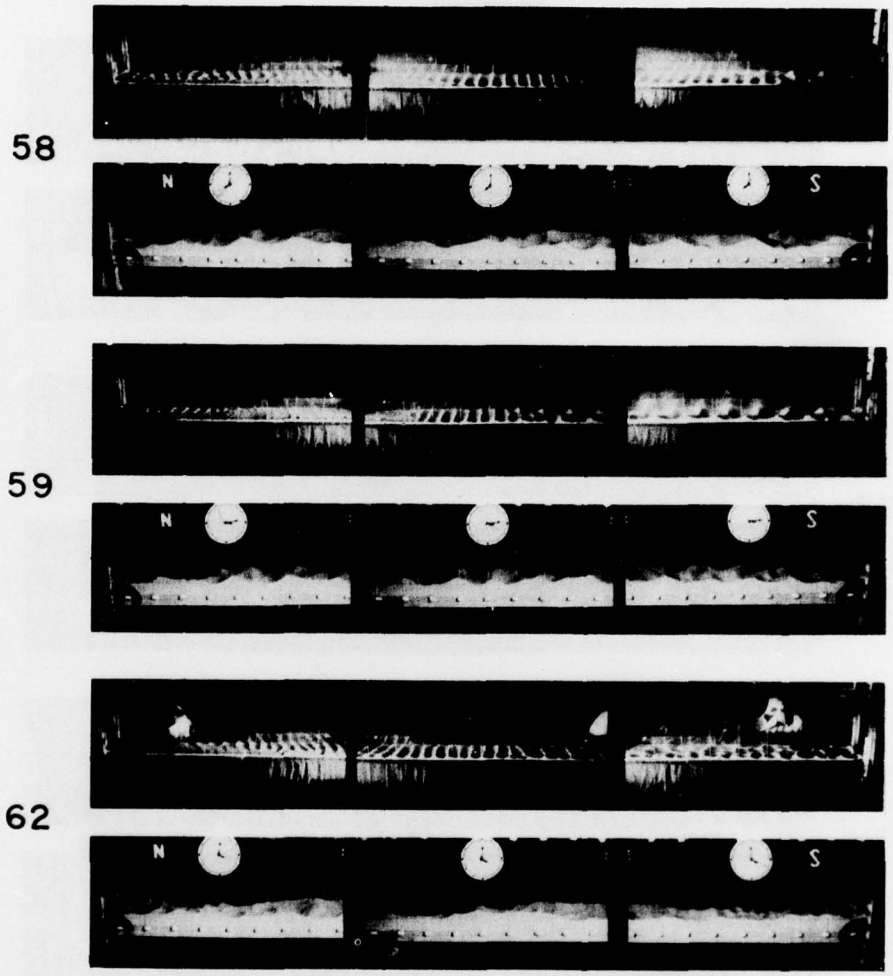

Figure B-2. Initial and final bed forms for experiments with the 0.18-millimeter sand. Experiment numbers shown at left of each pair of profiles.

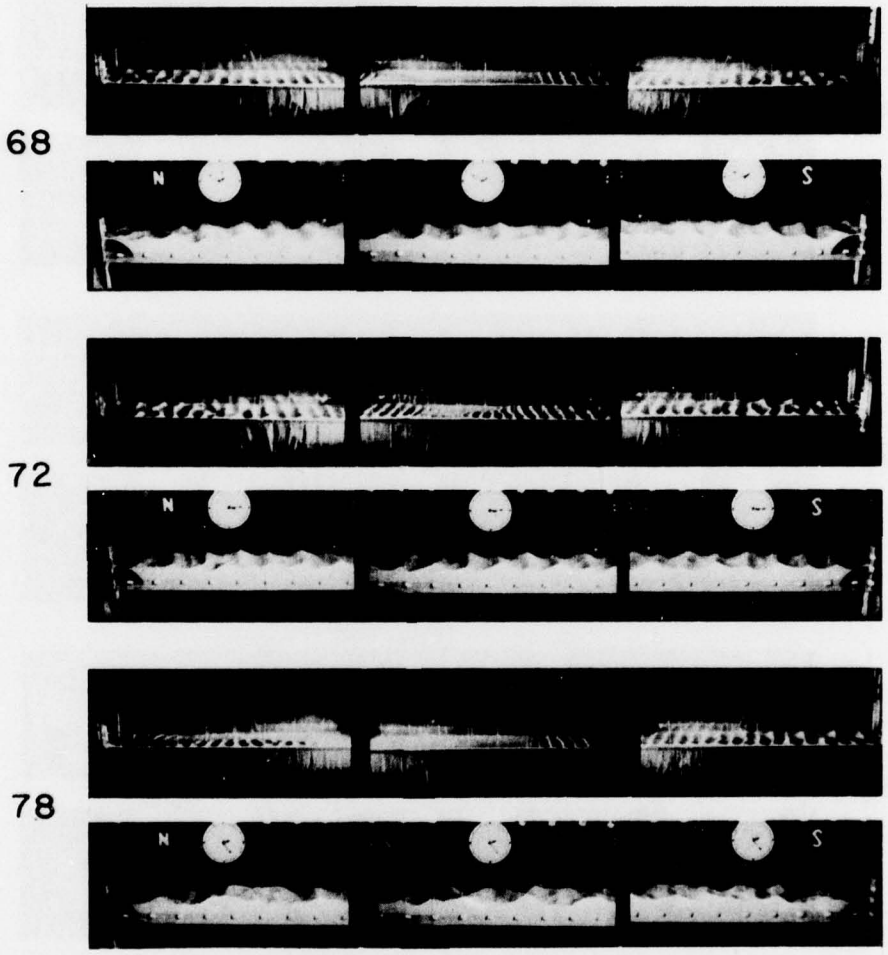

Figure B-2. Initial and final bed forms for experiments with the 0.18-millimeter sand. Experiment numbers shown at left of each pair of profiles.--Continued

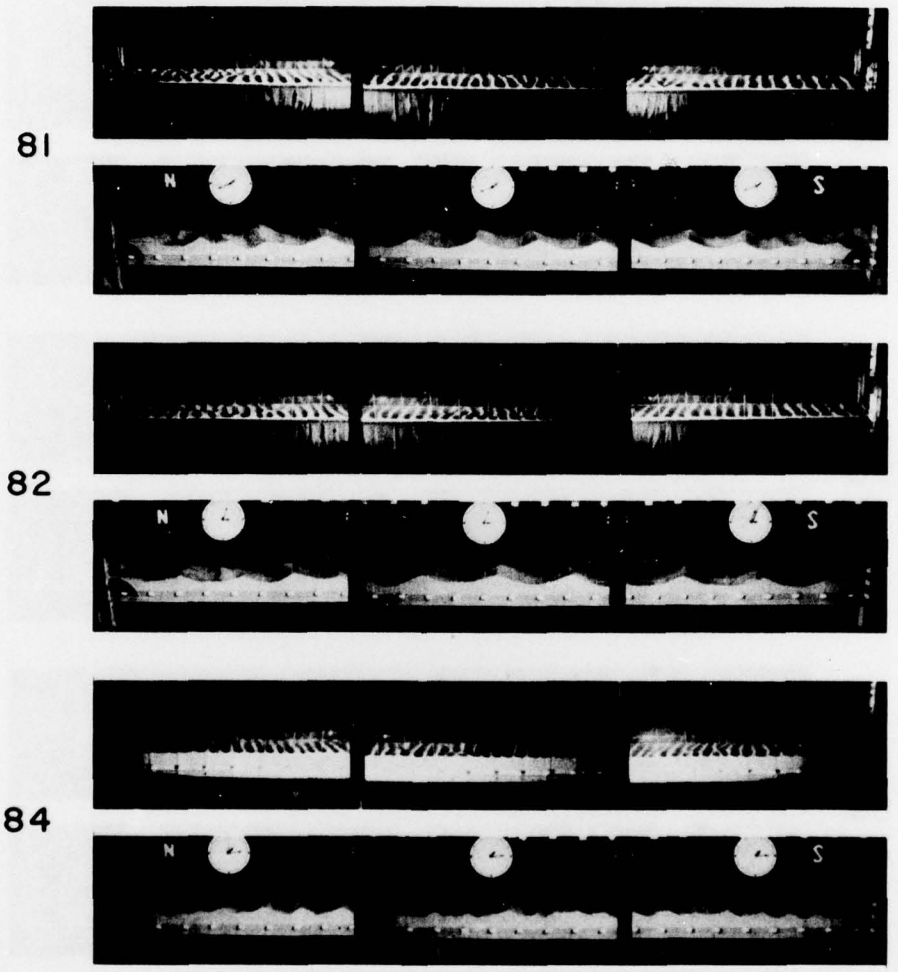

Figure B-2. Initial and final bed forms for experiments with the 0.18-millimeter sand. Experiment numbers shown at left of each pair of profiles.--Continued

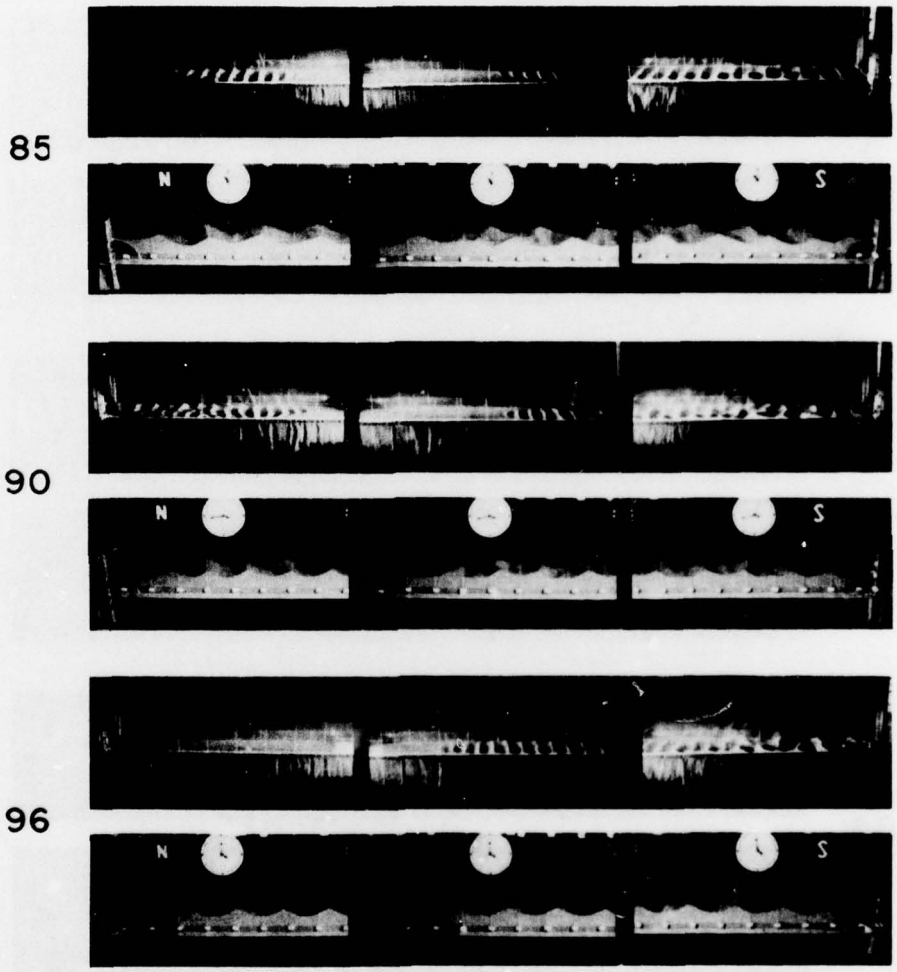

Figure B-3. Initial and final bed forms for experiments with the 0.21-millimeter sand. Experiment numbers shown at left of each pair of profiles.

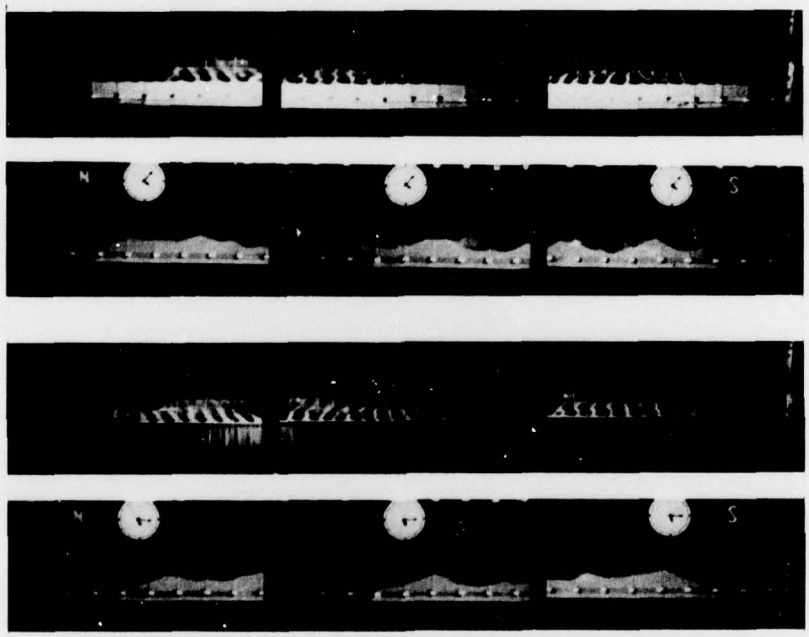

Figure B-3. Initial and final bed forms for experiments with the 0.21-millimeter sand. Experiment numbers shown at left of each pair of profiles.--Continued

Lofquist, Karl E. B.
Sand ripple growth in an oscillatory-flow water tunnel / by Karl E. B. Lofquist. -- Ft. Belvoir, Va. : U.S. Coastal Engineering Research Center ; Springfield, Va. : available from National Technical Information Service, 1978.
100 p. : ill. (Technical paper - U.S. Coastal Engineering Research Center ; no. 78-5)
CERC Agreement no. 76-30.
Bibliography : p. 83.
This report summarizes a laboratory study, including prototype conditions, of sand ripple growth in sinusoidal flow. The results will enable the coastal engineer to better predict and interpret equilibrium ripples in the offshore under both laboratory and field conditions.
1. Ripples (Sedimentary). 2. Beds. 3. Sand transport by waves. 4. Shore processes. I. Title. II. Series: U.S. Coastal Engineering Research Center. Technical paper no. 78-5.

TC203 .U581tp no. 78-5 627

Lofquist, Karl E. B.
Sand ripple growth in an oscillatory-flow water tunnel / by Karl E. B. Lofquist. -- Ft. Belvoir, Va. : U.S. Coastal Engineering Research Center ; Springfield, Va. : available from National Technical Information Service, 1978.
100 p. : ill. (Technical paper - U.S. Coastal Engineering Research Center ; no. 78-5)
CERC Agreement no. 76-30.
Bibliography : p. 83.
This report summarizes a laboratory study, including prototype conditions, of sand ripple growth in sinusoidal flow. The results will enable the coastal engineer to better predict and interpret equilibrium ripples in the offshore under both laboratory and field conditions.
1. Ripples (Sedimentary). 2. Beds. 3. Sand transport by waves. 4. Shore processes. I. Title. II. Series: U.S. Coastal Engineering Research Center. Technical paper no. 78-5.

TC203 .U581tp no. 78-5 627

Lofquist, Karl E. B.
Sand ripple growth in an oscillatory-flow water tunnel / by Karl E. B. Lofquist. -- Ft. Belvoir, Va. : U.S. Coastal Engineering Research Center ; Springfield, Va. : available from National Technical Information Service, 1978.
100 p. : ill. (Technical paper - U.S. Coastal Engineering Research Center ; no. 78-5)
CERC Agreement no. 76-30.
Bibliography : p. 83.
This report summarizes a laboratory study, including prototype conditions, of sand ripple growth in sinusoidal flow. The results will enable the coastal engineer to better predict and interpret equilibrium ripples in the offshore under both laboratory and field conditions.
1. Ripples (Sedimentary). 2. Beds. 3. Sand transport by waves. 4. Shore processes. I. Title. II. Series: U.S. Coastal Engineering Research Center. Technical paper no. 78-5.

TC203 .U581tp no. 78-5 627

Lofquist, Karl E. B.
Sand ripple growth in an oscillatory-flow water tunnel / by Karl E. B. Lofquist. -- Ft. Belvoir, Va. : U.S. Coastal Engineering Research Center ; Springfield, Va. : available from National Technical Information Service, 1978.
100 p. : ill. (Technical paper - U.S. Coastal Engineering Research Center ; no. 78-5)
CERC Agreement no. 76-30.
Bibliography : p. 83.
This report summarizes a laboratory study, including prototype conditions, of sand ripple growth in sinusoidal flow. The results will enable the coastal engineer to better predict and interpret equilibrium ripples in the offshore under both laboratory and field conditions.
1. Ripples (Sedimentary). 2. Beds. 3. Sand transport by waves. 4. Shore processes. I. Title. II. Series: U.S. Coastal Engineering Research Center. Technical paper no. 78-5.

TC203 .U581tp no. 78-5 627